

Multi-photon Neurophotonic: recent advances in imaging and manipulating neuronal circuits

Cécile Telliez^{1,*}, Ruth Sims¹, Giulia Faini¹, Pascal Berto^{1,2,3}, Eirini Papagiakoumou¹, Dimitrii Tanese¹, Nicolò Accanto^{1,4,*}

¹ Sorbonne Université, INSERM, CNRS, Institut de la Vision, F-75012 Paris, France

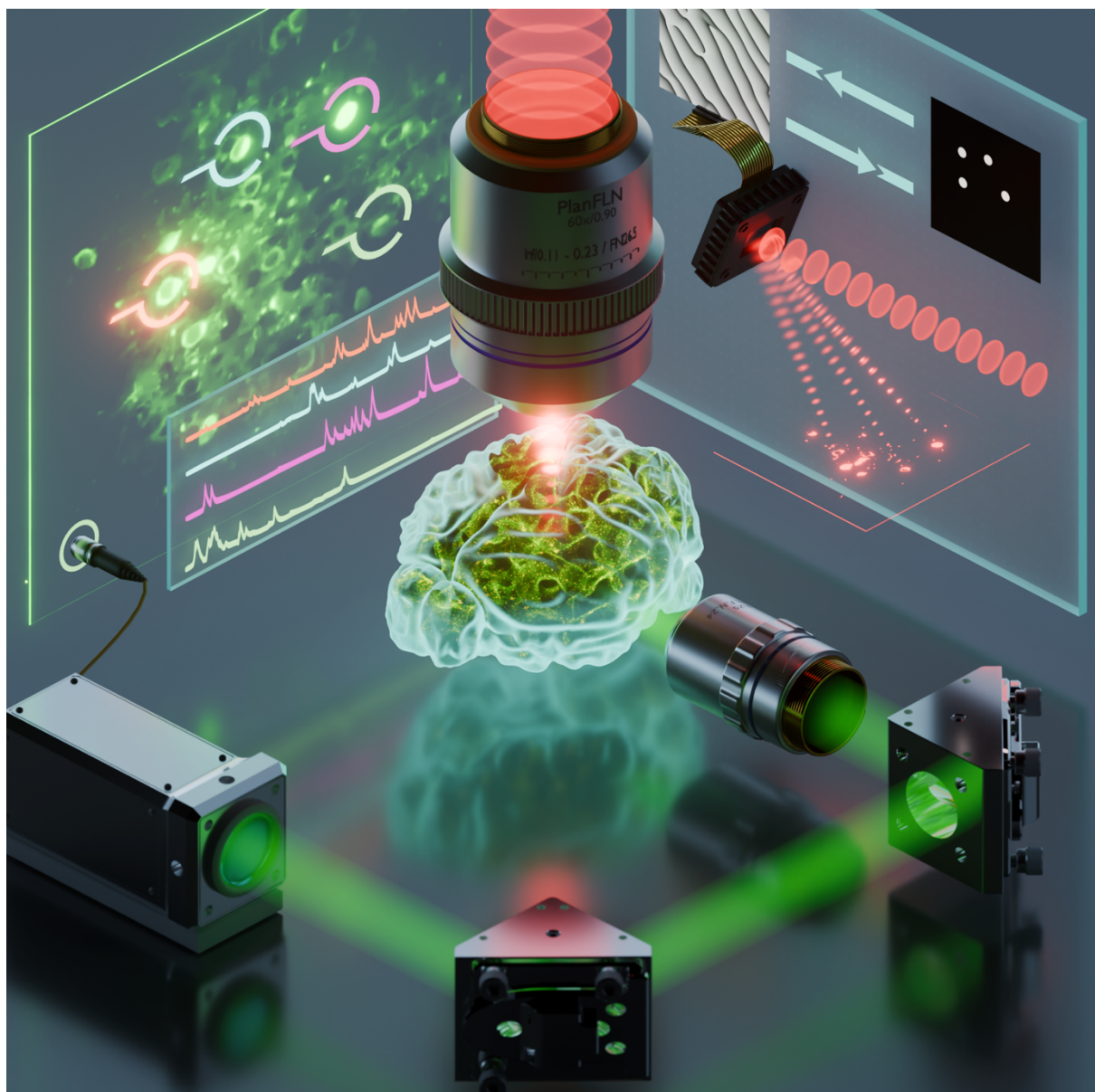
² Université Paris Cité, Paris 75006, France

³ Institut Universitaire de France (IUF), Paris 75231, France

⁴ Institute for Bioengineering of Catalonia (IBEC), Barcelona Institute of Science and Technology, Barcelona, Spain

*Nicolò Accanto, E-mail: nicolo.accanto@inserm.fr, naccanto@ibecbarcelona.eu

*Cécile Telliez, E-mail: cecile.telliez@inserm.fr



Cover Art

Author: Clément Molinier, Licence: <https://creativecommons.org/licenses/by/4.0/>

Artistic impression of a two-photon microscope setup used to image and optogenetically manipulate neuronal activity in the mouse brain.

A microscope objective focuses infrared laser pulses into the brain, where indicators of neuronal activity and optogenetic opsins are expressed.

The lateral projections provide a detailed view of:

- 1. The process of imaging neuronal activity, extracting activity traces from individual neurons over time.*
- 2. A spatial light modulator using computer-generated holography to precisely photostimulate specific neurons.*
At the bottom, an artistic representation depicts fluorescence light being detected by a photodetector.

Abstract

The possibility of using light to image and manipulate neuronal activity, at the heart of Neurophotonics, has provided new irreplaceable tools to study brain function. In particular, the combination of multiphoton microscopy and optogenetics allows researchers to interact with neuronal circuits with single-cell resolution in living brain tissues.

However, significant optical challenges remain to empower new discoveries in Neuroscience. This article focuses on three critical areas for future development: 1) expanding imaging and optogenetic stimulation to larger fields of view and faster acquisition speeds, while maintaining single-cell resolution and minimizing photodamage; 2) enabling access to deeper brain regions to study currently inaccessible neuronal circuits; and 3) developing optical techniques for studying natural behaviours in freely moving animals. For each of these challenges, we review the current state-of-the-art and suggest future directions with the potential to transform the field.

Keywords

Neurophotonics; Multiphoton microscopy; Optogenetic photostimulation; Calcium and voltage imaging; Wavefront shaping; All-optical brain studies

Introduction

Functional imaging and optogenetics

Neuronal circuits process information from the external world to shape our perception, memories, behaviour, and ultimately, our identities. Understanding how exactly this processing takes place is a fundamental question in Neuroscience. Over the past 20 years, several game changing neurophotonics technologies have emerged, which address this challenge by providing powerful optical means of interacting with neuronal networks, empowered by two significant breakthroughs in genetic engineering. First, Genetically Encoded Calcium and Voltage Indicators (GECIs and GEVIs), are fluorescent proteins that, once expressed in neurons, enable imaging of neuronal function by converting changes in calcium ion concentration (a proxy for neuronal activity; in the case of GECIs) or changes in cell membrane potential (directly reflecting neuronal activity; in the case of GEVIs) into fluorescence variations¹⁻⁴. Second, the optogenetics technology relies on genetically expressing light-

sensitive proteins, known as opsins, in specific neuronal populations, that enable researchers to control activity in those cells with light⁵⁻⁸. By illuminating opsin-expressing neurons, it is possible to reversibly switch their activity on or off at will, in function of the type of opsin used.

While imaging neuronal activity establishes correlations - such as which neurons fire in correlation with a specific external stimulus - introducing controlled perturbations by selectively activating or inhibiting neuronal activity enables the inference of causal links^{9,10} - such as whether a specific group of neurons drives certain behaviours. Experiments in which neuronal activity imaging and optogenetics photostimulation can be performed at the same time are named “all-optical” studies of the brain^{11,12}. In the past 15 years, they have been used for instance for mapping functional connectivity among neurons¹³⁻¹⁵ and elucidating the neural bases of perception¹⁶⁻²⁰ and behaviour^{14,19-23} in small living animal models (mostly rodents).

Although one-photon (1P) illumination methods (with visible light) for all-optical experiments have the advantage of simplicity and cost-effectiveness, and have been utilized in some studies²⁴⁻²⁹, they are in general limited by background fluorescence, poor axial confinement, and limited propagation (<200µm) through scattering tissues such as the brain. Consequently, most all-optical studies in mice, a widely used animal model, use two-photon Laser Scanning Microscopy (2P-LSM) for its superior tissue penetration and axial confinement³⁰⁻³². In this manuscript we will mainly focus on 2P studies of the brain, both for functional imaging and optogenetic photostimulation, while giving the relevant references for the newest 1P approaches and detailing the potential of 3P microscopy for reaching deeper brain regions.

Two-photon all optical studies of the brain

2P-LSM is today the gold standard for imaging neurons and neuronal activity *in vivo* in the mouse brain. By far, the most used GECI is the GCaMP family^{1-3,33-35}, whose absorption peak in the 2P regime sits around 920 nm. To construct an image (Fig. 1a, b), a near infrared (NIR) pulsed laser centred at 920 nm (typically Ti:Sapphire oscillators with <200fs pulse duration, 80MHz repetition rate and tens of nJ pulse energy) is focused by a microscope objective on a diffraction-limited spot that is raster scanned by a pair of galvanometric mirrors across the field of view (FOV). The fluorescence photons emitted by the activity indicator, are collected through the same objective and detected with a photomultiplier tube (PMT).

In a 2P all-optical experiment (Fig. 1a, c), a second NIR pulsed laser is used for optogenetic photostimulation. When using GCaMP as the activity indicator, the typical choice is to use red-shifted opsins^{13,16,19,21} that can be efficiently excited at near infrared wavelengths. This has the great advantage of meeting the high energy demands of optogenetic activation based on powerful laser amplifiers using Ytterbium-doped active media, which have seen significant industrial development in recent years, are centred around 1030-1070 nm, and can deliver ~300 fs laser pulses with low repetition rates (0.5-10 MHz) and very high energy (up to > 500 µJ). However, as most microbial opsins can also be excited at 920 nm, this configuration is prone to generate optical cross-talk, i.e. spurious activation of opsin-expressing neurons by the imaging laser. Strategies to minimise the cross-talk include³⁶: limiting the imaging laser power, imaging across larger FOVs to limit the dwell time per pixel, or switching to a configuration based on red-shifted GECIs and blue-shifted opsins^{37,38} that effectively minimise the spectral overlap.

To selectively photostimulate only the neurons of interest among those expressing an opsin, 2P stimulation is combined with light shaping techniques to split the laser beam into tens of spots that simultaneously illuminate target neurons (Fig. 1a). A preferred light shaping method is computer-generated holography (CGH)^{21,39-41}, implemented using a liquid crystal Spatial Light Modulator (SLM) (Fig. 1a, c). The SLM can either create multiple diffraction-limited spots that are spirally-scanned with galvanometric mirrors to illuminate the entire soma of neurons^{42,43}, or directly sculpt extended shapes (10-15µm disks) to target the soma in a scanless manner. In 2P holographic optogenetics, all targets are therefore illuminated simultaneously and we will thus refer to this holographic 2P

photostimulation process as ‘parallel’ excitation, as opposed to the serial nature of scanning excitation used for imaging.

Manuscript outline

As all-optical studies begin to advance our understanding of the brain, major optical challenges must be addressed. This article focuses on three key challenges (illustrated in Fig. 2), briefly reviews the current state of the art and outlines future directions that could significantly advance Neurophotonics. Part A explores methods for imaging large neuronal networks with high spatial resolution and speed. We discuss strategies for expanding the FOV in 2P imaging and photostimulation, achieving kHz imaging speeds for voltage indicators, and enabling ultrafast optogenetic activation of targeted neurons. We conclude with a discussion on limitations related to the tissue damage and strategies to scale up circuit investigations without exceeding photodamage threshold.

Part B focuses on the challenge of reaching deeper brain regions through scattering tissue. Depending on the depth, solutions include using longer excitation wavelengths, as in three-photon (3P) microscopy, adaptive optics and scattering compensation techniques, and micro-endoscopy.

Part C highlights advances in flexible and adaptable technologies designed to study natural behaviour in freely moving animals.

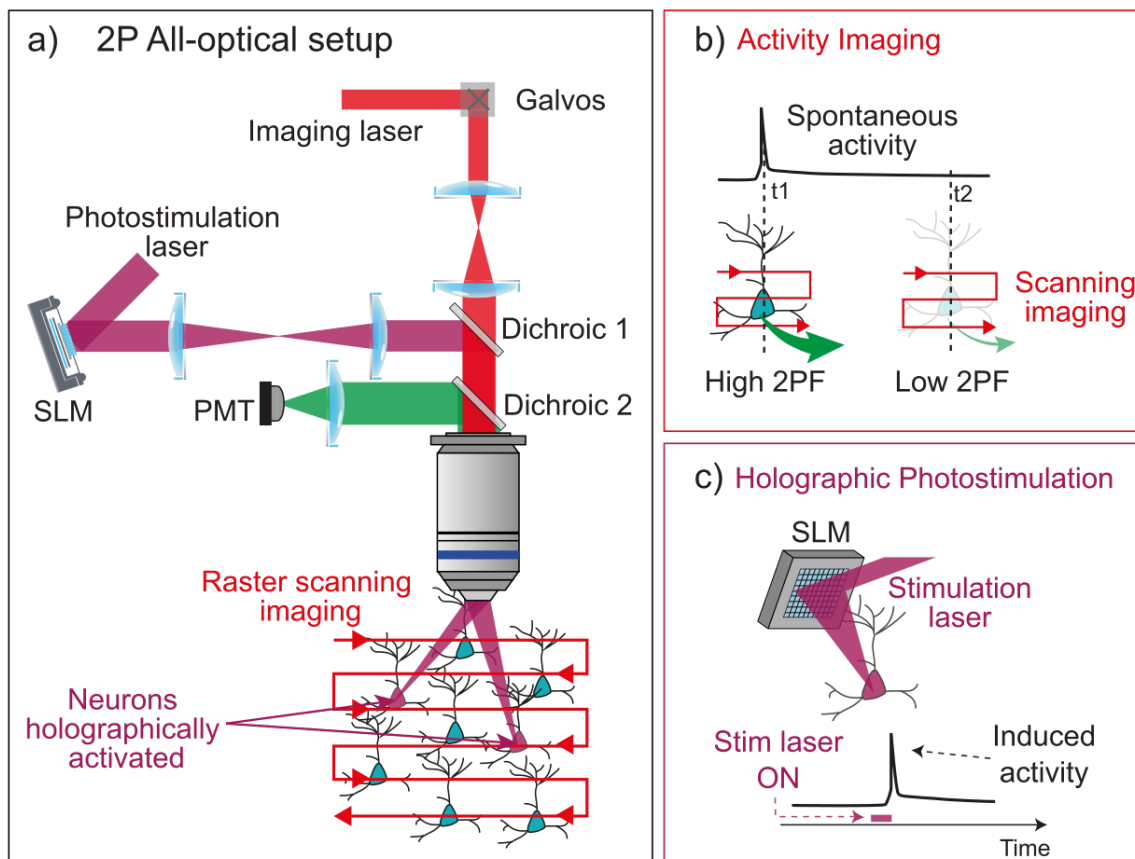


Figure 1. Two-photon all-optical studies of the brain

a) Setup for 2P all-optical studies of the brain, composed of an imaging path (red) to record the activity of neurons within a network and a photostimulation path (purple) to induce controlled optogenetic perturbations (here, activation of neurons). In the imaging path, a near-infrared (NIR) laser is raster-scanned across the field of view and the 2P fluorescence is recorded with a photomultiplier tube (PMT). Optogenetic stimulation is induced by shaping the light from a second NIR laser with a spatial light modulator (SLM), which redirects the light to precisely target the neurons of interest. **b),** Simplified

sketch of the 2P activity imaging process. Upon raster scanning of the imaging laser on the field of view, neurons expressing a fluorescent activity reporter emit a 2P fluorescence signal, with its intensity reflecting the level of spontaneous activity of the neuron. c) Simplified sketch of the 2P patterned optogenetic photostimulation processes. Upon brief patterned illumination from the SLM, a targeted neuron expressing an optogenetic actuator (or inhibitor; not shown) has its activity induced (or suppressed). 2PF: 2P fluorescence.

Part A. Precisely probing neuronal circuits across millimetre Fields of View and at kilohertz rates

In an ideal scenario, all-optical experiments would grant imaging and photostimulation access to an entire ensemble of neurons, with single-cell spatial resolution and at sufficient timescales for recording the time-dependent neuronal information and without altering the brain tissue under study.

Space

Neuronal circuits, from local to large-scale networks, involve thousands to millions of neurons⁴⁴ connected across distant brain regions⁴⁵, dynamically processing and integrating information. As a consequence, focusing solely on a single region or a subset of neurons may not fully capture how neurons encode information^{45,46}. To address this, all-optical microscopy techniques must be developed to record and manipulate the activity of multiple, large (~mm) brain areas involved in processing the information under study, while maintaining at least single-cell resolution. It is important to emphasize, however, that the performance of an all-optical setup is not solely determined by the optics. In the case of single-cell optogenetic photostimulation, for example, the spatial resolution also depends on the expression pattern of the opsins. Neuronal cell bodies are often densely surrounded by neurites of neighbouring cells, and if opsins are expressed in these neurites, even two-photon (2P) stimulation targeted to a single cell body can inadvertently activate dendrites or axons of nearby neurons, effectively reducing spatial resolution. To overcome this issue, soma-targeted opsins have been developed, which confine opsin expression to the cell body while excluding it from neuronal processes, thereby enhancing the spatial precision of photostimulation⁴⁷⁻⁴⁹.

Time

In neuronal computation, information is electrically encoded through changes in membrane potential. Smaller variation of this potential, below a certain threshold and defined as sub-threshold fluctuations, serve as graded analogue signal within neurons, while supra-threshold changes trigger Action Potentials (APs) – brief (few ms) electrical spikes that propagate to downstream neurons. Neurons fire APs at precise times (on the ms scale) and specific frequencies (from a few Hz to several hundreds of Hz), with some neurons firing in synchrony while others do not. Additionally, in some brain areas, *e.g.* superficial cortical layers, neuronal activity is generally sparse in time, with activation being mostly asynchronous and infrequent, with many neurons remaining silent for extended periods⁵⁰⁻⁵³. All these temporal dynamics might be crucial for encoding sensation, cognition, and action in neural circuits⁵⁴⁻⁵⁶. Whether information is encoded in the firing rate, the precise spike time or a combination of both⁵⁷, being able to optogenetically replicate naturally occurring spatiotemporal activity patterns, or interfere with them with high temporal accuracy is of fundamental importance for a better understanding of the neuronal code. From the imaging point of view, the kinetics of the activity reporter (calcium or voltage indicator) filter the dynamics of neuronal events and dictate the necessary acquisition frame rates to faithfully detect reported events. Calcium indicators capture changes in calcium concentration linked to AP generation and can be imaged effectively at frame rates from a few Hz to tens of Hz. In contrast, the faster and emerging voltage indicators require kHz frame rates to report both APs as well as subthreshold membrane potential changes.

Balancing Spatial and Temporal Resolution

In sequential processes like typical 2P-LSM, one inherently has to accept trades off between the number of recorded positions, imaging speed and Signal-to-Noise Ratio (SNR). Striking a balance is crucial to maintain temporal resolution sufficient for capturing relevant activity events, while maximizing the number of recorded neurons and maintaining sufficient SNR to faithfully report activity. This necessitates strategic compromises to balance coverage, detail, imaging speed, and minimizing photodamage. In contrast, holographic optogenetics splits the laser beam to illuminate multiple neurons in parallel by using a SLM, effectively decoupling space and time. While previous reviews have already covered some of these trades off, especially from the point of view of imaging⁵⁸⁻⁶³, this section will focus on unsolved challenges that have to be overcome to expand the FOV and the speed of functional imaging (calcium or voltage) and optogenetic photostimulation, while keeping light-induced damage of the sample within acceptable limits.

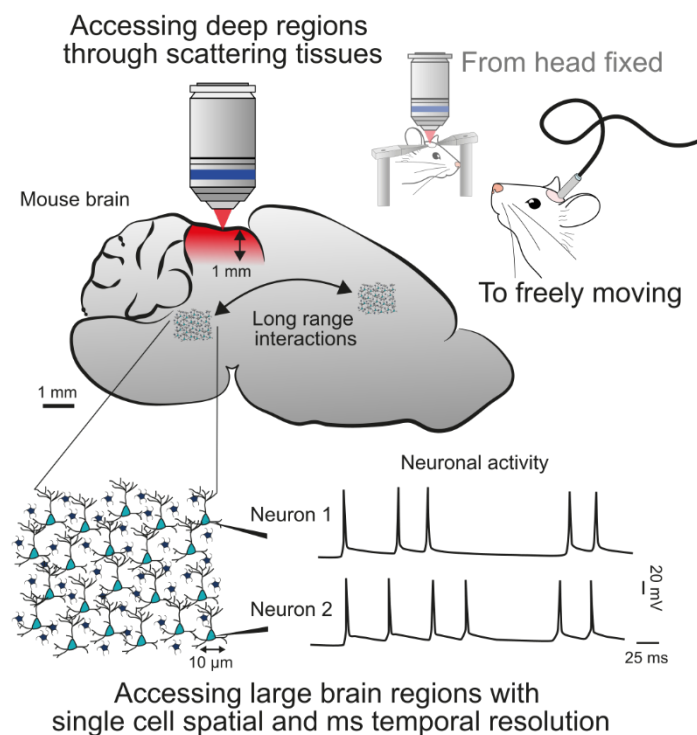


Figure 2. Current challenges in all-optical brain interrogation.

Current challenges in all-optical brain interrogation include: 1) imaging deep, down to a mm, within brain tissue, where scattering and absorption limit light penetration and signal quality; 2) adapting optical systems to freely moving animals, requiring miniaturization of microscopes and stable imaging and stimulation; and 3) achieving larger-scale, high-speed, and accurate imaging and stimulation of neuronal networks across broader brain regions.

Large scale calcium imaging

In the past years, different groups have developed large FOV^{59,64-68} (up to ~ 5 mm in diameter) 2P microscopes (also called 2P mesoscopes) for calcium imaging with single neuron spatial resolution. These mesoscopes (see Fig. 3a), based on custom designed lenses, carefully assembled scan engines made of different scanning mirrors in cascade, and microscope objectives with low aberrations, large pupils and wide accepting angles, can produce either faster acquisition (~ 50 Hz) on multiple smaller regions across the whole 5 mm FOV (as in Ref.^{66,67}), or slower acquisition speeds (~ 1 Hz) of the entire

FOV⁶⁴, with the possibility to acquire multiple planes at the same time^{65,68}, thus leading to the quasi simultaneous calcium imaging of up to ~ 1 million neurons^{46,65}.

One of the challenges associated with extremely powerful 2P mesoscopes is their current limited availability, largely confined to a few selected laboratories. While commercial versions of the 2P mesoscope of Ref.⁶⁴ (Thorlabs) or of Ref.⁶⁷ (Pacific Optica), are emerging, widespread adoption within neuroscience laboratories remains a crucial goal for the coming years. To this end, solutions that sacrifice some optical performance but within an easier and more cost-effective implementation could facilitate broader dissemination, especially when based on off-the-shelf components (as in Ref.^{69,70}).

Pushing even beyond the spatial scales attainable with a 2P mesoscope, some research groups have explored techniques for parallel or sequential study of spatially separated regions, even centimeters apart^{71–74}. Parallelized systems (Fig. 3a) have been developed using either dual beam paths with separate microscope objectives^{71,72} or multiple millimeter-sized lenses (GRIN lenses) coupled to a single objective⁷³. While the former offers superior resolution and detection efficiency, it is limited to simultaneous imaging of only two distant areas. The latter option, although theoretically more flexible, still requires complex alignment procedures. Inscopix recently introduced a 1P microscope variant, the Quartet system, employing four optical fibers, enabling more straightforward imaging of up to four different brain regions in mice. Expanding similar techniques, based on optical fibers, into the 2P domain holds promise for future advancements.

Finally, 1P widefield microscopes with camera detection inherently enable snapshot imaging, achieving millimetre (or even centimetre) scale FOVs and frame rates of tens of Hz^{75–78}. However, the large background fluorescence, limited axial confinement and penetration depth of 1P techniques make it difficult to identify real individual neuron activity. Investing in the further development of computational methods to demix fluorescence traces^{79–82}, as well as developing new smart approaches that combine structured illumination and adaptive optics⁸³, could be a promising direction. Computational innovations are also boosting 1P Light Field Microscopy^{84,85} – which further expands mesoscale access by enabling scanless 3D imaging at tens of Hz- by supporting its scalability, enabling near single-cell signal extraction, and extending depth access to a few hundreds of microns.

Large scale holographic optogenetic photostimulation

If the FOV achievable by a conventional 2P microscope has recently been expanded to the 5x5 mm² limit^{64,67,86}, the laterally accessible FOV of a holographic 2P setup has, until now, been constrained to approximately 1x1 mm² due to the inherent limitations of standard SLMs (see Ref.^{16,87}). The most commonly used SLMs for 2P phase-modulation consist of a 2D matrix of $\sim 10^6$ liquid-crystal pixels. In a standard CGH configuration, the SLM is placed in the conjugate plane of the microscope objective pupil (see Fig. 3b). Two relay lenses of focal lengths f_1 and f_2 are used to image the SLM screen at the objective pupil and to completely fill it. Let L_{SLM} be the lateral SLM screen size, the maximum holographic FOV at the sample plane (L_{FOV}) can be expressed as follows⁸⁸:

$$L_{\text{FOV}} = 2 \frac{f_{\text{obj}}}{M} \tan(\theta_{\text{SLM}}) = \frac{D_{\text{SLM}}}{NA_{\text{obj}}} \tan(\theta_{\text{SLM}}) = \frac{\lambda N_{\text{pix}}}{2 NA_{\text{obj}}} \quad (1)$$

where f_{obj} and NA_{obj} are the focal length and numerical aperture (NA) of the objective, that can be related to the objective pupil diameter (D_{Pup}) by the relation $D_{\text{Pup}} = 2 NA_{\text{obj}} f_{\text{obj}}$; $M = \frac{f_2}{f_1} \approx \frac{D_{\text{Pup}}}{L_{\text{SLM}}}$ is the magnification between the SLM and pupil plane; θ_{SLM} is the maximal half angle that the SLM can introduce, which depends on the laser wavelength (λ) and the SLM pixel size (d_{pix}): $\tan(\theta_{\text{SLM}}) = \frac{\lambda}{2 d_{\text{pix}}}$. The full SLM angular steering capabilities extends to $\pm \theta_{\text{SLM}}$. N_{pix} is the number of SLM pixels in a line $L_{\text{SLM}} = N_{\text{pix}} d_{\text{pix}}$. For typical commercial SLMs, screen sizes are around 15 mm, pixel sizes are 8-20 μm , giving a full angular coverage of about $\pm 3.7^\circ$ and $\pm 1.5^\circ$ at $\lambda \approx 1 \mu\text{m}$. In comparison, 2P imaging mesoscopes with 5x5 mm² FOV use customized objectives (Fig. 3a) with $NA_{\text{obj}} = 0.5$, a very large pupil $D_{\text{Pup}} > 30$ mm and large acceptance angles $\theta_{\text{obj}} = \pm 5^\circ$. As schematically shown in Fig.

3b, because of the magnification needed to fill the objective pupil, the SLM angles that are already intrinsically smaller than mesoscopes acceptance angles, become even smaller at the objective entrance $\theta'_{\text{SLM}} < \theta_{\text{SLM}} < \theta_{\text{obj}}$. It follows that, coupling a standard SLM with a mesoscope objective, while filling its pupil, results in a holographically accessible FOV of $\sim 1 \times 1 \text{ mm}^2$, as demonstrated in Ref.⁸⁷, which is much smaller than the FOV accessible for imaging. For comparison, scanning mirrors used in 2P imaging mesoscopes, have a size of 5-20 mm and an optical scanning angle of $\sim \pm 20^\circ$.

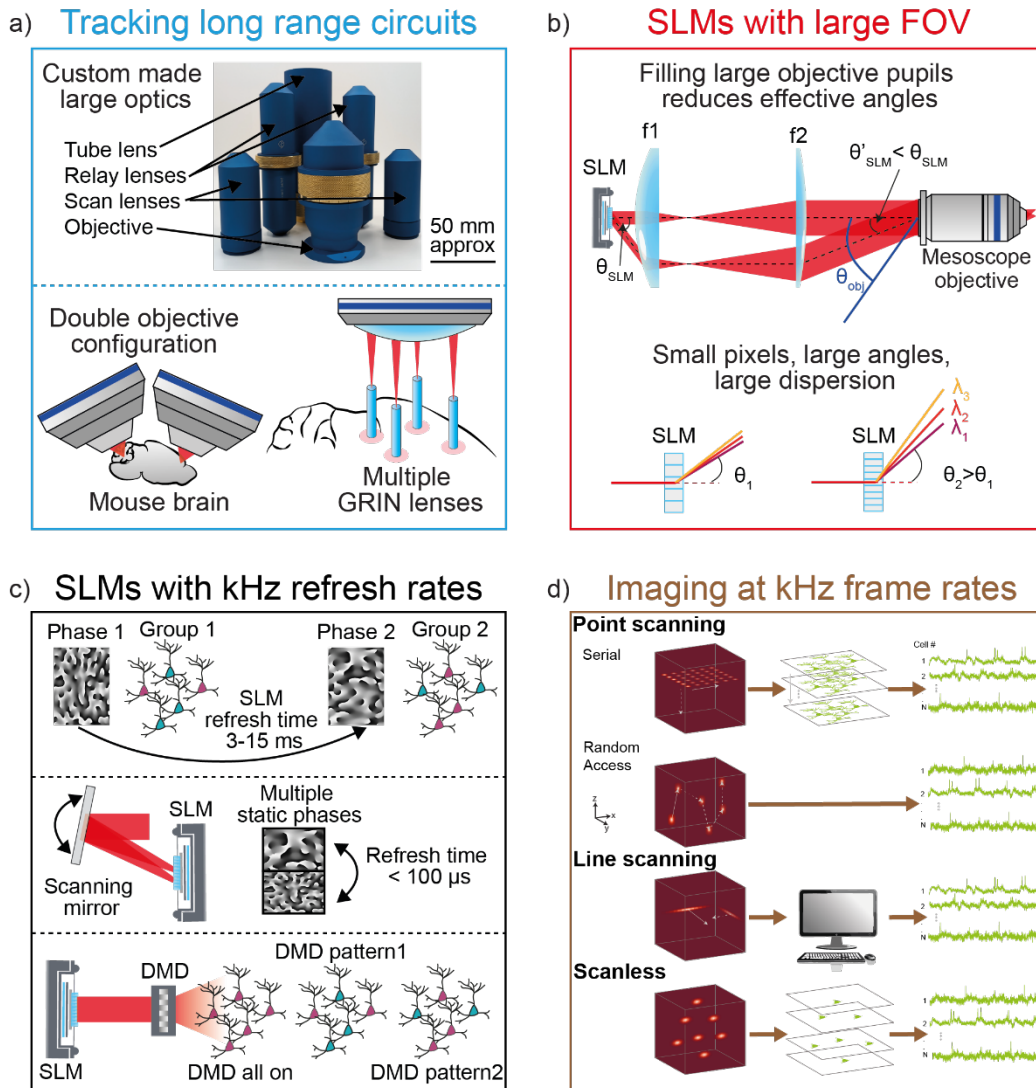


Figure 3. Strategies for fast and large 2P all-optical systems.

a) Large-Area Neuronal Activity Recording: neuronal activity across large regions can be recorded using custom-made large-field objectives and scanners (Courtesy of Pacific Optics under the licence <https://creativecommons.org/licenses/by/4.0/>, see also Ref.⁶⁷). Multiple areas can be accessed simultaneously by combining two objectives (as in^{71,72}) or using multiple GRIN lenses⁷³. **b)** Limitations that constrain the FOV accessible to a SLM positioned in the conjugate plane of the objective pupil, with the assumption that the objective pupil is fully illuminated. Top panel: filling the large pupil of mesoscope objectives (diameter > 30 mm) when using standard SLMs does not reach the acceptance angles of these objectives. Bottom panel: reducing the size of the SLM pixels increases the maximum achievable diffraction angles but also introduces significant chromatic dispersion. In 2P optogenetics this reduces the 2P photostimulation efficiency for spots generated off-centre. **c)** SLMs with kHz refresh rates. In holographic optogenetics, the refresh rate of liquid crystal SLMs is relatively slow (3-15ms) and limits the maximum rate at which holograms can be projected and thus patterns reconfigured. To overcome this, fast (<100 μ s) addressing of a multi-hologram SLM with galvanometric mirrors has been

developed⁸⁹. Another approach combines a slow SLM with a fast DMD, which act as a rapid (10kHz) area-specific shutter of the SLM-defined patterns⁹⁰. **d)** State-of-the-art approaches for 2P imaging at kHz frame rates include serial scanning and scanless techniques. Simulated excitation point spread functions are shown on the left panels, with extracted single-cell activity traces on the right. Serial scanning methods can be divided into point-scanning, random access methods^{91,92}, and line-scanning tomography⁹³. Point-scanning uses a single diffraction-limited spot to image a volume via lateral and axial displacement, with fluorescence detected by PMTs. Random access methods scan targeted pixel sets of interest with acousto-optic deflectors^{94,95}, while line-scanning acquires angular projection of the FOV, and single-cell neuronal activity is recovered computationally. Scanless methods simultaneously illuminate several ROIs (using temporally-focused, low-NA Gaussian, holographic or phase-contrast shaped beams⁹⁶) and use camera detection to preserve spatial cell information.

To develop a 2P holographic mesoscope, as derived from Eq (1), one must increase the total number of SLM pixels. This can be done in two ways: 1) by decreasing the pixel size d_{pix} while keeping the SLM size L_{SLM} constant, which increases the steering angle, or 2) by increasing the SLM size while keeping the pixel size constant, reducing the SLM-to-objective magnification.

SLM models following the first strategy already exist, such as the Holoeye GAEA-2.1, with 4160 x 2464 pixels of 3.74 μm . If this creates larger steering angles, it also generates high dispersions as each wavelength of a laser pulse sees a slightly different phase and is reflected at different angles (Fig. 3b bottom panel). As shown in Ref.⁹⁷, for the bandwidths typically used in 2P optogenetics (central wavelength = 1030 nm, with a $1/e^2$ width < 30 nm), this greatly reduces the 2P efficiency at the sample plane, and makes such a strategy practically nonviable. A possible solution, could be to design specific optical elements that could compensate the SLM induced dispersion, as discussed in Ref.⁹⁸.

The second strategy, *i.e.* using SLMs with a larger screen and larger pixels, as in Ref.¹⁶, could be more suitable as it avoids undesired dispersion that can reduce 2P efficiency. Fabrication and cost-effective commercialization of similar SLMs is needed to deliver next generation 2P holographic mesoscopes.

Another possible route to increase the accessible FOV is to couple the SLM with a scanning device that can produce larger angles, an idea already explored in Ref.⁹⁷ to produce quasi simultaneous patterning on very distant areas. In a different direction, tuneable meta-surfaces^{99,100} were shown to produce large FOV holograms⁹⁹, and broadband meta-surface holograms were also demonstrated¹⁰¹. New developments in this field could attempt to produce large scale tuneable meta-surface SLMs, with high throughputs (> 80%), large steering angles (> $\pm 10^\circ$) and wavelength independent operation across typical laser bandwidth used in 2P optogenetic photostimulation experiments.

Kilohertz 2P voltage imaging

Calcium imaging with GECIs is widely used for all-optical neurophysiology and it permits the activity of large numbers of neurons to be recorded simultaneously^{64,65,67,71,102,103}. Calcium transients generally last significantly longer (tens to hundreds of ms) than the underlying voltage fluctuations, facilitating the detection of neural activity (as they require slower imaging frame rates to achieve Nyquist sampling), but also limiting the quantification of spike firing rates and timing (the temporal resolution is limited by the duration of the calcium transient), particularly in the case of high-frequency trains of APs, as confirmed by simultaneous calcium and voltage imaging studies¹⁰⁴. Furthermore, GECIs are not well-suited for detecting sub-threshold voltage changes (*i.e.* small changes in the membrane potential that do not cause neurons to fire) or hyperpolarisations resulting from synaptic and neuromodulatory inputs¹⁰⁵.

Voltage indicators, which transduce changes in membrane potential into changes in optical signals, promise to address many of these challenges¹⁰⁶, and tremendous research efforts have been focused on developing bright and sensitive GEVIs^{29,95,107–110}. Detecting single APs requires millisecond recording precision, such that voltage indicators typically necessitate orders of magnitude faster imaging rates than with GECIs (kHz imaging rates). Similarly, the small signals associated with sub-threshold post-

synaptic changes in membrane potential (\sim mV, with respect to \sim 100 mV when an AP is fired) can only be detected using highly sensitive imaging approaches.

To overcome these challenges, optical voltage imaging experiments have generally relied on widefield, 1P illumination and camera detection, to maximize the number of fluorescence photons generated and collected^{111–113}. To approach single-cell resolution, background “crosstalk” from out-of-focus fluorescence has been reduced by using genetic approaches to achieve sparse labelling^{114,115} and/or targeted illumination based on amplitude or phase modulation^{29,116–120}.

As already discussed, to further reduce out-of-focus fluorescence and reach deeper regions, the optical sectioning and longer excitation wavelengths inherent to multi-photon excitation microscopy can be exploited. However, the acquisition rate of conventional 2P-LSM is limited and millisecond transients, such as APs, can only be reliably detected by drastically reducing the FOV^{121–124}. More specialised imaging approaches, based on spatial and/ or temporal multiplexing (in which the laser beam is divided into several beamlets that scan the sample at different spatial locations and/ or with a relative delay of tens of nanoseconds) can record neural activity across much larger areas at kilohertz rates^{93,109,125–129} and can now operate close to the fundamental limit of fluorescence lifetime of the fluorescent proteins used (2–3 ns^{130,131}).

Although classical or multiplexed approaches are valuable for imaging densely packed brain regions such as the hippocampus¹¹⁰, neurons in other brain regions, and in particular, the cell membranes where GEVIs are expressed, generally occupy a small fraction of the total imaging volume, and make classical raster scan trajectories use the finite photon budget inefficiently¹²⁹.

One approach capable of operating beyond this fundamental limit is to exclusively target regions of interest without spending time on dark or non-interesting regions of the sample. A subset of these techniques, random-access microscopy^{91,92} (RAM), commonly uses acousto-optic devices in conjunction with holography to quickly (within \sim 20 μ s) scan the laser beam from one neuron to the next^{94,95} (Fig. 3d). An exciting advancement of these methods demonstrated the use of high-speed 1D phase modulators to increase the point scanning rate of random-access microscopy by almost a factor of seven (down to \sim 3 μ s)¹³². However, methods based on 1D phase modulation currently impose strict symmetry constraints on the output patterns¹³³, and the use of extended patterns to excite fluorescence at multiple points simultaneously results in the generation of out-of-focus fluorescence which can degrade signal-to-background ratio. Recently, deep 2P voltage imaging down to layers 5 and 6 of mouse cortex, was demonstrated at near-kHz frame rate, in a polygon-galvo scanning microscope combined with an adaptive excitation module¹³⁴, which selectively gates photon delivery to regions of interest during full FOV scanning. An alternative targeted voltage imaging approach is based on the combination of holography (using a SLM) with temporal focusing^{135,136}, and high-speed camera detection⁹⁶ (Fig. 3d). This method maintains single-cell resolution, even in scattering tissue, but further characterisation of the fundamental imaging depth as compared with sequential approaches is necessary.

Ultrafast 2P optogenetics

Combining 2P CGH with advancements in fast-photocycle (few ms opening and closing kinetics), somatargeted (*i.e.* whose expression is restricted to the neuron cell body) opsins, has permitted to elicit APs with sub-millisecond precision^{47,48,137–139}, and achieve high spiking rates up to 100 Hz^{138,139}, while keeping near single-cell spatial resolution. This precision and resolution allow the recreation of spatiotemporally precise activity patterns in single or multiple neurons in parallel, closely mimicking the physiological temporal dynamics observed in neural circuits.

However, re-playing different temporal patterns in multiple cells on the ms level is challenging due to the relatively slow refresh rates of liquid crystal-based SLMs that can vary between \sim 20 ms^{43,48,137,139} and 3 ms (or 2 ms in overdrive mode)¹⁶ for the fastest models, limited by the time required for liquid crystal molecules to rotate under specific voltages (Fig. 3c).

Alternative technologies offer faster refresh rates but suffer from other limitations: ferroelectric SLMs¹⁴⁰ can function at kHz refresh rates but only allow binary phase modulation to be generated; digital micromirror devices (DMDs)¹⁴¹ can typically reach >10 kHz but only in binary amplitude modulation, which strongly limits light efficiency in sparse targeting and therefore restricts usage to mainly 1P activation^{142–146}. Recently, MEMS (micro-electromechanical system) technology offering both phase modulation and kHz switching rates in the visible spectrum has emerged¹⁴⁷, and while still in its early stages, future progress is likely to expand its use to the NIR.

Some groups have found workarounds, such as combining an SLM for generating illumination patterns with a DMD acting as a fast shutter for each spot⁹⁰, or tiling an SLM into independent phase masks accessible with an upstream scan unit at over 20 kHz⁸⁹ (Fig. 3c). These techniques require only the addition of a few optical elements (a DMD or a scanner, respectively) to holographic light shaping systems and could be easily implemented in labs already equipped with holographic technology. Increasing illumination reconfiguration speed has enabled the creation of sub-millisecond controlled temporal delays in the successive activation of two cells for the first time with 2P optogenetics⁸⁹, paving the way towards unrestricted playing of neural activation.

A real technological breakthrough for 2P optogenetics would be to develop systems capable of both mesoscopic holographic access (see Section: *Large scale holographic optogenetic photostimulation*) and ultrafast light-shaping reconfiguration, for large-scale and rapid neuronal activation. This might allow for instance to activate neurons in separated but connected brain regions to simulate or intentionally perturb the propagation of neuronal signals (on the ms scale) from one region to the other.

Ultrafast SLMs will not only be highly effective for inducing precisely timed neuronal activity through 2P photostimulation, but, as described in the next section, by taking advantage of the opsin photocycle, they can also help reduce the total power needed to quasi-simultaneously photostimulate large groups of neurons. On the 2P imaging side, techniques that are a mix of parallel and sequential RAMP approaches could be designed with ultrafast SLMs, in which a group of neurons is simultaneously excited before rapidly switching to a different group. Finally, in part B, we will discuss adaptive optics and wavefront shaping approaches to counteract aberrations and scattering and thus, access deeper brain regions, which critically depend on the availability of rapid and stable SLMs.

Scaling up circuit investigation within the limits of the sample

Achieving larger FOVs and faster acquisition speeds, or increasing the number of neurons targeted for simultaneous photostimulation (which can be necessary to induce detectable behavioral changes) often requires higher laser power, particularly in deep and scattering brain tissue, and can result in long and challenging acquisitions. In this section, we will first examine the potential risks of photodamage and photo-induced alterations to the sample, before discussing how leveraging specific properties of the sample can help minimize the required laser power, reduce artefacts, and maximize the overall efficiency and output of these experiments.

Photo-induced damages and artefacts

Among the various types of laser-induced damage and undesired effects we can list thermal damages, non-linear photodamage and artefactual neuronal responses.

Linear or thermal damages result from prolonged linear absorption of light; this is directly related to the amount of energy deposited on the sample, determined by the average power and duration of illumination. This heating is primarily driven by linear absorption of NIR light by biological tissues¹⁴⁸, especially water¹⁴⁹, and although heat is dissipated by blood flow, local or diffuse temperature increases can still occur. Even small temperature variations (<2K) can influence various physiological aspects^{150–154} and larger increases (2-8K) can lead to irreversible damage to the brain tissue, including protein denaturation and cell death^{155,156}. Temperature changes can disrupt the function of proteins

such as opsins and other ionic channels, altering neuronal activity^{157–164}, and have broader implications like unintended behavioural alterations, such as body motion or changes in brain-wide neural dynamics^{165,166}. These effects can ultimately bias experiments. Interestingly, while brain heating is usually an undesired side effect, targeted photoheating of neurons expressing thermosensitive channels can be exploited to modulate neuronal activity, a technique known as thermogenetics^{167–169}. In standard 2P-LSM, using a conventional Ti:Sapphire laser (<200fs, 80 MHz), power levels typically range from a few to around 100 mW, and mouse brain studies have estimated a global brain temperature increase of about 2 K/100 mW¹⁴⁸. For optogenetic activation, low-repetition rate lasers (<300fs, 0.5-10 MHz) with high pulse energy maximize 2P excitation while keeping the power per target down to a few mWs^{16,19,48,138,170}. During multi-cell (~100 targets within a volume of a few hundred cubic microns) photostimulation, simulations predict a global rise of 1K with localized “hot spots” of ~2K confined to a few micrometres and dissipating within milliseconds¹⁴⁹. Therefore, heating threshold can get close to the operational ranges of both imaging and stimulation experiments and can pose a practical limit to the number of neurons that can be investigated. Careful monitoring thermal effects, for instance with experimentally-validated temperature simulation models¹⁴⁹, is essential, along with solutions for mitigating heating, as detailed in the following.

While high-peak power pulses can reduce photoheating, they may cause nonlinear damage due to the intense and localized electric fields they generate. These effects can result in photochemical damage, photoablation of tissues, optical breakdown, cell death, and the release of toxic substances into surrounding tissue, which can alter the overall behaviour of the organism under study^{155,171}. Nonlinear damage has been observed at pulse energies in the range of 10 to 100s of pJ/μm², sometimes only few fold apart from the working power conditions of both 2P imaging and photostimulation^{48,89,172,173}. However, this concern becomes more significant in 3P excitation, which requires even higher peak power levels.

Finally, excitation light can elicit unwanted neuronal or behavioural responses by interacting with other photosensitive elements in the organism, such as photoreceptors in mammalian retinas, which can be activated by NIR light¹⁷⁴, or fish larvae that detect certain NIR wavelengths and exhibit light-avoidance behaviour as a response¹⁷⁵.

Experiment optimization leveraging the properties of the sample

Specific properties of neurons in the brain, of activity indicators (GECIs and GEVIs) and opsins can be exploited to reduce laser power, minimize measurements, and shorten or simplify recordings. This not only reduces photodamage, but also improves experimental throughput and decreases data size to be stored and processed. We will now present practical examples that take advantage of the spatiotemporal sparsity of neural activity and connections, as well as the slow opsin photocycle. In addition to optimizing optical strategies, it is important to highlight that continuous developments in GECIs, GEVIs and opsins^{2,59,176} are also essential for significantly reducing laser power requirements and minimizing photodamage.

Leveraging spatiotemporal sparsity for functional imaging

As discussed earlier (Introduction and Section: *kilohertz 2P voltage imaging*), neurons in some brain regions are sparsely distributed, and their activity can be sparse in both space and time. This makes conventional point-scanning inefficient, often recording from inactive regions, which slows down imaging speed and unnecessarily inflates data size. Spatiotemporal sparsity can be leveraged to optimize and speed up functional imaging using two key strategies:

(1) *Exploiting structural spatial sparsity* by restricting imaging to voxels of interest rather than raster scanning the full FOV. This reduces the number of measurements and thereby increases imaging speed and reduces data size, while also lowering energy deposition on the sample; RAMP techniques^{91,92,177} use this principle. However, its overall speed and signal-to-noise ratio (SNR) remain constrained by the sequential nature of target-by-target sampling.

(2) *Utilizing functional spatiotemporal sparsity* to allow reconstruction of individual activities from imaging where the full FOV is captured in fewer measurements using spatially extended point spread functions (PSFs). These parallelized sampling methods fall into two main categories: (i) scanning spatially extended point spread functions (PSFs) with single-pixel detectors (i.e. PMT) (reviewed in refs^{30,58,178}), or (ii) using scanless illumination with multi-pixel detectors (i.e. camera). In the first case, the scanned PSF can be an engineered single point (e.g., a Temporally-Focused low-NA Gaussian spot¹⁷⁹, a Bessel beam¹⁸⁰, a V-shaped PSF¹⁸¹), a line⁹³, or multibeam illumination (such as multiplexed sets of points distributed in 3D for multi-plane imaging⁹⁸). A drawback of the approaches above is their reduced spatial resolution and increased crosstalk between emitters, simultaneously recorded by the single detector. In scanless imaging^{26,96,182,183} instead, the camera preserves spatial information about emitters. However, as imaging depth increases, scattering progressively disrupts this spatial encoding and leads to signal loss.

In both cases, demixing algorithms^{184–186} can help mitigate these issues by using known fluorescent dynamics of activity reporters and brain activity sparsity to separate overlapping signals. Such approaches have successfully reconstructed fluorescent transients from highly intermixed signals, like scattering patterns through multimode fibers¹⁸⁷ or diffusing tissues¹⁸⁸. Interestingly, the combination of dynamic illumination patterns and temporal sparsity may further improve demixing performances^{116,189,190}. Moreover, as the field transitions from calcium to voltage imaging—where fluorescent transients are faster and more temporally intertwined—these demixing methods will become even more critical.

Leveraging sparse connections and functions for circuit photostimulation

2P optogenetic photostimulation can be used to selectively activate or silence even one individual neuron within an ensemble. While cell-by-cell photostimulation can help identify neuronal functions and map synaptic connections, scaling this approach to larger circuits (involving thousands of neurons) remains challenging and often inefficient, as it requires many measurements.

A key example is synaptic connectivity mapping. Neurons communicate through synapses, where activation of a pre-synaptic neuron generates an electrical signal in the post-synaptic neuron if they are connected. Sequentially photostimulating (one-by-one) hundreds of potential pre-synaptic cells while recording (with an electrode) from a single post-synaptic neuron can partially map the functional connectivity of local circuits^{47,49,191–196}. Yet, this method is inefficient due to the sparse nature of synaptic connections, leading to many photostimulations that fail to evoke a response in the post-synaptic cell.

To overcome this inefficiency, similar to parallelized imaging, group testing approaches have been proposed^{197–199}. Instead of stimulating neurons one by one, multiple neurons are activated simultaneously to integrate their inputs on the post-synaptic neuron. This approach, recently validated experimentally^{194,196,200}, combined with signal reconstruction techniques, is an example of compressed sensing²⁰¹, and can more efficiently probe the full population. By reducing the number of required stimulations, this approach enables faster network mapping with fewer recordings, making it also particularly useful when the effects of single-cell activation are subtle or challenging to detect. As pioneering studies of visual encoding¹⁵, locomotion²¹, and sensory modulation^{12,18–20} have demonstrated, precise multicell photostimulation will likely become a standard tool in Neuroscience.

Exploiting the opsins photocycle for power-efficient multi-cell photostimulation

Unlike fluorophores, which have nanosecond relaxation times, opsins exhibit a slower photocycle, staying open for several milliseconds after excitation. Leveraging this characteristic, along with the ability to generate rapid holographic stimulation patterns (see Section: *Ultrafast 2P optogenetics*), a novel cyclic illumination protocol has been developed to maximize the number of activated cells within a fixed power budget⁸⁹. Instead of splitting the laser power across all targeted neurons, subgroups are activated sequentially and the illumination is delivered in short bursts (50 μ s) to each subgroup. Due

to their slow relaxation, opsins in the first subgroup remain active while the laser moves to the others. By cycling back and repeating this process, all neurons can spike nearly simultaneously, while the overall power consumption is significantly reduced compared to simultaneously targeting the entire neuronal ensemble⁸⁹.

To conclude part A, we have discussed challenges and perspectives for increasing the FOV and speed of photostimulation and imaging. A clear path for future developments is to merge together the efforts towards larger FOV and faster performances, both for 2P imaging and 2P photostimulation, which often advance in parallel without being implemented in the same platform. As we have seen in this section, the very nature of the sample under study will have to be considered to design specific strategies that minimize tissue damage and optimize recordings.

Part B. Accessing deep brain regions

Brain tissue challenges light propagation due to absorption and scattering. With increasing depth z within the tissue, the light intensity $I(z)$ decreases exponentially^{31,202}:

$$I(z) \propto e^{-z/\ell_e}$$

where ℓ_e is the extinction length, defined as $\ell_e = \ell_{\text{abs}} + \ell_s$, with ℓ_{abs} and ℓ_s representing the absorption and scattering length, respectively. Absorption in biological tissues is mainly due to water, but for wavelengths shorter than ~ 1400 nm, the extinction length is primarily dominated by scattering.

Compared to the visible spectrum, longer, NIR wavelengths experience less scattering ($140\mu\text{m} < \ell_s < 260\mu\text{m}$ for $800\text{nm} < \lambda < 1100\text{nm}$ compared to $\ell_s < 110\mu\text{m}$ for $\lambda < 700\text{nm}$ ²⁰³) and are thus beneficial for deeper all-optical experiments. This advantage can be exploited by using red-shifted calcium indicators or optogenetic actuators (opsins), though spectral cross-talk between the two must be considered^{48,204,205} to be combined in all-optical experiments. Switching to 2P excitation, which uses NIR lasers and provides increased axial confinement, is often the best choice for precise all-optical experiments in the scattering mouse brain³¹.

However, the depth at which 2P microscopes can effectively image is constrained by a loss of contrast linked to the appearance of out-of-focus fluorescence as the excitation power is increased to compensate for depth loss^{206–208}. For the mouse brain, this generally limits 2P functional imaging to 0.6–0.7mm below the surface with green calcium indicators^{209–212} and slightly deeper, up to 0.85mm with red-shifted calcium reporters²¹³, overall limiting experiments to the upper layers of the cortex.

To reach deeper brain regions, different and complementary strategies have been pursued: 1) transitioning towards even longer excitation wavelengths by switching to a three-photon (3P) excitation regime; 2) correcting scattering-induced wavefront deformations with adaptive optics and wavefront shaping; 3) implanting minimally invasive devices to relay light from the surface to the deep brain regions of interest.

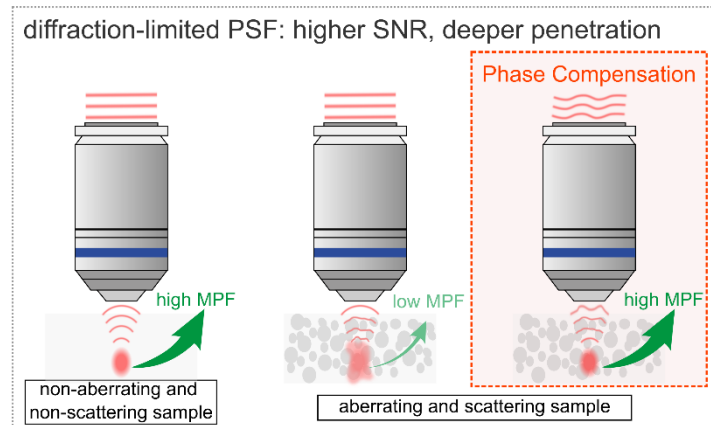
Three-photon excitation microscopy.

Three-photon excitation microscopy (reviewed here^{214,215}; Fig. 4a) enables deeper brain access by using longer wavelengths for excitation, and by further reducing out-of-focus excitation thanks to its higher non-linearity. In the NIR range, wavelengths around 1300 nm and 1700nm offer optimal scattering/absorption trade-offs ($\ell_e \approx 250\text{--}300\mu\text{m}$ at 1300nm; $\ell_e \approx 400\mu\text{m}$ at 1700nm)^{203,216,217}, and also align with the tripled frequencies of green and red-emitting fluorophores.

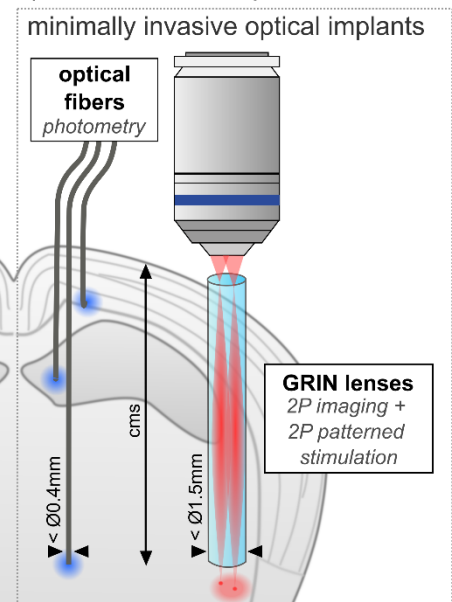
Due to the low 3P action cross-sections of fluorophores²¹⁸, 3P imaging has only been possible thanks to the development of low-duty cycle amplified lasers ($\sim 1\text{MHz}$, sub-100 fs, pulse energies in the hundreds of nJ) operating in the 1300/1700nm spectral regions²⁰³. In vivo 3P calcium imaging using 1300nm excitation of GCaMP has been demonstrated²¹⁹ and widely adopted^{211,220–222}, notably allowing imaging through all cortical layers and reaching the hippocampus at a 1mm depth in the mouse brain.

Similarly, 1700nm excitation of red-shifted GECIs (jRGECOs)¹²⁹ has enabled deep cortical imaging in the mouse brain (up to $z=0.75\text{mm}$). However, despite improvements²¹³, red-shifted indicators remain several times dimmer than GCaMP, which limits their maximal fluorescence recording depth. Unlike 2P imaging, which is limited by contrast loss at depth, 3P imaging maintains minimal background noise at greater depths due to its higher order of non-linearity^{216,223,224}, but is rather limited by challenges in experimentally generating and/or collecting sufficient signal, and/or tissue heating¹⁷⁸. Theoretically, 3P microscopy at 1300 nm and 1700 nm could maintain contrast up to 9 extinction lengths (ℓ_e)^{203,225} (approximately 2.5-3.5mm depth). Experimentally, however, maximum reported imaging depths are typically around $5\ell_e$ ^{226,227} with bright dyes or quantum dots, and drop to about $4\ell_e$ ^{211,222,228}, and $2\ell_e$ ¹²⁹ with green and red GECIs, respectively, owing to their lower brightness.

a) Adaptive Optics and Wavefront Shaping



b) Microendoscopy



c) Three-Photon Microscopy

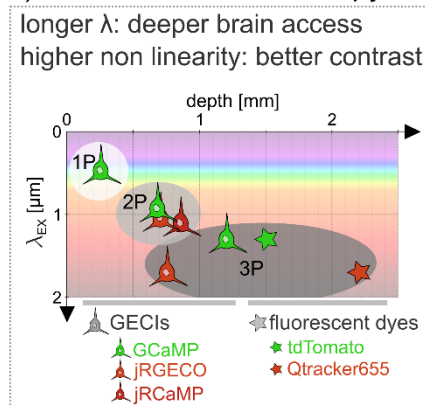


Figure 4. Strategies for deeper brain access.

a) Adaptive Optics. In absence of aberrations, a diffraction-limited focal spot is formed in a point-scanning microscope, leading to high multi-photon fluorescence (MPF) generation. Inside a scattering medium such as brain tissue, mismatches in the refractive index distort the wavefront, resulting in a distorted, enlarged focus and reduced MPF. Pre-shaping the wavefront to compensate for tissue aberrations allows for the recovery of a tight focus and high MPF. **b) Micro-Endoscopy.** Minimally invasive optical implants enable optical access to brain regions at centimetre depths. Thin optical fibers ($< \varnothing 0.4\text{mm}$) can record fluorescence from a specific region (1P photometry) and are multiplexable. GRIN lenses ($< \varnothing 1.5\text{mm}$) can be coupled to a 2P all-optical system to perform 2P point-scanning imaging and 2P patterned optogenetic stimulation. **c) Three-Photon Excitation Microscopy.** Longer NIR

wavelengths and higher-order non-linearity help maintain imaging contrast at millimetre depths. Maximum recorded imaging depths for GECIs under 1P, 2P and 3P excitation and different excitation wavelengths are shown. For comparison, maximum imaging depths of fluorescent dyes and quantum dots under 3PE are also represented.

Enhancing the brightness of GECIs or developing functionalized quantum dots for calcium sensing²²⁶ could extend 3P calcium imaging depths within the $5\ell_e$ limit achieved by dyes and quantum dots. Complementary strategies to enhance fluorescence generation include optimizing system transmittance (with customized optics²⁰³, appropriate immersion media²²⁹, underfilling the pupil of high NA objectives²³⁰) and employing adaptive optics^{231–234}. Photon budget can also be optimized by using Adaptive Excitation Sources (AES)¹²⁹, which synchronizes laser pulse delivery with pixels of interest during raster scanning of the FOV. AES have significantly boosted fluorescent signals while keeping average powers—and thus temperature rises—low. This approach holds significant potential for addressing both heating challenges and the low imaging frame rates in raster scanning configurations, which are limited by the ~ 1 MHz repetition rates of laser sources in 3P microscopy. On the fluorescence detection side, there is great potential for improving photon collection efficiency, with an estimated three-fold margin for enhancement²³⁵. Strategies for optimizing detection efficiency include using low-magnification high-NA objective lenses^{236,237} and specialized PMTs²³⁸ designed for 3P microscopy.

As of today, 3P microscopy is primarily used for imaging of neurons and neuronal activity. Parallel developments aimed at reaching greater depths for optogenetic photostimulation may in the future extend all-optical experiments to the deepest regions of the mouse cortex. However, 3P optogenetic photostimulation²³⁹ might be limited by the higher energy demands of optogenetic activation compared to point-scanning imaging. Such experiments could benefit from the development of lasers with higher deliverable energies.

Adaptive optics, wavefront shaping

Light focusing within deep brain tissues is degraded by optical aberrations and scattering, both caused by refractive index and surface inhomogeneities (see Fig. 4a). These effects broaden the excitation PSF, resulting not only in reduced spatial resolution but also in decreased focal intensity, and consequently diminished fluorescent signal in multiphoton microscopy, particularly for higher-order processes²⁴⁰. Compensating for this focal intensity loss by increasing power can heighten the risks of linear and non-linear damage, while the enlarged PSF can also lead to signal contamination from structures outside the diffraction-limited spot during deep calcium imaging experiments^{241,242}. Although scattering and optical aberrations both impact focus, resolution, and contrast, they differ in their compensation challenges in biological tissue. Optical aberrations arise from smooth, low-frequency refractive index variations over larger spatial scales, typically caused by structures larger than the wavelength of the NIR laser, such as brain layers or blood vessels²⁴³, and can be corrected using adaptive optics. In contrast, scattering results from high-frequency, fast variations in the refractive index caused by structures comparable in size to the wavelength of light (e.g. cells, nuclei, organelles etc.)²⁴³. This leads to a speckle pattern – i.e. a deterministic interference pattern from randomly distributed coherent sources – that is much harder to compensate for using traditional correction methods and that poses a significant challenge in today's research.

Correcting optical aberrations: Adaptive Optics

Originally developed for astronomy²⁴⁴, Adaptive Optics (AO) has proven highly effective in correcting aberrations in multiphoton microscopy, resulting in enhanced contrast and diffraction-limited imaging at increased depths (typ. maximum 0.7mm in 2P²⁴⁵, 1.2mm in 3P^{231–234}). While large structures (e.g., neuronal bodies $\sim 10 \mu\text{m}$) partially compensate for the reduced intensity caused by PSF enlargement due to the excitation of more fluorophores, this effect critically limits the imaging depth for smaller

structures^{242,246} (e.g., dendrites, spines). AO operates by measuring aberrations and dynamically compensating for them using a wavefront corrector, such as an SLM or a deformable mirror. Over the past few years, numerous AO implementations have been proposed and applied to brain imaging (see review in ref.^{244,247,248}). They can be broadly categorized depending on whether they rely on direct or indirect wavefront sensing techniques. Briefly, direct methods typically employ a Shack-Hartmann wavefront sensor to measure in a single shot the distorted wavefront originating from a spatially coherent "guide star", e.g. formed by the 2P excitation of a red-shifted dye^{242,245,249–251}. Indirect methods, a.k.a. 'sensorless' methods, estimate the aberrated wavefront by sequentially adjusting the pattern on the wavefront corrector to maximize a focusing metric (e.g. by monitoring 2P fluorescence signals), by means of an optimisation generally performed through a zonal (e.g. pupil segmentation^{252,253}) or a modal approach (e.g. Zernike modes scan^{254,255}).

Direct methods are fast, provide high measurement accuracy for optimal correction, and can be used with time-varying fluorescent signals, such as those in calcium imaging²⁵⁶. In contrast, indirect methods do not often require guide stars, are more robust to scattering, and are simpler to implement since they only require a wavefront corrector. Moreover, the recent development of wavefront correctors that work in transmission^{257,258} is expected to further promote the dissemination of AO in Neurophotonics. These devices eliminate the need for additional beam-folding optics and can be directly placed at the pupil of the microscope objective, making integration easier. Although these correctors are relatively slow (typically few ms) and limited in the number of modes they can address, they are sufficient for correcting low order aberrations which can be considered as quasi-static in microscopy and can be described typically by 7-11 Zernike radial orders²⁴⁴.

Correcting scattering: Wavefront Shaping

However, it should be emphasized that the correction of smooth, low-order aberrations can only enhance ballistic contributions. Yet, at depths higher than the scattering length ℓ_s (typ. $\ell_s=150\ \mu\text{m}$ at λ_{2P} , and $\ell_s=300\text{-}400\ \mu\text{m}$ at λ_{3P} in the brain), scattered light becomes predominant. It typically accounts for more than 99% of the deposited energy at depths beyond $5\ell_s$. Over the past decade, significant advances have been made in the development of techniques for understanding and controlling light propagation in complex media (see review^{202,259}). In particular, "wavefront shaping" holds the promise of harnessing scattered photons to enable deep imaging in brain tissues, overcoming the limitations imposed by the exponential attenuation of ballistic photons with increasing depth. It involves not only compensating for low-order aberration as in conventional AO, but also correcting the high-order wavefront distortions – mainly composed of optical vortices²⁶⁰ – induced by multiple scattering. Performing such phase correction²⁶¹ using a non-linear optical feedback²⁶² is particularly challenging since (i) it requires probing/controlling wavefront distortions that involve thousands to millions of spatial modes to focus light. Additionally, (ii) to reach optimal performances, the phase compensation must be carried out faster than the speckle decorrelation time which corresponds to the time at which the wavefront loses correlation with its earlier state (typ. below $\sim 1\text{ms}$ at millimetres depth in living mouse brain²⁶³). Note that correcting more persistent modes is still possible but comes at the cost of reduced signal enhancement²⁶⁴. Finally, (iii) the scattering compensation is only effective over a limited FOV determined by the angular memory effect range, which is related to the intrinsic isoplanatism of the scattering process (typ. from tens of μm at shallow depth to the size of a speckle grain at large depth). Performing imaging through scattering media on a large FOV ideally requires estimating the so-called "Transmission Matrix" (TM), which linearly relates the input field to the output field^{265,266}. A recent study²⁶⁷ has demonstrated the possibility of measuring the TM using a 2P signal, a computational framework, and a single-pixel detector (e.g. a PMT). This represents a significant advancement over traditional camera-based strategies, which generally lack the sensitivity for deep imaging in strong multiple scattering regime.

Over the past few years, significant efforts have been made to address this challenge in the context of multiphoton brain imaging²⁵⁹. Briefly, indirect, iterative, interferometric methods such as IMPACT²⁶⁸, F-SHARP²⁶⁹, α -FSS²³⁴, DASH²⁷⁰, have already demonstrated impressive 2P and 3P signal enhancement

(typ. 1-2 order of magnitude) *in vivo*, but mainly at moderate depth (*i.e.* in an intermediate scattering regime) in brain tissue or through the intact skull (*i.e.* through a static scattering medium). Moreover, conjugated²⁷¹ and multi-pupil²⁷² correcting strategies have proven relatively efficient at extending the corrected FOV to a certain extent, but innovative solutions are required for larger-scale correction. Considering the giant number of TM modes that must be probed for large-scale correction in the multiple scattering regime, strategies based on random access – which exploit neuronal sparsity – should be prioritized, as they minimize the number of isoplanatic patches requiring measurement and correction. A recent approach²⁷³ combining fast (40 kHz) AOD-based wavefront shaping with 3D random-access scanning has shown great promise for providing fast, iterative multi-patch correction in transcranial imaging. However, despite important speed improvement, these indirect methods remain iterative, requiring multiple SLM updates for each patch, keeping them well below the potential performance limits of current SLM refresh rates. In contrast, a single-shot “digital optical phase conjugation” method has been recently demonstrated in model sample using 1P fluorescence guide stars²⁶⁰, by exploiting the large spectral bandwidth of forward multiple-scattering media²⁷⁴ along with a high-resolution wavefront sensor capable of reconstructing speckle fields²⁷⁵. Extending this approach to two-photon guide stars and coupling it with multiplexed wavefront sensor schemes²⁷⁶ presents an intriguing prospect for probing multiple isoplanatic patches in a single-shot. Across these strategies, the availability of an ultra-fast SLM²⁷⁷ (typ. 0.1-1MHz) with a high number of modes and working in the NIR would be a true game changer, significantly accelerating measurement in feedback-based methods and/or speeding up compensation in various correction strategies.

Minimally invasive implants: GRIN lenses and fibers and wavefront shaping.

Many behaviourally relevant brain structures lie below 1 mm inside the brain²⁷⁸, beyond the current reach of optimized (3P, AO) microscopes. Presently, the only viable approach to get optical access to them is the implantation of a relay system (Fig. 4c) that has to be minimally invasive, while ensuring access to a sufficiently large FOV and to high quality optical recordings. There are two main families of widely used relays: gradient refractive index (GRIN) lenses, and optical fibers (Fig.4b).

GRIN lenses are small cylinders of glass (diameter < 1.5 mm, several mm long), which serve as imaging relays^{279,280}. Their main drawback is their large optical aberrations that eventually limit the accessible FOV to a size smaller than the GRIN lens diameter. Proposed solutions include adaptive optics²⁸¹⁻²⁸³ and correction lenses at the GRIN lens entrance^{284,285}. Commercial GRIN lenses (for instance from Grintech, Ref.²⁸⁶) can offer field and chromatic corrections, at the cost of larger diameters and increased invasiveness. GRIN lenses have been used for 2P all-optical experiments with CGH in both superficial²⁸⁷ and deep^{14,288} brain regions. Advanced techniques have increased the available FOV, through using multiple GRIN lenses, coupled to a single objective, to simultaneously study several brain regions⁷³, or through a GRIN lens-micropism assembly that give access to full panoramic views of an entire brain column²⁸⁹. Micropism assemblies, recently extended for deeper brain access^{290,291}, offer a lower-aberration alternative to GRIN lenses.

Using optical fibers to guide the light has the advantage of being truly minimally invasive, as typical fiber diameters are in the range of 50-400 μm ^{278,292}. Fiber photometry experiments, in which all the cells expressing an activity reporter are simultaneously excited and detected through the fiber^{278,292}, or fiber optic widefield 1P optogenetic photostimulation are a relatively common technique in Neuroscience. These experiments can be improved by using multiple fibers²⁹³ and by engineering the fiber tip and exploiting plasmonic effects to enable optical access to different points within the same fiber^{294,295}.

By using SLMs and wavefront shaping²⁰², it is possible to turn a multimode optical fiber (MMF) into an imaging device^{296,297}, which has recently allowed researchers to record morphological images and neuronal activity in very deep brain structures²⁹⁸. In this case, wavefront shaping techniques, similar to the ones described above in the context of scattering, allow researchers to focus and scan a laser

beam through the MMF to construct an image. In the future, shaping two different lasers with separate SLMs could allow simultaneous imaging and photostimulation.

A limitation of these approaches is their sensitivity to fiber bending and deformations, which has so far limited their use to static fiber conditions. As we will detail in the next section, optical fibers could be the ideal platform for both deep brain (thanks to their small footprint) and studies in freely moving animals (exploiting their flexibility). However, wavefront shaping through fibers in dynamic conditions has so far remained elusive. As different groups are currently tackling this problem^{299–302}, we expect that powerful solutions will emerge in the near future.

Part C. Freely moving mice

The all-optical techniques described so far are restricted to the use of head-restrained animals, which limits behavioural studies. Understanding how neuronal circuits affect certain types of behaviour, necessarily calls for new methods that should be capable of studying animals engaged in naturalistic behavioural tasks. Recent efforts focus on developing lightweight (< 5g) miniaturized wearable systems for optically studying neuronal activity in freely moving rodents (for comprehensive reviews, see Ref^{303–305}). Many of those systems have been only used for calcium imaging, with few notable example of all-optical experiments^{24,25,306}. Miniaturized optical systems fall in 3 main families (Fig. 5).

1P Miniscopes are complete microscopes that fit on the animal's head, featuring miniaturized LEDs and CMOS cameras. They share the aforementioned advantages and drawbacks of 1P microscopes: they are a cost-effective solution, offer large (up to 5-10 mm) FOVs^{75,307,308} at high acquisition rates (up to 500 Hz³⁰⁹), but are limited in penetration depth and affected by high fluorescence background due to poor z resolution. To extend miniscopes to all-optical studies, a new system was proposed²⁵, utilizing an optical fiber to transmit visible laser light from the optical table to the animal head and a miniaturized DMD for patterned optogenetic photostimulation with near single-neuron resolution. 1P miniscopes are already routinely used in combination with GRIN lenses to reach deep brain regions in freely moving mice. To minimize invasiveness, it was recently proposed¹⁸⁷ to implant a short (8 cm) optical fiber instead of a GRIN lens and detect the fluorescence from GECIs backpropagating through the fiber with the miniscope camera. By using non-negative matrix factorization algorithms, it could be possible to temporally demix neuronal activity traces as each neuron would produce a recognisable spatial fingerprint on the camera. Going a step further, and making use of a miniaturized DMD²⁵, in the future it might become possible to perform wavefront shaping directly at the animal head through the same short optical fiber to focus a visible laser beam to the locations of choice. In this way one could at the same time record demixed calcium activity traces and photostimulate neurons with the DMD, all in a compact and cost-effective device, that would have the advantage that with short fibers almost completely implanted, the risk of wavefront distortions due to fiber bending could be minimized. Another innovation in portable, real-time, large FOV imaging is the 1P masked-based lens-less miniscope technique³¹⁰, which substitutes bulk optics with a thin optical mask and additionally provides scanless volumetric access.

Miniaturized Multiphoton Microscopes utilize single-core optical fibers to transmit the NIR laser beam from the optical table to a head-mounted microscope equipped with miniaturized optics and 2D scanners (mostly MEMS^{222,311}, but also fiber scanner³¹²); fluorescence is also fiber-collected and detected by synchronized PMTs. They offer high-resolution 2P^{311–313} and 3P^{228,314} calcium imaging with FOVs up to ~ 1mm³¹³ and frame rates <50 Hz, and potential z-scanning using miniaturized tuneable lenses³¹¹. A key limitation of these devices is that they have not yet been coupled to 2P optogenetic photostimulation. A possible solution could be to develop a miniaturized phase-only SLM, for instance based on reconfigurable thermo-optics^{315–317} or metasurfaces³¹⁸ to be placed directly at the animal head after the fiber. Most SLMs usually operate in reflection mode, such that integrating them into an optical system demands the optical path to be folded, thus increasing weight and volume. Thermo-

optics and metasurfaces instead, can operate in transmission, which is very appealing to develop highly compact and low-weight devices.

Fiber Bundle-based Microscopes utilize multi-core fibers, also known as fiber bundles, consisting of thousands of individual cores (diameter of 2-10 μ m), enabling them to function as imaging systems. They relay optical signals between the optical table and a miniaturized objective (e.g., GRIN lens) on the animal's head. Typical elements for 2D imaging (standard galvo scanners) and patterned optogenetic activation (SLMs) remain on the optical table (except for z-scanning tuneable lenses^{319,320}) and do not require miniaturization. The accessible FOV depends on the bundle's diameter (up to 1.5mm) and the optical system's magnification at the fiber output. These microscopes support both 1P^{24,321,322} and 2P^{306,319,320} imaging, as well as 2P CGH using an SLM before the fiber that has recently demonstrated optogenetic activation with single-cell precision in freely moving mice³⁰⁶.

We expect performance to greatly benefit from novel bundle architectures, such as bundles with a larger diameter and higher core number, which must still be flexible enough to allow animals to freely move. In this sense, leached fiber bundles, which lack a shared clad between all the cores, could be a potential solution to maintain flexibility, but to our knowledge they are only produced in standard lengths/diameters by two manufacturers (Schott, Sumita), with little or no customization available. Finally, similar to what described in the previous section for multimode fibers, wavefront shaping methods through fiber bundles are also capable of focusing laser light with no additional micro-optics^{302,323,324}. At the same time, imaging through fiber bundles using holographic detection and computational reconstruction methods are also being extensively investigated^{300,325,326}. Hybrid approaches that leverage on wavefront shaping and computational methods to enhance existing fiber bundle-based microscopes could be a way to explore in the future.

It is foreseeable that research towards freely moving studies will in the future merge with that of minimally invasive components to reach deeper brain regions (Section: *Minimally invasive implants: GRIN lenses and fibers and wavefront shaping*). In order to rapidly advance with both, it is necessary to invest in the broad availability and improvement of miniaturized components. High resolution 3D printing is a promising way to fabricate aberration corrected miniaturized optics, even on the tip of optical fibers, but are so far restricted to only a handful of research groups³²⁷⁻³³². Tunable metasurfaces^{99,100} designed from the beginning for neurophotonics applications might provide extremely valuable components to best study neuronal circuits in freely moving animals.

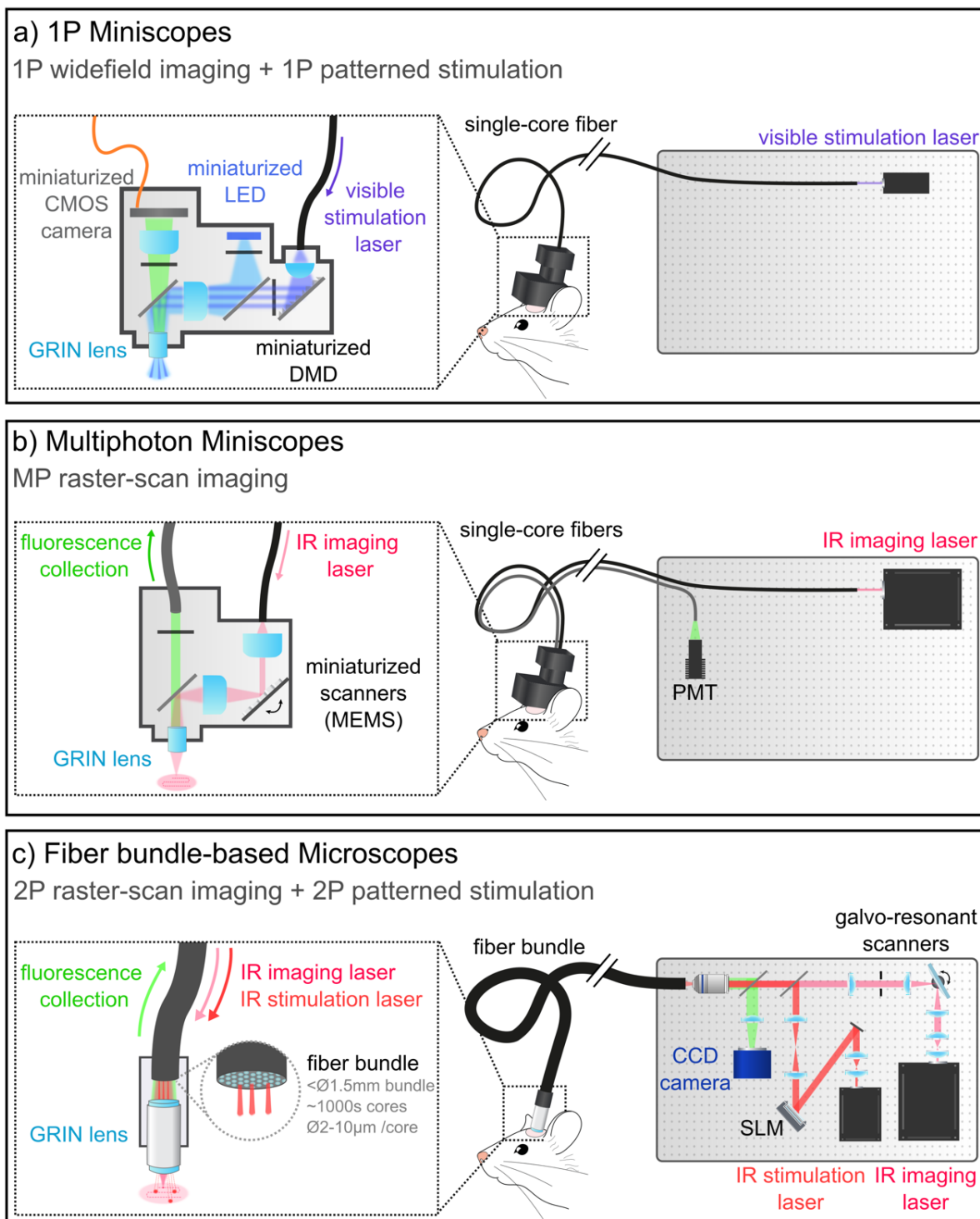


Figure 5. Optical systems for all-optical experiments in freely moving mice.

This figure illustrates miniaturized microscopes (centre), with a detailed view of the optical components on the animal's head (left) and those remaining on the optical table (right). **a)** 1P miniscopes for functional imaging are fully mounted on the animal's head and include miniaturized LEDs and CMOS cameras. Some systems incorporate 1P patterned illumination (1P MAPSI²⁵) for optogenetic stimulation by integrating a Digital Micromirror Device (DMD) and relaying a visible laser from the optical table to the miniscope using a single-core fiber. **b)** In 2P Miniaturized Microscopes, the NIR imaging laser is delivered via fiber to miniaturized scanners (MEMS) on the miniscope for 2P point-scan imaging. Fluorescence is collected through another fiber and detected by a PMT. Currently, 2P miniaturized microscopes do not support 2P patterned optogenetic stimulation. **c)** In Fiber Bundle-based

Microscopes, standard optical systems for 2P point scanning (galvo-resonant scanners) and 2P patterned optogenetic stimulation (SLM) are located on the optical table. Both lasers are relayed to a GRIN lens on the animal's head via a fiber bundle, which also collects fluorescence.

Conclusions

All-optical systems that combine the recording of neuronal activity with controlled optogenetic perturbation offer highly promising methodologies for neuroscience research in small animal models. As optical techniques rapidly evolve, this manuscript has focused on highlighting emerging advancements and required improvements in key technological components and approaches. While this review has not primarily focused on the development of indicators or actuators, it is important to emphasize that optics alone will not be sufficient to address all the challenges faced by neurophotronics. Advancing the field will require the development of more sensitive and soma-targeted opsins, brighter and more reliable indicators for calcium and voltage, and the minimization of spectral crosstalk between opsins and indicators. These represent critical areas for improvement that will have a significant impact on the future of Neurophotronics. In what follows, we summarize some of the key technological advancements and challenges discussed in this manuscript:

Commercialization of State-of-the-Art Techniques

The commercialization of large and advanced technologies developed in specialized labs is critical for broader adoption in research environments with strong biology and neuroscience expertise but less familiarity with complex optics. While 2P all-optical microscopes are becoming more accessible, new key technologies require either all-in-one solutions or modular components that can be integrated into existing systems. In microscopy, the commercialization and widespread adoption of 2P mesoscopes for ultra-wide calcium imaging and kHz imaging modules would mark a significant advance. A breakthrough solution would be a multi-functional microscope capable of seamlessly handling large FOV, kHz speeds, 2P-3P imaging, and freely moving configurations. On the laser side, current offerings meet key needs with powerful Ytterbium-doped laser amplifiers for multi-cell 2P optogenetic activation and optical parametric amplifiers (OPAs) for 3P microscopy. However, commercialization of AES (Adaptive Excitation Source) technology as an integrable module for deep 3P imaging would further extend capabilities, and stronger 3P laser sources may still be required for deep all-optical experiments. Tuneable high-power lasers, such as OPAs, that cover the full wavelength range used in 2P optogenetics (approximately 800-1200 nm) could improve spectral opsin matching³⁷, thereby reducing power demands and minimizing heat generation during multi-cell stimulation.

Optimization of SLMs and off-the-shelf optical components

As we have seen throughout this manuscript, phase-only SLMs are likely one of the most critical optical elements for all-optical brain neurophotronics. Researchers need larger-screen SLMs with more pixels to extend FOE for on/off activity modulation in optogenetics and higher-speed SLMs (>kHz) for naturalistic optogenetic activity replay, random access microscopy, scattering correction and compressed sensing strategies. Miniaturized SLMs working in transmission using thermo-optics or metasurfaces would enable compact systems for freely moving animal experiments. It is also key to optimize the performance, accessibility and customization possibilities of standard optical components (e.g., specialized PMTs and objectives for 3PM, low-aberration GRIN lenses), and miniaturized optical components (e.g., MEMS scanners, DMDs, tuneable lenses, filters, detectors). Miniaturized custom optics can also be produced using advanced 3D printers, such as Nanoscribe^{330,331}; however, these printers are currently prohibitively expensive, making it inefficient for each lab to own one. Therefore, establishing more companies that offer custom design services would significantly enhance accessibility. Fiber optics are increasingly used in microscopy and offer crucial advancements for multi-region imaging, deep tissue imaging, and flexible systems for freely moving experiments with

maintained precision, as well as multi-colour light patterning. For further progress, research labs require the development of custom fiber such as large-diameter bundles with more cores, bend-resilient fibers for wavefront shaping, and higher NA multimode fibers for improved signal collection.

Advancements in software and data methodologies

Advancements in software and signal reconstruction algorithms are essential for maximizing the impact of all-optical experiments. Demixing algorithms could revive the use of 1P techniques in mini-, micro- and meso-scopes, particularly for large-field, fast imaging (e.g., voltage imaging); and extend the depth limits of standard multiphoton and fiber-bundle-based microscopes. As data volumes grow, developing robust pipelines for processing large datasets will be critical. Equally important is providing open access to this data, enabling other research groups to analyse it or use it to create computational models, fostering greater collaboration and accelerating discoveries. Additionally, integrated software and hardware solutions to implement fast and optimized multi-cell stimulation protocols will facilitate large-scale network analysis with minimal data and reduced photodamage.

We believe that advancements in these areas will be crucial for driving the next wave of progress in Neurophotonics. These innovations will not only enhance the precision and capabilities of optical techniques but also spur new discoveries in Neuroscience, ultimately deepening our understanding of brain function. They will enable establishing precise correlations between brain activity and complex behaviours (e.g., social interactions or motor behaviours) in natural, freely-moving conditions. Moreover, advancements in micro-endoscopy, adaptive optics, and multiphoton microscopy will allow exploration of deep brain structures involved in higher-order cognitive functions like memory and decision-making. High-speed recordings, in particular the emerging field of voltage imaging, along with millisecond-precise optogenetic manipulation, could help resolve the long-standing debate on whether information in the brain is temporally encoded in the form of spike timing or spike frequency. Finally, large-field-of-view imaging will enable full-brain or even full-animal studies in small organisms (like *C. elegans* or zebrafish), shedding light on long-range connectivity and inter-regional communication.

Funding Sources

The authors acknowledge support from HORIZON EUROPE European Research Council (DEEPER, 101016787, C.T. and E.P.); European Research Council (HoloVis ERC2019-ADG-885090, C.T.); National Institutes of Health (1RF1NS128772-01, C.T. and R.S.; 1R01NS136027-01A1, R.S.); the Agence National de la Recherche (PEMGet M22JRAR039, G.F.); the Institut Universitaire de France (P.B.); the IHU Foresight 2024 ('HOLOCO', D.T); Sorbonne University ('PARSEC', EMRG-10/2023, D.T.); the European Union (European Research Council, ERC) under grant agreement No 101116227 (2P-BRAINSCOPY project, N.A.). Views and opinions expressed are however those of the author(s) only and do not necessarily reflect those of the European Union or European Research Council (ERC). Neither the European Union nor the granting authority can be held responsible for them.

Acknowledgments

The authors thanks all the Emiliani group and Hilton B. de Aguiar for fruitful discussion, as well as Clément Molinier for providing the cover art image.

References

- (1) Tian, L.; Hires, S. A.; Mao, T.; Huber, D.; Chiappe, M. E.; Chalasani, S. H.; Petreanu, L.; Akerboom, J.; McKinney, S. A.; Schreiter, E. R.; Bargmann, C. I.; Jayaraman, V.; Svoboda, K.; Looger, L. L. Imaging Neural Activity in Worms, Flies and Mice with Improved GCaMP Calcium Indicators. *Nat. Methods* **2009**, *6* (12), 875–881. <https://doi.org/10.1038/nmeth.1398>.
- (2) Lin, M. Z.; Schnitzer, M. J. Genetically Encoded Indicators of Neuronal Activity. *Nat. Neurosci.* **2016**, *19* (9), 1142–1153. <https://doi.org/10.1038/nn.4359>.
- (3) Grienberger, C.; Konnerth, A. Imaging Calcium in Neurons. *Neuron* **2012**, *73* (5), 862–885. <https://doi.org/10.1016/j.neuron.2012.02.011>.
- (4) Xu, Y.; Zou, P.; Cohen, A. E. Voltage Imaging with Genetically Encoded Indicators. *Curr. Opin. Chem. Biol.* **2017**, *39*, 1–10. <https://doi.org/10.1016/j.cbpa.2017.04.005>.
- (5) Boyden, E. S.; Zhang, F.; Bamberg, E.; Nagel, G.; Deisseroth, K. Millisecond-Timescale, Genetically Targeted Optical Control of Neural Activity. *Nat. Neurosci.* **2005**, *8* (9), 1263–1268. <https://doi.org/10.1038/nn1525>.
- (6) Fenno, L.; Yizhar, O.; Deisseroth, K. The Development and Application of Optogenetics. *Annu. Rev. Neurosci.* **2011**, *34* (1), 389–412. <https://doi.org/10.1146/annurev-neuro-061010-113817>.
- (7) Deisseroth, K. Optogenetics: 10 Years of Microbial Opsins in Neuroscience. *Nature Neuroscience*. 2015, pp 1213–1225. <https://doi.org/10.1038/nn.4091>.
- (8) Deisseroth, K. Optogenetics. *Nature Methods*. 2011, pp 26–29. <https://doi.org/10.1038/nmeth.f.324>.
- (9) O'Connor, D. H.; Huber, D.; Svoboda, K. Reverse Engineering the Mouse Brain. *Nature* **2009**, *461* (7266), 923–929. <https://doi.org/10.1038/nature08539>.
- (10) Panzeri, S.; Harvey, C. D.; Piasini, E.; Latham, P. E.; Fellin, T. Cracking the Neural Code for Sensory Perception by Combining Statistics, Intervention, and Behavior. *Neuron* **2017**, *93* (3), 491–507. <https://doi.org/10.1016/j.neuron.2016.12.036>.
- (11) Emiliani, V.; Cohen, A. E.; Deisseroth, K.; Häusser, M. All-Optical Interrogation of Neural Circuits. *J. Neurosci.* **2015**, *35* (41), 13917–13926. <https://doi.org/10.1523/JNEUROSCI.2916-15.2015>.
- (12) Russell, L. E.; Dalglish, H. W. P.; Nutbrown, R.; Gauld, O. M.; Herrmann, D.; Fişek, M.; Packer, A. M.; Häusser, M. All-Optical Interrogation of Neural Circuits in Behaving Mice. *Nat. Protoc.* **2022**, *17* (7), 1579–1620. <https://doi.org/10.1038/s41596-022-00691-w>.
- (13) Chettih, S. N.; Harvey, C. D. Single-Neuron Perturbations Reveal Feature-Specific Competition in V1. *Nature* **2019**, *567* (7748), 334–340. <https://doi.org/10.1038/s41586-019-0997-6>.
- (14) Jennings, J. H.; Kim, C. K.; Marshel, J. H.; Raffiee, M.; Ye, L.; Quirin, S.; Pak, S.; Ramakrishnan, C.; Deisseroth, K. Interacting Neural Ensembles in Orbitofrontal Cortex for Social and Feeding Behaviour. *Nature* **2019**, *565* (7741), 645–649. <https://doi.org/10.1038/s41586-018-0866-8>.
- (15) Spampinato, G. L. B.; Ronzitti, E.; Zampini, V.; Ferrari, U.; Trapani, F.; Khabou, H.; Agraval, A.; Dalkara, D.; Picaud, S.; Papagiakoumou, E.; Marre, O.; Emiliani, V. All-Optical Inter-Layers Functional Connectivity Investigation in the Mouse Retina. *Cell Reports Methods* **2022**, *2* (8), 100268. <https://doi.org/10.1016/j.crmeth.2022.100268>.
- (16) Marshel, J. H.; Kim, Y. S.; Machado, T. A.; Quirin, S.; Benson, B.; Kadmon, J.; Raja, C.;

- Chibukhchyan, A.; Ramakrishnan, C.; Inoue, M.; Shane, J. C.; McKnight, D. J.; Yoshizawa, S.; Kato, H. E.; Ganguli, S.; Deisseroth, K. Cortical Layer-Specific Critical Dynamics Triggering Perception. *Science* (80-.). **2019**, *365* (6453). <https://doi.org/10.1126/science.aaw5202>.
- (17) Dagleish, H. W. P.; Russell, L. E.; Packer, A. M.; Roth, A.; Gauld, O. M.; Greenstreet, F.; Thompson, E. J.; Häusser, M. How Many Neurons Are Sufficient for Perception of Cortical Activity? *Elife* **2020**, *9*, 1–99. <https://doi.org/10.7554/eLife.58889>.
- (18) Russell, L. E.; Fişek, M.; Yang, Z.; Tan, L. P.; Packer, A. M.; Dagleish, H. W. P.; Chettih, S. N.; Harvey, C. D.; Häusser, M. The Influence of Cortical Activity on Perception Depends on Behavioral State and Sensory Context. *Nat. Commun.* **2024**, *15* (1). <https://doi.org/10.1038/s41467-024-46484-5>.
- (19) Gill, J. V.; Lerman, G. M.; Zhao, H.; Stetler, B. J.; Rinberg, D.; Shoham, S. Precise Holographic Manipulation of Olfactory Circuits Reveals Coding Features Determining Perceptual Detection. *Neuron* **2020**, *108* (2), 382–393.e5. <https://doi.org/10.1016/j.neuron.2020.07.034>.
- (20) Carrillo-Reid, L.; Han, S.; Yang, W.; Akrouh, A.; Yuste, R. Controlling Visually Guided Behavior by Holographic Recalling of Cortical Ensembles. *Cell* **2019**, *178* (2), 447–457.e5. <https://doi.org/10.1016/j.cell.2019.05.045>.
- (21) dal Maschio, M.; Donovan, J. C.; Helmbrecht, T. O.; Baier, H. Linking Neurons to Network Function and Behavior by Two-Photon Holographic Optogenetics and Volumetric Imaging. *Neuron* **2017**, *94* (4), 774–789.e5. <https://doi.org/10.1016/j.neuron.2017.04.034>.
- (22) Robinson, N. T. M.; Descamps, L. A. L.; Russell, L. E.; Buchholz, M. O.; Bicknell, B. A.; Antonov, G. K.; Lau, J. Y. N.; Nutbrown, R.; Schmidt-Hieber, C.; Häusser, M. Targeted Activation of Hippocampal Place Cells Drives Memory-Guided Spatial Behavior. *Cell* **2020**, *183* (6), 1586–1599.e10. <https://doi.org/10.1016/j.cell.2020.09.061>.
- (23) Daie, K.; Svoboda, K.; Druckmann, S. Targeted Photostimulation Uncovers Circuit Motifs Supporting Short-Term Memory. *Nat. Neurosci.* **2021**, *24* (2), 259–265. <https://doi.org/10.1038/s41593-020-00776-3>.
- (24) Szabo, V.; Ventalon, C.; De Sars, V.; Bradley, J.; Emiliani, V. Spatially Selective Holographic Photoactivation and Functional Fluorescence Imaging in Freely Behaving Mice with a Fiberscope. *Neuron* **2014**, *84* (6), 1157–1169. <https://doi.org/10.1016/j.neuron.2014.11.005>.
- (25) Zhang, J.; Hughes, R. N.; Kim, N.; Fallon, I. P.; Bakhurin, K.; Kim, J.; Severino, F. P. U.; Yin, H. H. A One-Photon Endoscope for Simultaneous Patterned Optogenetic Stimulation and Calcium Imaging in Freely Behaving Mice. *Nat. Biomed. Eng.* **2022**, *7* (4), 499–510. <https://doi.org/10.1038/s41551-022-00920-3>.
- (26) Bovetti, S.; Moretti, C.; Zucca, S.; Dal Maschio, M.; Bonifazi, P.; Fellin, T. Simultaneous High-Speed Imaging and Optogenetic Inhibition in the Intact Mouse Brain. *Sci. Rep.* **2017**, *7* (1), 40041. <https://doi.org/10.1038/srep40041>.
- (27) Zhang, Y.; Oertner, T. G. Optical Induction of Synaptic Plasticity Using a Light-Sensitive Channel. **2007**, *4* (2), 139–141. <https://doi.org/10.1038/NMETH988>.
- (28) Zhang, F.; Wang, L. P.; Brauner, M.; Liewald, J. F.; Kay, K.; Watzke, N.; Wood, P. G.; Bamberg, E.; Nagel, G.; Gottschalk, A.; Deisseroth, K. Multimodal Fast Optical Interrogation of Neural Circuitry. *Nature* **2007**, *446* (7136), 633–639. <https://doi.org/10.1038/nature05744>.
- (29) Hochbaum, D. R.; Zhao, Y.; Farhi, S. L.; Klapoetke, N.; Werley, C. A.; Kapoor, V.; Zou,

- P.; Kralj, J. M.; MacLaurin, D.; Smedemark-Margulies, N.; Saulnier, J. L.; Boulting, G. L.; Straub, C.; Cho, Y. K.; Melkonian, M.; Wong, G. K. S.; Harrison, D. J.; Murthy, V. N.; Sabatini, B. L.; Boyden, E. S.; Campbell, R. E.; Cohen, A. E. All-Optical Electrophysiology in Mammalian Neurons Using Engineered Microbial Rhodopsins. *Nat. Methods* **2014**, *11* (8), 825–833. <https://doi.org/10.1038/NMETH.3000>.
- (30) Yang, W.; Yuste, R. In Vivo Imaging of Neural Activity. *Nat. Methods* **2017**, *14* (4), 349–359. <https://doi.org/10.1038/nmeth.4230>.
- (31) Helmchen, F.; Denk, W. Deep Tissue Two-Photon Microscopy. *Nat. Methods* **2005**, *2* (12), 932–940. <https://doi.org/10.1038/nmeth818>.
- (32) Svoboda, K.; Yasuda, R. Principles of Two-Photon Excitation Microscopy and Its Applications to Neuroscience. *Neuron* **2006**, *50* (6), 823–839. <https://doi.org/10.1016/j.neuron.2006.05.019>.
- (33) Nakai, J.; Ohkura, M.; Imoto, K. A High Signal-to-Noise Ca²⁺ Probe Composed of a Single Green Fluorescent Protein. *Nat. Biotechnol.* **2001**, *19* (2), 137–141. <https://doi.org/10.1038/84397>.
- (34) Rose, T.; Goltstein, P. M.; Portugues, R.; Griesbeck, O. Putting a Finishing Touch on GECIs. *Front. Mol. Neurosci.* **2014**, *7*, 1–15. <https://doi.org/10.3389/fnmol.2014.00088>.
- (35) Zhang, Y.; Looger, L. L. Fast and Sensitive GCaMP Calcium Indicators for Neuronal Imaging. *J. Physiol.* **2024**, *602* (8), 1595–1604. <https://doi.org/10.1113/JP283832>.
- (36) Adesnik, H.; Abdeladim, L. Probing Neural Codes with Two-Photon Holographic Optogenetics. *Nat. Neurosci.* **2021**, *24* (10), 1356–1366. <https://doi.org/10.1038/s41593-021-00902-9>.
- (37) Forli, A.; Pisoni, M.; Printz, Y.; Yizhar, O.; Fellin, T. Optogenetic Strategies for High-Efficiency All-Optical Interrogation Using Blue-Light-Sensitive Opsins. *Elife* **2021**, *10*, 1–25. <https://doi.org/10.7554/eLife.63359>.
- (38) Fu, T.; Arnoux, I.; Döring, J.; Backhaus, H.; Watari, H.; Stasevicius, I.; Fan, W.; Stroh, A. Exploring Two-Photon Optogenetics beyond 1100 Nm for Specific and Effective All-Optical Physiology. *iScience* **2021**, *24* (3). <https://doi.org/10.1016/j.isci.2021.102184>.
- (39) Papagiakoumou, E.; Anselmi, F.; Bègue, A.; De Sars, V.; Glückstad, J.; Isacoff, E. Y.; Emiliani, V. Scanless Two-Photon Excitation of Channelrhodopsin-2. *Nat. Methods* **2010**, *7* (10), 848–854. <https://doi.org/10.1038/nmeth.1505>.
- (40) Bègue, A.; Papagiakoumou, E.; Leshem, B.; Conti, R.; Enke, L.; Oron, D.; Emiliani, V. Two-Photon Excitation in Scattering Media by Spatiotemporally Shaped Beams and Their Application in Optogenetic Stimulation. *Biomed. Opt. Express* **2013**, *4* (12), 2869. <https://doi.org/10.1364/boe.4.002869>.
- (41) Pégard, N. C.; Mardinly, A. R.; Oldenburg, I. A.; Sridharan, S.; Waller, L.; Adesnik, H. Three-Dimensional Scanless Holographic Optogenetics with Temporal Focusing (3D-SHOT). *Nat. Commun.* **2017**, *8* (1), 1–14. <https://doi.org/10.1038/s41467-017-01031-3>.
- (42) Rickgauer, J. P.; Tank, D. W. Two-Photon Excitation of Channelrhodopsin-2 at Saturation. *Proc. Natl. Acad. Sci.* **2009**, *106* (35), 15025–15030. <https://doi.org/10.1073/pnas.0907084106>.
- (43) Packer, A. M.; Peterka, D. S.; Hirtz, J. J.; Prakash, R.; Deisseroth, K.; Yuste, R. Two-Photon Optogenetics of Dendritic Spines and Neural Circuits. *Nat. Methods* **2012**, *9* (12), 1202–1205. <https://doi.org/10.1038/nmeth.2249>.
- (44) Alivisatos, A. P.; Chun, M.; Church, G. M.; Greenspan, R. J.; Roukes, M. L.; Yuste, R.

- The Brain Activity Map Project and the Challenge of Functional Connectomics. *Neuron* **2012**, 74 (6), 970–974. <https://doi.org/10.1016/j.neuron.2012.06.006>.
- (45) Machado, T. A.; Kauvar, I. V.; Deisseroth, K. Multiregion Neuronal Activity: The Forest and the Trees. *Nat. Rev. Neurosci.* **2022**, 23 (11), 683–704. <https://doi.org/10.1038/s41583-022-00634-0>.
- (46) Manley, J.; Lu, S.; Barber, K.; Demas, J.; Kim, H.; Meyer, D.; Traub, F. M.; Vaziri, A. Simultaneous, Cortex-Wide Dynamics of up to 1 Million Neurons Reveal Unbounded Scaling of Dimensionality with Neuron Number. *Neuron* **2024**, 1–16. <https://doi.org/10.1016/j.neuron.2024.02.011>.
- (47) Shemesh, O. A.; Tanese, D.; Zampini, V.; Linghu, C.; Piatkevich, K.; Ronzitti, E.; Papagiakoumou, E.; Boyden, E. S.; Emiliani, V. Temporally Precise Single-Cell-Resolution Optogenetics. *Nat. Neurosci.* **2017**, 20 (12), 1796–1806. <https://doi.org/10.1038/s41593-017-0018-8>.
- (48) Mardinly, A. R.; Oldenburg, I. A.; Pégard, N. C.; Sridharan, S.; Lyall, E. H.; Chesnov, K.; Brohawn, S. G.; Waller, L.; Adesnik, H. Precise Multimodal Optical Control of Neural Ensemble Activity. *Nat. Neurosci.* **2018**, 21 (6), 881–893. <https://doi.org/10.1038/s41593-018-0139-8>.
- (49) Baker, C. A.; Elyada, Y. M.; Parra, A.; Bolton, M. M. Cellular Resolution Circuit Mapping with Temporal-Focused Excitation of Soma-Targeted Channelrhodopsin. *Elife* **2016**, 5 (AUGUST), 1–15. <https://doi.org/10.7554/eLife.14193>.
- (50) Vinje, W. E.; Gallant, J. L. Sparse Coding and Decorrelation in Primary Visual Cortex during Natural Vision. *Science (80-)*. **2000**, 287 (5456), 1273–1276. <https://doi.org/10.1126/science.287.5456.1273>.
- (51) Yoshida, T.; Ohki, K. Natural Images Are Reliably Represented by Sparse and Variable Populations of Neurons in Visual Cortex. *Nat. Commun.* **2020**, 11 (1), 872. <https://doi.org/10.1038/s41467-020-14645-x>.
- (52) Gauld, O. M.; Packer, A. M.; Russell, L. E.; Dagleish, H. W. P.; Iuga, M.; Sacadura, F.; Roth, A.; Clark, B. A.; Häusser, M. A Latent Pool of Neurons Silenced by Sensory-Evoked Inhibition Can Be Recruited to Enhance Perception. *Neuron* **2024**, 112 (14), 2386–2403.e6. <https://doi.org/10.1016/j.neuron.2024.04.015>.
- (53) Ohki, K.; Chung, S.; Ch'ng, Y. H.; Kara, P.; Reid, R. C. Functional Imaging with Cellular Resolution Reveals Precise Micro-Architecture in Visual Cortex. *Nature* **2005**, 433 (7026), 597–603. <https://doi.org/10.1038/nature03274>.
- (54) Panzeri, S.; Brunel, N.; Logothetis, N. K.; Kayser, C. Sensory Neural Codes Using Multiplexed Temporal Scales. *Trends Neurosci.* **2010**, 33 (3), 111–120. <https://doi.org/10.1016/j.tins.2009.12.001>.
- (55) Borst, A.; Theunissen, F. E. Information Theory and Neural Coding. *Nat. Neurosci.* **1999**, 2 (11), 947–957. <https://doi.org/10.1038/14731>.
- (56) Kumar, A.; Rotter, S.; Aertsen, A. Spiking Activity Propagation in Neuronal Networks: Reconciling Different Perspectives on Neural Coding. *Nat. Rev. Neurosci.* **2010**, 11 (9), 615–627. <https://doi.org/10.1038/nrn2886>.
- (57) Brette, R. Philosophy of the Spike: Rate-Based vs. Spike-Based Theories of the Brain. *Front. Syst. Neurosci.* **2015**, 9 (November), 1–14. <https://doi.org/10.3389/fnsys.2015.00151>.
- (58) Ji, N.; Freeman, J.; Smith, S. L. Technologies for Imaging Neural Activity in Large Volumes. *Nat. Neurosci.* **2016**, 19 (9), 1154–1164. <https://doi.org/10.1038/nn.4358>.
- (59) Kim, T. H.; Schnitzer, M. J. Fluorescence Imaging of Large-Scale Neural Ensemble

- Dynamics. *Cell* **2022**, *185* (1), 9–41. <https://doi.org/10.1016/j.cell.2021.12.007>.
- (60) Lecoq, J.; Orlova, N.; Grewe, B. F. Wide. Fast. Deep: Recent Advances in Multiphoton Microscopy of in Vivo Neuronal Activity. *J. Neurosci.* **2019**, *39* (46), 9042–9052. <https://doi.org/10.1523/JNEUROSCI.1527-18.2019>.
- (61) Weisenburger, S.; Vaziri, A. A Guide to Emerging Technologies for Large-Scale and Whole-Brain Optical Imaging of Neuronal Activity. *Annu. Rev. Neurosci.* **2018**, *41* (1), 431–452. <https://doi.org/10.1146/annurev-neuro-072116-031458>.
- (62) Wu, J.; Ji, N.; Tsia, K. K. Speed Scaling in Multiphoton Fluorescence Microscopy. *Nat. Photonics* **2021**, *15* (11), 800–812. <https://doi.org/10.1038/s41566-021-00881-0>.
- (63) Ota, K.; Oisi, Y.; Suzuki, T.; Ikeda, M.; Ito, Y.; Ito, T.; Uwamori, H.; Kobayashi, K.; Kobayashi, M.; Odagawa, M.; Matsubara, C.; Kuroiwa, Y.; Horikoshi, M.; Matsushita, J.; Hioki, H.; Ohkura, M.; Nakai, J.; Oizumi, M.; Miyawaki, A.; Aonishi, T.; Ode, T.; Murayama, M. Fast, Cell-Resolution, Contiguous-Wide Two-Photon Imaging to Reveal Functional Network Architectures across Multi-Modal Cortical Areas. *Neuron* **2021**, *109* (11), 1810–1824.e9. <https://doi.org/10.1016/j.neuron.2021.03.032>.
- (64) Sofroniew, N. J.; Flickinger, D.; King, J.; Svoboda, K. A Large Field of View Two-Photon Mesoscope with Subcellular Resolution for in Vivo Imaging. *Elife* **2016**, *5* (JUN2016), 1–20. <https://doi.org/10.7554/eLife.14472>.
- (65) Demas, J.; Manley, J.; Tejera, F.; Barber, K.; Kim, H.; Traub, F. M.; Chen, B.; Vaziri, A. High-Speed, Cortex-Wide Volumetric Recording of Neuroactivity at Cellular Resolution Using Light Beads Microscopy. *Nat. Methods* **2021**, *18* (9), 1103–1111. <https://doi.org/10.1038/s41592-021-01239-8>.
- (66) Clough, M.; Chen, I. A.; Park, S. W.; Ahrens, A. M.; Stirman, J. N.; Smith, S. L.; Chen, J. L. Flexible Simultaneous Mesoscale Two-Photon Imaging of Neural Activity at High Speeds. *Nat. Commun.* **2021**, *12* (1), 1–7. <https://doi.org/10.1038/s41467-021-26737-3>.
- (67) Yu, C. H.; Stirman, J. N.; Yu, Y.; Hira, R.; Smith, S. L. Diesel2p Mesoscope with Dual Independent Scan Engines for Flexible Capture of Dynamics in Distributed Neural Circuitry. *Nat. Commun.* **2021**, *12* (1). <https://doi.org/10.1038/s41467-021-26736-4>.
- (68) Lu, R.; Liang, Y.; Meng, G.; Zhou, P.; Svoboda, K.; Paninski, L.; Ji, N. Rapid Mesoscale Volumetric Imaging of Neural Activity with Synaptic Resolution. *Nat. Methods* **2020**, *17* (3), 291–294. <https://doi.org/10.1038/s41592-020-0760-9>.
- (69) Janiak, F. K.; Bartel, P.; Bale, M. R.; Yoshimatsu, T.; Komulainen, E.; Zhou, M.; Staras, K.; Prieto-Godino, L. L.; Euler, T.; Maravall, M.; Baden, T. Non-Telecentric Two-Photon Microscopy for 3D Random Access Mesoscale Imaging. *Nat. Commun.* **2022**, *13* (1), 1–20. <https://doi.org/10.1038/s41467-022-28192-0>.
- (70) Bumstead, J. R. Designing a Large Field-of-View Two-Photon Microscope Using Optical Invariant Analysis. *Neurophotonics* **2018**, *5* (02), 1. <https://doi.org/10.1117/1.nph.5.2.025001>.
- (71) Lecoq, J.; Savall, J.; Vučinić, D.; Grewe, B. F.; Kim, H.; Li, J. Z.; Kitch, L. J.; Schnitzer, M. J. Visualizing Mammalian Brain Area Interactions by Dual-Axis Two-Photon Calcium Imaging. *Nat. Neurosci.* **2014**, *17* (12), 1825–1829. <https://doi.org/10.1038/nn.3867>.
- (72) Wagner, M. J.; Kim, T. H.; Kadmon, J.; Nguyen, N. D.; Ganguli, S.; Schnitzer, M. J.; Luo, L. Shared Cortex-Cerebellum Dynamics in the Execution and Learning of a Motor Task. *Cell* **2019**, *177* (3), 669–682.e24. <https://doi.org/10.1016/j.cell.2019.02.019>.
- (73) Yang, M.; Zhou, Z.; Zhang, J.; Jia, S.; Li, T.; Guan, J.; Liao, X.; Leng, B.; Lyu, J.; Zhang, K.; Li, M.; Gong, Y.; Zhu, Z.; Yan, J.; Zhou, Y.; Liu, J. K.; Varga, Z.; Konnerth, A.; Tang, Y.;

- Gao, J.; Chen, X.; Jia, H. MATRIEX Imaging: Multiarea Two-Photon Real-Time in Vivo Explorer. *Light Sci. Appl.* **2019**, *8* (1), 109. <https://doi.org/10.1038/s41377-019-0219-x>.
- (74) Terada, S. I.; Kobayashi, K.; Ohkura, M.; Nakai, J.; Matsuzaki, M. Super-Wide-Field Two-Photon Imaging with a Micro-Optical Device Moving in Post-Objective Space. *Nat. Commun.* **2018**, *9* (1). <https://doi.org/10.1038/s41467-018-06058-8>.
- (75) Rynes, M. L.; Surinach, D. A.; Linn, S.; Laroque, M.; Rajendran, V.; Dominguez, J.; Hadjistemoulou, O.; Navabi, Z. S.; Ghanbari, L.; Johnson, G. W.; Nazari, M.; Mohajerani, M. H.; Kodandaramaiah, S. B. Miniaturized Head-Mounted Microscope for Whole-Cortex Mesoscale Imaging in Freely Behaving Mice. *Nat. Methods* **2021**, *18* (4), 417–425. <https://doi.org/10.1038/s41592-021-01104-8>.
- (76) Fan, J.; Suo, J.; Wu, J.; Xie, H.; Shen, Y.; Chen, F.; Wang, G.; Cao, L.; Jin, G.; He, Q.; Li, T.; Luan, G.; Kong, L.; Zheng, Z.; Dai, Q. Video-Rate Imaging of Biological Dynamics at Centimetre Scale and Micrometre Resolution. *Nat. Photonics* **2019**. <https://doi.org/10.1038/s41566-019-0474-7>.
- (77) Cardin, J. A.; Crair, M. C.; Higley, M. J. Mesoscopic Imaging: Shining a Wide Light on Large-Scale Neural Dynamics. *Neuron* **2020**, *108* (1), 33–43. <https://doi.org/10.1016/j.neuron.2020.09.031>.
- (78) Ren, C.; Komiyama, T. Characterizing Cortex-Wide Dynamics with Wide-Field Calcium Imaging. *J. Neurosci.* **2021**, *41* (19), 4160–4168. <https://doi.org/10.1523/JNEUROSCI.3003-20.2021>.
- (79) Zhang, Y.; Zhang, G.; Han, X.; Wu, J.; Li, Z.; Li, X.; Xiao, G.; Xie, H.; Fang, L.; Dai, Q. Rapid Detection of Neurons in Widefield Calcium Imaging Datasets after Training with Synthetic Data. *Nat. Methods* **2023**, *20* (5), 747–754. <https://doi.org/10.1038/s41592-023-01838-7>.
- (80) Sarafraz, H.; Nöbauer, T.; Kim, H.; Soldevila, F.; Gigan, S.; Vaziri, A. Speckle-Enabled in Vivo Demixing of Neural Activity in the Mouse Brain. *Biomed. Opt. Express* **2024**, *15* (6), 3586. <https://doi.org/10.1364/BOE.524521>.
- (81) Giovannucci, A.; Friedrich, J.; Gunn, P.; Kalfon, J.; Brown, B. L.; Koay, S. A.; Taxidis, J.; Najafi, F.; Gauthier, J. L.; Zhou, P.; Khakh, B. S.; Tank, D. W.; Chklovskii, D. B.; Pnevmatikakis, E. A. Caiman an Open Source Tool for Scalable Calcium Imaging Data Analysis. *Elife* **2019**, *8*. <https://doi.org/10.7554/eLife.38173>.
- (82) Dong, Z.; Mau, W.; Feng, Y.; Pennington, Z. T.; Chen, L.; Zaki, Y.; Rajan, K.; Shuman, T.; Aharoni, D.; Cai, D. J. Minian, an Open-Source Miniscope Analysis Pipeline. *Elife* **2022**, *11*, 1–37. <https://doi.org/10.7554/eLife.70661>.
- (83) Shi, R.; Chen, X.; Deng, J.; Liang, J.; Fan, K.; Zhou, F.; Tang, P.; Zhang, L.; Kong, L. Random-Access Wide-Field Mesoscopy for Centimetre-Scale Imaging of Biodynamics with Subcellular Resolution. *Nat. Photonics* **2024**, *18* (7), 721–730. <https://doi.org/10.1038/s41566-024-01422-1>.
- (84) Skocek, O.; Nöbauer, T.; Weigluny, L.; Martínez Traub, F.; Xia, C. N.; Molodtsov, M. I.; Grama, A.; Yamagata, M.; Aharoni, D.; Cox, D. D.; Golshani, P.; Vaziri, A. High-Speed Volumetric Imaging of Neuronal Activity in Freely Moving Rodents. *Nat. Methods* **2018**, *15* (6), 429–432. <https://doi.org/10.1038/s41592-018-0008-0>.
- (85) Nöbauer, T.; Zhang, Y.; Kim, H.; Vaziri, A. Mesoscale Volumetric Light-Field (MesoLF) Imaging of Neuroactivity across Cortical Areas at 18 Hz. *Nat. Methods* **2023**, *20* (4), 600–609. <https://doi.org/10.1038/s41592-023-01789-z>.
- (86) Tsai, P. S.; Mateo, C.; Field, J. J.; Schaffer, C. B.; Anderson, M. E.; Kleinfeld, D. Ultra-

- Large Field-of-View Two-Photon Microscopy. *Opt. Express* **2015**, *23* (11), 13833. <https://doi.org/10.1364/oe.23.013833>.
- (87) Abdeladim, L.; Shin, H.; Jagadisan, U. K.; Ogando, M. B.; Adesnik, H. Probing Inter-Areal Computations with a Cellular Resolution Two-Photon Holographic Mesoscope. *bioRxiv*. March 3, 2023. <https://doi.org/10.1101/2023.03.02.530875>.
- (88) Golan, L.; Reutsky, I.; Farah, N.; Shoham, S. Design and Characteristics of Holographic Neural Photo-Stimulation Systems. *J. Neural Eng.* **2009**, *6* (6). <https://doi.org/10.1088/1741-2560/6/6/066004>.
- (89) Faini, G.; Tanese, D.; Molinier, C.; Telliez, C.; Hamdani, M.; Blot, F.; Tourain, C.; de Sars, V.; Del Bene, F.; Forget, B. C.; Ronzitti, E.; Emiliani, V. Ultrafast Light Targeting for High-Throughput Precise Control of Neuronal Networks. *Nat. Commun.* **2023**, *14* (1), 1888. <https://doi.org/10.1038/s41467-023-37416-w>.
- (90) Brunstein, M.; Lubetzki, J.; Moutoussamy, C.; Li, W.; Barral, J. Fast 2-Photon Stimulation Using Holographic Patterns. *Opt. Express* **2023**, *31* (23), 39222. <https://doi.org/10.1364/oe.498644>.
- (91) Reddy, G. D.; Saggau, P. Fast Three-Dimensional Laser Scanning Scheme Using Acousto-Optic Deflectors. *J. Biomed. Opt.* **2005**, *10* (6), 064038. <https://doi.org/10.1117/1.2141504>.
- (92) Salomé, R.; Kremer, Y.; Dieudonné, S.; Léger, J. F.; Krichevsky, O.; Wyart, C.; Chatenay, D.; Bourdieu, L. Ultrafast Random-Access Scanning in Two-Photon Microscopy Using Acousto-Optic Deflectors. *J. Neurosci. Methods* **2006**, *154* (1–2), 161–174. <https://doi.org/10.1016/j.jneumeth.2005.12.010>.
- (93) Kazemipour, A.; Novak, O.; Flickinger, D.; Marvin, J. S.; Abdelfattah, A. S.; King, J.; Borden, P. M.; Kim, J. J.; Al-Abdullatif, S. H.; Deal, P. E.; Miller, E. W.; Schreiter, E. R.; Druckmann, S.; Svoboda, K.; Looger, L. L.; Podgorski, K. Kilohertz Frame-Rate Two-Photon Tomography. *Nat. Methods* **2019**, *16* (8), 778–786. <https://doi.org/10.1038/s41592-019-0493-9>.
- (94) Akemann, W.; Wolf, S.; Villette, V.; Mathieu, B.; Tangara, A.; Fodor, J.; Ventalon, C.; Léger, J. F.; Dieudonné, S.; Bourdieu, L. Fast Optical Recording of Neuronal Activity by Three-Dimensional Custom-Access Serial Holography. *Nat. Methods* **2022**, *19* (1), 100–110. <https://doi.org/10.1038/s41592-021-01329-7>.
- (95) Villette, V.; Chavarha, M.; Dimov, I. K.; Bradley, J.; Pradhan, L.; Mathieu, B.; Evans, S. W.; Chamberland, S.; Shi, D.; Yang, R.; Kim, B. B.; Ayon, A.; Jalil, A.; St-Pierre, F.; Schnitzer, M. J.; Bi, G.; Toth, K.; Ding, J.; Dieudonné, S.; Lin, M. Z. Ultrafast Two-Photon Imaging of a High-Gain Voltage Indicator in Awake Behaving Mice. *Cell* **2019**, *179* (7), 1590-1608.e23. <https://doi.org/10.1016/j.cell.2019.11.004>.
- (96) Sims, R. R.; Bendifallah, I.; Grimm, C.; Lafirdeen, A. S. M.; Domínguez, S.; Chan, C. Y.; Lu, X.; Forget, B. C.; St-Pierre, F.; Papagiakoumou, E.; Emiliani, V. Scanless Two-Photon Voltage Imaging. *Nat. Commun.* **2024**, *15* (1), 1–22. <https://doi.org/10.1038/s41467-024-49192-2>.
- (97) Sun, S.; Zhang, G.; Cheng, Z.; Gan, W.; Cui, M. Large-Scale Femtosecond Holography for near Simultaneous Optogenetic Neural Modulation. *Opt. Express* **2019**, *27* (22), 32228. <https://doi.org/10.1364/oe.27.032228>.
- (98) Yang, W.; Miller, J. eun K.; Carrillo-Reid, L.; Pnevmatikakis, E.; Paninski, L.; Yuste, R.; Peterka, D. S. Simultaneous Multi-Plane Imaging of Neural Circuits. *Neuron* **2016**, *89* (2), 269. <https://doi.org/10.1016/j.neuron.2015.12.012>.
- (99) Kim, J.; Seong, J.; Yang, Y.; Moon, S.-W.; Badloe, T.; Rho, J. Tunable Metasurfaces

- towards Versatile Metalenses and Metaholograms: A Review. *Adv. Photonics* **2022**, *4* (02), 1–16. <https://doi.org/10.1117/1.AP.4.2.024001>.
- (100) Kuznetsov, A. I.; Brongersma, M. L.; Yao, J.; Chen, M. K.; Levy, U.; Tsai, D. P.; Zheludev, N. I.; Faraon, A.; Arbabi, A.; Yu, N.; Chanda, D.; Crozier, K. B.; Kildishev, A. V.; Wang, H.; Yang, J. K. W.; Valentine, J. G.; Genevet, P.; Fan, J. A.; Miller, O. D.; Majumdar, A.; Fröch, J. E.; Brady, D.; Heide, F.; Veeraraghavan, A.; Engheta, N.; Alù, A.; Polman, A.; Atwater, H. A.; Thureja, P.; Paniagua-Dominguez, R.; Ha, S. T.; Barreda, A. I.; Schuller, J. A.; Staude, I.; Grinblat, G.; Kivshar, Y.; Peana, S.; Yelin, S. F.; Senichev, A.; Shalaev, V. M.; Saha, S.; Boltasseva, A.; Rho, J.; Oh, D. K.; Kim, J.; Park, J.; Devlin, R.; Pala, R. A. Roadmap for Optical Metasurfaces. *ACS Photonics* **2024**, *11* (3), 816–865. <https://doi.org/10.1021/acsp Photonics.3c00457>.
- (101) Wen, D.; Yue, F.; Li, G.; Zheng, G.; Chan, K.; Chen, S.; Chen, M.; Li, K. F.; Wong, P. W. H.; Cheah, K. W.; Yue Bun Pun, E.; Zhang, S.; Chen, X. Helicity Multiplexed Broadband Metasurface Holograms. *Nat. Commun.* **2015**, *6* (1), 8241. <https://doi.org/10.1038/ncomms9241>.
- (102) Stirman, J. N.; Smith, I. T.; Kudenov, M. W.; Smith, S. L. Wide Field-of-View, Multi-Region, Two-Photon Imaging of Neuronal Activity in the Mammalian Brain. *Nat. Biotechnol.* **2016**, *34* (8), 857–862. <https://doi.org/10.1038/nbt.3594>.
- (103) Chen, J. L.; Voigt, F. F.; Javadzadeh, M.; Krueppel, R.; Helmchen, F. Long-Range Population Dynamics of Anatomically Defined Neocortical Networks. *Elife* **2016**, *5* (MAY2016), 1–26. <https://doi.org/10.7554/eLife.14679>.
- (104) Lee, S.; Zhang, G.; Gomez, L. C.; Testa-Silva, G.; Hao, Y. A.; Hiramoto, A.; Jiang, D.; Roth, R. H.; Ding, J.; Clandinin, T. R.; Roska, B.; Feldman, D.; Ji, N.; Lin, M. Z. Improving Positively Tuned Voltage Indicators for Brightness and Kinetics. *bioRxiv* **2024**. <https://doi.org/10.1101/2024.06.21.599617>.
- (105) Zhu, M. H.; Jang, J.; Milosevic, M. M.; Antic, S. D. Population Imaging Discrepancies between a Genetically-Encoded Calcium Indicator (GECI) versus a Genetically-Encoded Voltage Indicator (GEVI). *Sci. Rep.* **2021**, *11* (1), 1–15. <https://doi.org/10.1038/s41598-021-84651-6>.
- (106) Peterka, D. S.; Takahashi, H.; Yuste, R. Imaging Voltage in Neurons. *Neuron* **2011**, *69* (1), 9–21. <https://doi.org/10.1016/j.neuron.2010.12.010>.
- (107) Abdelfattah, A. S.; Kawashima, T.; Singh, A.; Novak, O.; Liu, H.; Shuai, Y.; Huang, Y.-C.; Campagnola, L.; Seeman, S. C.; Yu, J.; Zheng, J.; Grimm, J. B.; Patel, R.; Friedrich, J.; Mensh, B. D.; Paninski, L.; Macklin, J. J.; Murphy, G. J.; Podgorski, K.; Lin, B.-J.; Chen, T.-W.; Turner, G. C.; Liu, Z.; Koyama, M.; Svoboda, K.; Ahrens, M. B.; Lavis, L. D.; Schreier, E. R. Bright and Photostable Chemigenetic Indicators for Extended in Vivo Voltage Imaging. *Science* (80-.). **2019**, *365* (6454), 699–704. <https://doi.org/10.1126/science.aav6416>.
- (108) Liu, Z.; Lu, X.; Villette, V.; Gou, Y.; Colbert, K. L.; Lai, S.; Guan, S.; Land, M. A.; Lee, J.; Assefa, T.; Zollinger, D. R.; Korympidou, M. M.; Vlasits, A. L.; Pang, M. M.; Su, S.; Cai, C.; Froudarakis, E.; Zhou, N.; Patel, S. S.; Smith, C. L.; Ayon, A.; Bizouard, P.; Bradley, J.; Franke, K.; Clandinin, T. R.; Giovannucci, A.; Tolia, A. S.; Reimer, J.; Dieudonné, S.; St-Pierre, F. Sustained Deep-Tissue Voltage Recording Using a Fast Indicator Evolved for Two-Photon Microscopy. *Cell* **2022**, *185* (18), 3408–3425.e29. <https://doi.org/10.1016/j.cell.2022.07.013>.
- (109) Platasa, J.; Ye, X.; Ahrens, A. M.; Liu, C.; Chen, I. A.; Davison, I. G.; Tian, L.; Pieribone, V. A.; Chen, J. L. High-Speed Low-Light in Vivo Two-Photon Voltage Imaging of Large

- Neuronal Populations. *Nat. Methods* **2023**, *20* (7), 1095–1103.
<https://doi.org/10.1038/s41592-023-01820-3>.
- (110) Evans, S. W.; Shi, D.-Q.; Chavarha, M.; Plitt, M. H.; Taxidis, J.; Madruga, B.; Fan, J. L.; Hwang, F.-J.; van Keulen, S. C.; Suomivuori, C.-M.; Pang, M. M.; Su, S.; Lee, S.; Hao, Y. A.; Zhang, G.; Jiang, D.; Pradhan, L.; Roth, R. H.; Liu, Y.; Dorian, C. C.; Reese, A. L.; Negrean, A.; Losonczy, A.; Makinson, C. D.; Wang, S.; Clandinin, T. R.; Dror, R. O.; Ding, J. B.; Ji, N.; Golshani, P.; Giocomo, L. M.; Bi, G.-Q.; Lin, M. Z. A Positively Tuned Voltage Indicator for Extended Electrical Recordings in the Brain. *Nat. Methods* **2023**, *20* (7), 1104–1113. <https://doi.org/10.1038/s41592-023-01913-z>.
- (111) Knöpfel, T.; Song, C. Optical Voltage Imaging in Neurons: Moving from Technology Development to Practical Tool. *Nat. Rev. Neurosci.* **2019**, *20* (12), 719–727.
<https://doi.org/10.1038/s41583-019-0231-4>.
- (112) Lu, X.; Wang, Y.; Liu, Z.; Gou, Y.; Jaeger, D.; St-Pierre, F. Widefield Imaging of Rapid Pan-Cortical Voltage Dynamics with an Indicator Evolved for One-Photon Microscopy. *Nat. Commun.* **2023**, *14* (1). <https://doi.org/10.1038/s41467-023-41975-3>.
- (113) Quicke, P.; Howe, C. L.; Foust, A. J. Balancing the Fluorescence Imaging Budget for All-Optical Neurophysiology Experiments. In *All-Optical Methods to Study Neuronal Function*; 2023; pp 49–74. https://doi.org/10.1007/978-1-0716-2764-8_2.
- (114) Quicke, P.; Song, C.; McKimm, E. J.; Milosevic, M. M.; Howe, C. L.; Neil, M.; Schultz, S. R.; Antic, S. D.; Foust, A. J.; Knöpfel, T. Single-Neuron Level One-Photon Voltage Imaging with Sparsely Targeted Genetically Encoded Voltage Indicators. *Front. Cell. Neurosci.* **2019**, *13*. <https://doi.org/10.3389/fncel.2019.00039>.
- (115) Kannan, M.; Vasan, G.; Haziza, S.; Huang, C.; Chrapkiewicz, R.; Luo, J.; Cardin, J. A.; Schnitzer, M. J.; Pieribone, V. A. Dual-Polarity Voltage Imaging of the Concurrent Dynamics of Multiple Neuron Types. *Science (80-.)*. **2022**, *378* (6619).
<https://doi.org/10.1126/science.abm8797>.
- (116) Parot, V. J.; Sing-Long, C.; Adam, Y.; Böhm, U. L.; Fan, L. Z.; Farhi, S. L.; Cohen, A. E. Compressed Hadamard Microscopy for High-Speed Optically Sectioned Neuronal Activity Recordings. *J. Phys. D. Appl. Phys.* **2019**, *52* (14).
<https://doi.org/10.1088/1361-6463/aafe88>.
- (117) Fan, L. Z.; Kheifets, S.; Böhm, U. L.; Wu, H.; Piatkevich, K. D.; Xie, M. E.; Parot, V.; Ha, Y.; Evans, K. E.; Boyden, E. S.; Takesian, A. E.; Cohen, A. E. All-Optical Electrophysiology Reveals the Role of Lateral Inhibition in Sensory Processing in Cortical Layer 1. *Cell* **2020**, *180* (3), 521-535.e18.
<https://doi.org/10.1016/j.cell.2020.01.001>.
- (118) Xiao, S.; Lowet, E.; Gritton, H. J.; Fabris, P.; Wang, Y.; Sherman, J.; Mount, R. A.; Tseng, H.; Man, H.-Y.; Straub, C.; Piatkevich, K. D.; Boyden, E. S.; Mertz, J.; Han, X. Large-Scale Voltage Imaging in Behaving Mice Using Targeted Illumination. *iScience* **2021**, *24* (11), 103263. <https://doi.org/10.1016/j.isci.2021.103263>.
- (119) Adam, Y.; Kim, J. J.; Lou, S.; Zhao, Y.; Xie, M. E.; Brinks, D.; Wu, H.; Mostajo-Radji, M. A.; Kheifets, S.; Parot, V.; Chettih, S.; Williams, K. J.; Gmeiner, B.; Farhi, S. L.; Madisen, L.; Buchanan, E. K.; Kinsella, I.; Zhou, D.; Paninski, L.; Harvey, C. D.; Zeng, H.; Arlotta, P.; Campbell, R. E.; Cohen, A. E. Voltage Imaging and Optogenetics Reveal Behaviour-Dependent Changes in Hippocampal Dynamics. *Nature* **2019**, *569* (7756), 413–417.
<https://doi.org/10.1038/s41586-019-1166-7>.
- (120) Foust, A. J.; Zampini, V.; Tanese, D.; Papagiakoumou, E.; Emiliani, V. Computer-Generated Holography Enhances Voltage Dye Fluorescence Discrimination in

- Adjacent Neuronal Structures. *NeuroPhotonics* **2015**, 2 (2), 021007.
<https://doi.org/10.1117/1.nph.2.2.021007>.
- (121) Acker, C. D.; Yan, P.; Loew, L. M. Single-Voxel Recording of Voltage Transients in Dendritic Spines. *Biophys. J.* **2011**, 101 (2), L11–L13.
<https://doi.org/10.1016/j.bpj.2011.06.021>.
- (122) Roome, C. J.; Kuhn, B. Simultaneous Dendritic Voltage and Calcium Imaging and Somatic Recording from Purkinje Neurons in Awake Mice. *Nat. Commun.* **2018**, 9 (1), 1–14. <https://doi.org/10.1038/s41467-018-05900-3>.
- (123) Brinks, D.; Klein, A. J.; Cohen, A. E. Two-Photon Lifetime Imaging of Voltage Indicating Proteins as a Probe of Absolute Membrane Voltage. *Biophys. J.* **2015**, 109 (5), 914–921. <https://doi.org/10.1016/j.bpj.2015.07.038>.
- (124) Fisher, J. A. N.; Barchi, J. R.; Welle, C. G.; Kim, G. H.; Kosterin, P.; Obaid, A. L.; Yodh, A. G.; Contreras, D.; Salzberg, B. M. Two-Photon Excitation of Potentiometric Probes Enables Optical Recording of Action Potentials from Mammalian Nerve Terminals in Situ. *J. Neurophysiol.* **2008**, 99 (3), 1545–1553.
<https://doi.org/10.1152/jn.00929.2007>.
- (125) Wu, J.; Liang, Y.; Chen, S.; Hsu, C. L.; Chavarha, M.; Evans, S. W.; Shi, D.; Lin, M. Z.; Tsia, K. K.; Ji, N. Kilohertz Two-Photon Fluorescence Microscopy Imaging of Neural Activity in Vivo. *Nat. Methods* **2020**, 17 (3), 287–290. <https://doi.org/10.1038/s41592-020-0762-7>.
- (126) Kulkarni, R. U.; Vandenberghe, M.; Thunemann, M.; James, F.; Andreassen, O. A.; Djurovic, S.; Devor, A.; Miller, E. W. In Vivo Two-Photon Voltage Imaging with Sulfonated Rhodamine Dyes. *ACS Cent. Sci.* **2018**, 4 (10), 1371–1378.
<https://doi.org/10.1021/acscentsci.8b00422>.
- (127) Bando, Y.; Wenzel, M.; Yuste, R. Simultaneous Two-Photon Imaging of Action Potentials and Subthreshold Inputs in Vivo. *Nat. Commun.* **2021**, 12 (1), 1–12.
<https://doi.org/10.1038/s41467-021-27444-9>.
- (128) Cornejo, V. H.; Ofer, N.; Yuste, R. Voltage Compartmentalization in Dendritic Spines in Vivo. *Science (80-.)*. **2022**, 375 (6576), 82–86.
<https://doi.org/10.1126/science.abg0501>.
- (129) Li, B.; Wu, C.; Wang, M.; Charan, K.; Xu, C. An Adaptive Excitation Source for High-Speed Multiphoton Microscopy. *Nat. Methods* **2020**, 17 (2), 163–166.
<https://doi.org/10.1038/s41592-019-0663-9>.
- (130) Bindels, D. S.; Haarbosch, L.; Van Weeren, L.; Postma, M.; Wiese, K. E.; Mastop, M.; Aumonier, S.; Gotthard, G.; Royant, A.; Hink, M. A.; Gadella, T. W. J. MScarlet: A Bright Monomeric Red Fluorescent Protein for Cellular Imaging. *Nat. Methods* **2016**, 14 (1), 53–56. <https://doi.org/10.1038/nmeth.4074>.
- (131) Akerboom, J.; Chen, T. W.; Wardill, T. J.; Tian, L.; Marvin, J. S.; Mutlu, S.; Calderón, N. C.; Esposti, F.; Borghuis, B. G.; Sun, X. R.; Gordus, A.; Orger, M. B.; Portugues, R.; Engert, F.; Macklin, J. J.; Filosa, A.; Aggarwal, A.; Kerr, R. A.; Takagi, R.; Kracun, S.; Shigetomi, E.; Khakh, B. S.; Baier, H.; Lagnado, L.; Wang, S. S. H.; Bargmann, C. I.; Kimmel, B. E.; Jayaraman, V.; Svoboda, K.; Kim, D. S.; Schreiter, E. R.; Looger, L. L. Optimization of a GCaMP Calcium Indicator for Neural Activity Imaging. *J. Neurosci.* **2012**, 32 (40), 13819–13840. <https://doi.org/10.1523/JNEUROSCI.2601-12.2012>.
- (132) Berlage, C.; Böhm, U. L.; Sanchez Moreno, A.; Ledderose, J.; Gidon, A.; Larkum, M. E.; Plested, A.; Judkewitz, B. High-Speed Three-Dimensional Random Access Scanning with a Linear SLM. *Optica* **2024**, 11 (12), 1639.

- <https://doi.org/10.1364/OPTICA.536853>.
- (133) Akemann, W.; Bourdieu, L. Acousto-Optic Holography for Pseudo-Two-Dimensional Dynamic Light Patterning. *APL Photonics* **2024**, *9* (4).
<https://doi.org/10.1063/5.0185857>.
- (134) Zhao, S.; Hebert, E.; Gruzdeva, A.; Mahishi, D.; Takahashi, H.; Lee, S.; Hao, Y.; Lin, M.; Yapici, N.; Xu, C. Deep Two-Photon Voltage Imaging with Adaptive Excitation. *bioRxiv* **2024**. <https://doi.org/10.21203/rs.3.rs-5434919/v1>.
- (135) Papagiakoumou, E.; de Sars, V.; Oron, D.; Emiliani, V. Patterned Two-Photon Illumination by Spatiotemporal Shaping of Ultrashort Pulses. *Opt. Express* **2008**, *16* (26), 22039. <https://doi.org/10.1364/OE.16.022039>.
- (136) Papagiakoumou, E.; Ronzitti, E.; Emiliani, V. Scanless Two-Photon Excitation with Temporal Focusing. *Nat. Methods* **2020**, *17* (6), 571–581.
<https://doi.org/10.1038/s41592-020-0795-y>.
- (137) Chaigneau, E.; Ronzitti, E.; Gajowa, M. A.; Soler-Llavina, G. J.; Tanese, D.; Brureau, A. Y. B.; Papagiakoumou, E.; Zeng, H.; Emiliani, V. Two-Photon Holographic Stimulation of ReaChR. *Front. Cell. Neurosci.* **2016**, *10* (OCT2016).
<https://doi.org/10.3389/fncel.2016.00234>.
- (138) Chen, I.-W.; Ronzitti, E.; Lee, B. R.; Daigle, T. L.; Dalkara, D.; Zeng, H.; Emiliani, V.; Papagiakoumou, E. In Vivo Sub-Millisecond Two-Photon Optogenetics with Temporally Focused Patterned Light. *J. Neurosci.* **2019**, *39* (18), 1785–18.
<https://doi.org/10.1523/JNEUROSCI.1785-18.2018>.
- (139) Ronzitti, E.; Conti, R.; Zampini, V.; Tanese, D.; Foust, A. J.; Klapoetke, N.; Boyden, E. S.; Papagiakoumou, E.; Emiliani, V. Submillisecond Optogenetic Control of Neuronal Firing with Two-Photon Holographic Photoactivation of Chronos. *J. Neurosci.* **2017**, *37* (44), 10679–10689. <https://doi.org/10.1523/JNEUROSCI.1246-17.2017>.
- (140) Hossack, W. J.; Theofanidou, E.; Crain, J.; Heggarty, K.; Birch, M. High-Speed Holographic Optical Tweezers Using a Ferroelectric Liquid Crystal Microdisplay. *Opt. Express* **2003**, *11* (17), 2053. <https://doi.org/10.1364/oe.11.002053>.
- (141) Hornbeck, L. J. Digital Light Processing for High-Brightness High-Resolution Applications. In *Projection Displays III*; Wu, M. H., Ed.; 1997; Vol. 3013, pp 27–40.
<https://doi.org/10.1117/12.273880>.
- (142) Kim, S.; Moon, H. S.; Vo, T. T.; Kim, C. H.; Im, G. H.; Lee, S.; Choi, M.; Kim, S. G. Whole-Brain Mapping of Effective Connectivity by fMRI with Cortex-Wide Patterned Optogenetics. *Neuron* **2023**, *111* (11), 1732-1747.e6.
<https://doi.org/10.1016/j.neuron.2023.03.002>.
- (143) Rullan, M.; Benzinger, D.; Schmidt, G. W.; Miliias-Argeitis, A.; Khammash, M. An Optogenetic Platform for Real-Time, Single-Cell Interrogation of Stochastic Transcriptional Regulation. *Mol. Cell* **2018**, *70* (4), 745-756.e6.
<https://doi.org/10.1016/j.molcel.2018.04.012>.
- (144) Sakai, S.; Ueno, K.; Ishizuka, T.; Yawo, H. Parallel and Patterned Optogenetic Manipulation of Neurons in the Brain Slice Using a DMD-Based Projector. *Neurosci. Res.* **2013**, *75* (1), 59–64. <https://doi.org/10.1016/j.neures.2012.03.009>.
- (145) Warp, E.; Agarwal, G.; Wyart, C.; Friedmann, D.; Oldfield, C. S.; Conner, A.; Del Bene, F.; Arrenberg, A. B.; Baier, H.; Isacoff, E. Y. Emergence of Patterned Activity in the Developing Zebrafish Spinal Cord. *Curr. Biol.* **2012**, *22* (2), 93–102.
<https://doi.org/10.1016/j.cub.2011.12.002>.
- (146) Zhu, P.; Fajardo, O.; Shum, J.; Zhang Schäerer, Y. P.; Friedrich, R. W. High-Resolution

- Optical Control of Spatiotemporal Neuronal Activity Patterns in Zebrafish Using a Digital Micromirror Device. *Nat. Protoc.* **2012**, *7* (7), 1410–1425. <https://doi.org/10.1038/nprot.2012.072>.
- (147) Rocha, J. C. A.; Wright, T.; Bütaitè, U. G.; Carpenter, J.; Gordon, G. S. D.; Phillips, D. B. Fast and Light-Efficient Wavefront Shaping with a MEMS Phase-Only Light Modulator. *arXiv* **2024**. <https://doi.org/10.48550/arXiv.2409.01289>.
- (148) Podgorski, K.; Ranganathan, G. Brain Heating Induced by Near-Infrared Lasers during Multiphoton Microscopy. *J. Neurophysiol.* **2016**, *116* (3), 1012–1023. <https://doi.org/10.1152/jn.00275.2016>.
- (149) Picot, A.; Dominguez, S.; Liu, C.; Chen, I. W.; Tanese, D.; Ronzitti, E.; Berto, P.; Papagiakoumou, E.; Oron, D.; Tessier, G.; Forget, B. C.; Emiliani, V. Temperature Rise under Two-Photon Optogenetic Brain Stimulation. *Cell Rep.* **2018**, *24* (5), 1243–1253.e5. <https://doi.org/10.1016/j.celrep.2018.06.119>.
- (150) Feller, G. Protein Folding at Extreme Temperatures: Current Issues. *Semin. Cell Dev. Biol.* **2018**, *84*, 129–137. <https://doi.org/10.1016/j.semcdb.2017.09.003>.
- (151) Lapidus, L. J. Protein Unfolding Mechanisms and Their Effects on Folding Experiments. *F1000Research* **2017**, *6*, 1723. <https://doi.org/10.12688/f1000research.12070.1>.
- (152) Los, D. A.; Murata, N. Membrane Fluidity and Its Roles in the Perception of Environmental Signals. *Biochim. Biophys. Acta - Biomembr.* **2004**, *1666* (1–2), 142–157. <https://doi.org/10.1016/j.bbamem.2004.08.002>.
- (153) Leach, M. D.; Cowen, L. E. Membrane Fluidity and Temperature Sensing Are Coupled via Circuitry Comprised of Ole1, Rsp5, and Hsf1 in *Candida Albicans*. *Eukaryot. Cell* **2014**, *13* (8), 1077–1084. <https://doi.org/10.1128/EC.00138-14>.
- (154) Ma, D. K.; Li, Z.; Lu, A. Y.; Sun, F.; Chen, S.; Rothe, M.; Menzel, R.; Sun, F.; Horvitz, H. R. Acyl-CoA Dehydrogenase Drives Heat Adaptation by Sequestering Fatty Acids. *Cell* **2015**, *161* (5), 1152–1163. <https://doi.org/10.1016/j.cell.2015.04.026>.
- (155) Thomsen, S. PATHOLOGIC ANALYSIS OF PHOTOTHERMAL AND PHOTOMECHANICAL EFFECTS OF LASER–TISSUE INTERACTIONS. *Photochem. Photobiol.* **1991**, *53* (6), 825–835. <https://doi.org/10.1111/j.1751-1097.1991.tb09897.x>.
- (156) Dewhirst, M. W.; Viglianti, B. L.; Lora-Michiels, M.; Hanson, M.; Hoopes, P. J. Basic Principles of Thermal Dosimetry and Thermal Thresholds for Tissue Damage from Hyperthermia. *Int. J. Hyperth.* **2003**, *19* (3), 267–294. <https://doi.org/10.1080/0265673031000119006>.
- (157) Wells, J.; Kao, C.; Konrad, P.; Milner, T.; Kim, J.; Mahadevan-Jansen, A.; Jansen, E. D. Biophysical Mechanisms of Transient Optical Stimulation of Peripheral Nerve. *Biophys. J.* **2007**, *93* (7), 2567–2580. <https://doi.org/10.1529/biophysj.107.104786>.
- (158) Yang, F.; Zheng, J. High Temperature Sensitivity Is Intrinsic to Voltage-Gated Potassium Channels. *Elife* **2014**, *3*, e03255. <https://doi.org/10.7554/eLife.03255>.
- (159) Shibasaki, K.; Suzuki, M.; Mizuno, A.; Tominaga, M. Effects of Body Temperature on Neural Activity in the Hippocampus: Regulation of Resting Membrane Potentials by Transient Receptor Potential Vanilloid 4. *J. Neurosci.* **2007**, *27* (7), 1566–1575. <https://doi.org/10.1523/JNEUROSCI.4284-06.2007>.
- (160) Sabatini, B. L.; Regehr, W. G. Timing of Neurotransmission at Fast Synapses in the Mammalian Brain. *Nature* **1996**, *384* (6605), 170–172. <https://doi.org/10.1038/384170a0>.
- (161) Stujenske, J. M.; Spellman, T.; Gordon, J. A. Modeling the Spatiotemporal Dynamics of Light and Heat Propagation for InVivo Optogenetics. *Cell Rep.* **2015**, *12* (3), 525–534.

- <https://doi.org/10.1016/j.celrep.2015.06.036>.
- (162) Hodgkin, A. L.; Katz, B. The Effect of Sodium Ions on the Electrical Activity of the Giant Axon of the Squid. *J. Physiol.* **1949**, *108* (1), 37–77.
<https://doi.org/10.1113/jphysiol.1949.sp004310>.
- (163) Shapiro, M. G.; Homma, K.; Villarreal, S.; Richter, C.-P.; Bezanilla, F. Infrared Light Excites Cells by Changing Their Electrical Capacitance. *Nat. Commun.* **2012**, *3* (1), 736.
<https://doi.org/10.1038/ncomms1742>.
- (164) Chimere, C.; Movileanu, L.; Pezeshki, S.; Winterhalter, M.; Kleinekathöfer, U. Transport at the Nanoscale: Temperature Dependence of Ion Conductance. *Eur. Biophys. J.* **2008**, *38* (1), 121–125. <https://doi.org/10.1007/s00249-008-0366-0>.
- (165) Pavlidou, E.; Hagel, C.; Panteliadis, C. Febrile Seizures: Recent Developments and Unanswered Questions. *Child's Nerv. Syst.* **2013**, *29* (11), 2011–2017.
<https://doi.org/10.1007/s00381-013-2224-3>.
- (166) Aronov, D.; Fee, M. S. Natural Changes in Brain Temperature Underlie Variations in Song Tempo during a Mating Behavior. *PLoS One* **2012**, *7* (10), 1–10.
<https://doi.org/10.1371/journal.pone.0047856>.
- (167) Ermakova, Y. G.; Lanin, A. A.; Fedotov, I. V.; Roshchin, M.; Kelmanson, I. V.; Kulik, D.; Bogdanova, Y. A.; Shokhina, A. G.; Bilan, D. S.; Staroverov, D. B.; Balaban, P. M.; Fedotov, A. B.; Sidorov-Biryukov, D. A.; Nikitin, E. S.; Zheltikov, A. M.; Belousov, V. V. Thermogenetic Neurostimulation with Single-Cell Resolution. *Nat. Commun.* **2017**, *8* (1), 15362. <https://doi.org/10.1038/ncomms15362>.
- (168) Roshchin, M.; Ermakova, Y. G.; Lanin, A. A.; Chebotarev, A. S.; Kelmanson, I. V.; Balaban, P. M.; Zheltikov, A. M.; Belousov, V. V.; Nikitin, E. S. Thermogenetic Stimulation of Single Neocortical Pyramidal Neurons Transfected with TRPV1-L Channels. *Neurosci. Lett.* **2018**, *687* (September), 153–157.
<https://doi.org/10.1016/j.neulet.2018.09.038>.
- (169) Bernstein, J. G.; Garrity, P. A.; Boyden, E. S. Optogenetics and Thermogenetics: Technologies for Controlling the Activity of Targeted Cells within Intact Neural Circuits. *Curr. Opin. Neurobiol.* **2012**, *22* (1), 61–71.
<https://doi.org/10.1016/j.conb.2011.10.023>.
- (170) Yang, W.; Carrillo-Reid, L.; Bando, Y.; Peterka, D. S.; Yuste, R. Simultaneous Two-Photon Imaging and Two-Photon Optogenetics of Cortical Circuits in Three Dimensions. *Elife* **2018**, *7*, 1–21. <https://doi.org/10.7554/eLife.32671>.
- (171) Deng, W.; Goldys, E. M.; Farnham, M. M.; Pilowsky, P. M. Optogenetics, the Intersection between Physics and Neuroscience: Light Stimulation of Neurons in Physiological Conditions. *Am. J. Physiol. Integr. Comp. Physiol.* **2014**, *307* (11), R1292–R1302. <https://doi.org/10.1152/ajpregu.00072.2014>.
- (172) Hopt, A.; Neher, E. Highly Nonlinear Photodamage in Two-Photon Fluorescence Microscopy. *Biophys. J.* **2001**, *80* (4), 2029–2036. [https://doi.org/10.1016/S0006-3495\(01\)76173-5](https://doi.org/10.1016/S0006-3495(01)76173-5).
- (173) Ji, N.; Magee, J. C.; Betzig, E. High-Speed, Low-Photodamage Nonlinear Imaging Using Passive Pulse Splitters. *Nat. Methods* **2008**, *5* (2), 197–202.
<https://doi.org/10.1038/nmeth.1175>.
- (174) Vinberg, F.; Palczewska, G.; Zhang, J.; Komar, K.; Wojtkowski, M.; Kefalov, V. J.; Palczewski, K. Sensitivity of Mammalian Cone Photoreceptors to Infrared Light. *Neuroscience* **2019**, *416*, 100–108.
<https://doi.org/10.1016/j.neuroscience.2019.07.047>.

- (175) Hartmann, S.; Vogt, R.; Kunze, J.; Rauschert, A.; Kuhnert, K.-D.; Wanzenböck, J.; Lamatsch, D. K.; Witte, K. Zebrafish Larvae Show Negative Phototaxis to Near-Infrared Light. *PLoS One* **2018**, *13* (11), e0207264. <https://doi.org/10.1371/journal.pone.0207264>.
- (176) Emiliani, V.; Entcheva, E.; Hedrich, R.; Hegemann, P.; Konrad, K. R.; Lüscher, C.; Mahn, M.; Pan, Z. H.; Sims, R. R.; Vierock, J.; Yizhar, O. Optogenetics for Light Control of Biological Systems. *Nat. Rev. Methods Prim.* **2022**, *2* (1). <https://doi.org/10.1038/s43586-022-00136-4>.
- (177) Li, Y.; Guo, S.; Mattison, B.; Hu, J.; Man, K. N. M.; Yang, W. High-Speed Two-Photon Microscopy with Adaptive Line-Excitation. *Optica* **2024**, *11* (8), 1138. <https://doi.org/10.1364/optica.529930>.
- (178) Xu, C.; Nedergaard, M.; Fowell, D. J.; Friedl, P.; Ji, N. Multiphoton Fluorescence Microscopy for in Vivo Imaging. *Cell* **2024**, *187* (17), 4458–4487. <https://doi.org/10.1016/j.cell.2024.07.036>.
- (179) Prevedel, R.; Verhoef, A. J.; Pernía-Andrade, A. J.; Weisenburger, S.; Huang, B. S.; Nöbauer, T.; Fernández, A.; Delcour, J. E.; Golshani, P.; Baltuska, A.; Vaziri, A. Fast Volumetric Calcium Imaging across Multiple Cortical Layers Using Sculpted Light. *Nat. Methods* **2016**, *13* (12), 1021–1028. <https://doi.org/10.1038/nmeth.4040>.
- (180) Lu, R.; Sun, W.; Liang, Y.; Kerlin, A.; Bierfeld, J.; Seelig, J. D.; Wilson, D. E.; Scholl, B.; Mohar, B.; Tanimoto, M.; Koyama, M.; Fitzpatrick, D.; Orger, M. B.; Ji, N. Video-Rate Volumetric Functional Imaging of the Brain at Synaptic Resolution. *Nat. Neurosci.* **2017**, *20* (4), 620–628. <https://doi.org/10.1038/nn.4516>.
- (181) Song, A.; Charles, A. S.; Koay, S. A.; Gauthier, J. L.; Thiberge, S. Y.; Pillow, J. W.; Tank, D. W. Volumetric Two-Photon Imaging of Neurons Using Stereoscopy (VTWINS). *Nat. Methods* **2017**, *14* (4), 420–426. <https://doi.org/10.1038/nmeth.4226>.
- (182) Zhang, T.; Hernandez, O.; Chrapkiewicz, R.; Shai, A.; Wagner, M. J.; Zhang, Y.; Wu, C. H.; Li, J. Z.; Inoue, M.; Gong, Y.; Ahanonu, B.; Zeng, H.; Bito, H.; Schnitzer, M. J. Kilohertz Two-Photon Brain Imaging in Awake Mice. *Nat. Methods* **2019**, *16* (11), 1119–1122. <https://doi.org/10.1038/s41592-019-0597-2>.
- (183) Quirin, S.; Jackson, J.; Peterka, D. S.; Yuste, R. Simultaneous Imaging of Neural Activity in Three Dimensions. *Front. Neural Circuits* **2014**, *8* (APR). <https://doi.org/10.3389/fncir.2014.00029>.
- (184) Zhou, P.; Resendez, S. L.; Rodriguez-Romaguera, J.; Jimenez, J. C.; Neufeld, S. Q.; Giovannucci, A.; Friedrich, J.; Pnevmatikakis, E. A.; Stuber, G. D.; Hen, R.; Kheirbek, M. A.; Sabatini, B. L.; Kass, R. E.; Paninski, L. Efficient and Accurate Extraction of in Vivo Calcium Signals from Microendoscopic Video Data. *Elife* **2018**, *7*. <https://doi.org/10.7554/eLife.28728>.
- (185) Nöbauer, T.; Skocek, O.; Pernía-Andrade, A. J.; Weilguny, L.; Traub, F. M.; Molodtsov, M. I.; Vaziri, A. Video Rate Volumetric Ca²⁺ Imaging across Cortex Using Seeded Iterative Demixing (SID) Microscopy. *Nat. Methods* **2017**, *14* (8), 811–818. <https://doi.org/10.1038/nmeth.4341>.
- (186) Pnevmatikakis, E. A.; Soudry, D.; Gao, Y.; Machado, T. A.; Merel, J.; Pfau, D.; Reardon, T.; Mu, Y.; Lacefield, C.; Yang, W.; Ahrens, M.; Bruno, R.; Jessell, T. M.; Peterka, D. S.; Yuste, R.; Paninski, L. Simultaneous Denoising, Deconvolution, and Demixing of Calcium Imaging Data. *Neuron* **2016**, *89* (2), 285. <https://doi.org/10.1016/j.neuron.2015.11.037>.
- (187) Rimoli, C. V.; Moretti, C.; Soldevila, F.; Brémont, E.; Ventalon, C.; Gigan, S. Demixing

- Fluorescence Time Traces Transmitted by Multimode Fibers. *Nat. Commun.* **2024**, *15* (1), 6286. <https://doi.org/10.1038/s41467-024-50306-z>.
- (188) Moretti, C.; Gigan, S. Readout of Fluorescence Functional Signals through Highly Scattering Tissue. *Nat. Photonics* **2020**, *14* (6), 361–364. <https://doi.org/10.1038/s41566-020-0612-2>.
- (189) Ducros, M.; Houssem, Y. G.; Bradley, J.; De Sars, V.; Charpak, S. Encoded Multisite Two-Photon Microscopy. *Proc. Natl. Acad. Sci. U. S. A.* **2013**, *110* (32), 13138–13143. <https://doi.org/10.1073/pnas.1307818110>.
- (190) Escobet-Montalbán, A.; Spesyvtsev, R.; Chen, M.; Saber, W. A.; Andrews, M.; Herrington, C. S.; Mazilu, M.; Dholakia, K. Wide-Field Multiphoton Imaging through Scattering Media without Correction. *Sci. Adv.* **2018**, *4* (10). <https://doi.org/10.1126/sciadv.aau1338>.
- (191) Izquierdo-Serra, M.; Hirtz, J. J.; Shababo, B.; Yuste, R. Two-Photon Optogenetic Mapping of Excitatory Synaptic Connectivity and Strength. *iScience* **2018**, *8*, 15–28. <https://doi.org/10.1016/j.isci.2018.09.008>.
- (192) Hage, T. A.; Bosma-Moody, A.; Baker, C. A.; Kratz, M. B.; Campagnola, L.; Jarsky, T.; Zeng, H.; Murphy, G. J. Synaptic Connectivity to L2/3 of Primary Visual Cortex Measured by Two-Photon Optogenetic Stimulation. *Elife* **2022**, *11*, 1–46. <https://doi.org/10.7554/elife.71103>.
- (193) Printz, Y.; Patil, P.; Mahn, M.; Benjamin, A.; Litvin, A.; Levy, R.; Bringmann, M.; Yizhar, O. Determinants of Functional Synaptic Connectivity among Amygdala-Projecting Prefrontal Cortical Neurons in Male Mice. *Nat. Commun.* **2023**, *14* (1). <https://doi.org/10.1038/s41467-023-37318-x>.
- (194) Triplett, M. A.; Gajowa, M.; Antin, B.; Sadahiro, M.; Adesnik, H.; Paninski, L. Rapid Learning of Neural Circuitry from Holographic Ensemble Stimulation Enabled by Model-Based Compressed Sensing. *bioRxiv* **2022**, 2022–09. <https://doi.org/10.1101/2022.09.14.507926>.
- (195) McRaven, C.; Tanese, D.; Zhang, L.; Yang, C.-T.; Ahrens, M.; Emiliani, V.; Koyama, M. High-Throughput Cellular-Resolution Synaptic Connectivity Mapping in Vivo with Concurrent Two-Photon Optogenetics and Volumetric Ca²⁺ Imaging. *bioRxiv* **2020**, 2020.02.21.959650.
- (196) Chen, I.-W.; Chan, C. Y.; Navarro, P.; de Sars, V.; Ronzitti, E.; Oweiss, K.; Tanese, D.; Emiliani, V. High-Throughput in Vivo Synaptic Connectivity Mapping of Neuronal Micro-Circuits Using Two-Photon Holographic Optogenetics and Compressive Sensing. *bioRxiv* **2023**. <https://doi.org/10.1101/2023.09.11.557026>.
- (197) Dmitri, C. Reconstruction of Sparse Circuits Using Multi-Neuronal Excitation (RESCUME). *Front. Neurosci.* **2010**, *4*. <https://doi.org/10.3389/conf.fnins.2010.03.00067>.
- (198) Navarro, P.; Oweiss, K. Compressive Sensing of Functional Connectivity Maps from Patterned Optogenetic Stimulation of Neuronal Ensembles. *Patterns* **2023**, *4* (10), 100845. <https://doi.org/10.1016/j.patter.2023.100845>.
- (199) Shababo, B.; Paige, B.; Pakman, A.; Paninski, L. Bayesian Inference and Online Experimental Design for Mapping Neural Microcircuits. In *Advances in Neural Information Processing Systems*; 2013; pp 1–9.
- (200) Xue, Y.; Waller, L.; Adesnik, H.; Pégard, N. Three-Dimensional Multi-Site Random Access Photostimulation (3D-MAP). *Elife* **2022**, *11*, 1–27. <https://doi.org/10.7554/eLife.73266>.

- (201) Rani, M.; Dhok, S. B.; Deshmukh, R. B. A Systematic Review of Compressive Sensing: Concepts, Implementations and Applications. *IEEE Access* **2018**, *6*, 4875–4894. <https://doi.org/10.1109/ACCESS.2018.2793851>.
- (202) Gigan, S.; Katz, O.; de Aguiar, H. B.; Andresen, E. R.; Aubry, A.; Bertolotti, J.; Bossy, E.; Bouchet, D.; Brake, J.; Brasselet, S.; Bromberg, Y.; Cao, H.; Chaigne, T.; Cheng, Z.; Choi, W.; Čížmár, T.; Cui, M.; Curtis, V. R.; Defienne, H.; Hofer, M.; Horisaki, R.; Horstmeyer, R.; Ji, N.; LaViolette, A. K.; Mertz, J.; Moser, C.; Mosk, A. P.; Pégard, N. C.; Piestun, R.; Popoff, S.; Phillips, D. B.; Psaltis, D.; Rahmani, B.; Rigneault, H.; Rotter, S.; Tian, L.; Vellekoop, I. M.; Waller, L.; Wang, L.; Weber, T.; Xiao, S.; Xu, C.; Yamilov, A.; Yang, C.; Yılmaz, H. Roadmap on Wavefront Shaping and Deep Imaging in Complex Media. *J. Phys. Photonics* **2022**, *4* (4), 042501. <https://doi.org/10.1088/2515-7647/ac76f9>.
- (203) Horton, N. G.; Wang, K.; Kobat, D.; Clark, C. G.; Wise, F. W.; Schaffer, C. B.; Xu, C. In Vivo Three-Photon Microscopy of Subcortical Structures within an Intact Mouse Brain. *Nat. Photonics* **2013**, *7* (3), 205–209. <https://doi.org/10.1038/nphoton.2012.336>.
- (204) Akerboom, J.; Carreras Calderón, N.; Tian, L.; Wabnig, S.; Prigge, M.; Tolö, J.; Gordus, A.; Orger, M. B.; Severi, K. E.; Macklin, J. J.; Patel, R.; Pulver, S. R.; Wardill, T. J.; Fischer, E.; Schüler, C.; Chen, T.-W.; Sarkisyan, K. S.; Marvin, J. S.; Bargmann, C. I.; Kim, D. S.; Kügler, S.; Lagnado, L.; Hegemann, P.; Gottschalk, A.; Schreiter, E. R.; Looger, L. L. Genetically Encoded Calcium Indicators for Multi-Color Neural Activity Imaging and Combination with Optogenetics. *Front. Mol. Neurosci.* **2013**, *6* (FEB), 1–29. <https://doi.org/10.3389/fnmol.2013.00002>.
- (205) Forli, A.; Vecchia, D.; Binini, N.; Succol, F.; Bovetti, S.; Moretti, C.; Nespoli, F.; Mahn, M.; Baker, C. A.; Bolton, M. M.; Yizhar, O.; Fellin, T. Two-Photon Bidirectional Control and Imaging of Neuronal Excitability with High Spatial Resolution In Vivo. *Cell Rep.* **2018**, *22* (11), 3087–3098. <https://doi.org/10.1016/j.celrep.2018.02.063>.
- (206) Kobat, D.; Horton, N. G.; Xu, C. In Vivo Two-Photon Microscopy to 1.6-Mm Depth in Mouse Cortex. *J. Biomed. Opt.* **2011**, *16* (10), 106014. <https://doi.org/10.1117/1.3646209>.
- (207) Cheng, X.; Sadegh, S.; Zilpelwar, S.; Devor, A.; Tian, L.; Boas, D. A. Comparing the Fundamental Imaging Depth Limit of Two-Photon, Three-Photon, and Non-Degenerate Two-Photon Microscopy. *Opt. Lett.* **2020**, *45* (10), 2934. <https://doi.org/10.1364/ol.392724>.
- (208) Theer, P.; Hasan, M. T.; Denk, W. Two-Photon Imaging to a Depth of 1000 Mm in Living Brains by Use of a Ti:Al₂O₃ Regenerative Amplifier. *Opt. Lett.* **2003**, *28* (12), 1022. <https://doi.org/10.1364/OL.28.001022>.
- (209) Bharioke, A.; Munz, M.; Brignall, A.; Kosche, G.; Eizinger, M. F.; Ledergerber, N.; Hillier, D.; Gross-Scherf, B.; Conzelmann, K. K.; Macé, E.; Roska, B. General Anesthesia Globally Synchronizes Activity Selectively in Layer 5 Cortical Pyramidal Neurons. *Neuron* **2022**, *110* (12), 2024–2040.e10. <https://doi.org/10.1016/j.neuron.2022.03.032>.
- (210) Francioni, V.; Padamsey, Z.; Rochefort, N. L. High and Asymmetric Somato-Dendritic Coupling of v1 Layer 5 Neurons Independent of Visual Stimulation and Locomotion. *Elife* **2019**, *8*, 1–25. <https://doi.org/10.7554/eLife.49145>.
- (211) Weisenburger, S.; Tejera, F.; Demas, J.; Chen, B.; Manley, J.; Sparks, F. T.; Martínez Traub, F.; Daigle, T.; Zeng, H.; Losonczy, A.; Vaziri, A. Volumetric Ca²⁺ Imaging in the Mouse Brain Using Hybrid Multiplexed Sculpted Light Microscopy. *Cell* **2019**, *177* (4),

- 1050-1066.e14. <https://doi.org/10.1016/j.cell.2019.03.011>.
- (212) Voigts, J.; Deister, C. A.; Moore, C. I. Layer Ensembles Can Selectively Regulate the Behavioral Impact and Layer-Specific Representation of Sensory Deviants. *Elife* **2020**, *9*, 1–39. <https://doi.org/10.7554/eLife.48957>.
- (213) Dana, H.; Mohar, B.; Sun, Y.; Narayan, S.; Gordus, A.; Hasseman, J. P.; Tsegaye, G.; Holt, G. T.; Hu, A.; Walpita, D.; Patel, R.; Macklin, J. J.; Bargmann, C. I.; Ahrens, M. B.; Schreiter, E. R.; Jayaraman, V.; Looger, L. L.; Svoboda, K.; Kim, D. S. Sensitive Red Protein Calcium Indicators for Imaging Neural Activity. *Elife* **2016**, *5* (MARCH2016), 1–24. <https://doi.org/10.7554/eLife.12727>.
- (214) Wang, T.; Xu, C. Three-Photon Neuronal Imaging in Deep Mouse Brain. *Optica* **2020**, *7* (8), 947. <https://doi.org/10.1364/optica.395825>.
- (215) Xiao, Y.; Deng, P.; Zhao, Y.; Yang, S.; Li, B. Three-Photon Excited Fluorescence Imaging in Neuroscience: From Principles to Applications. *Front. Neurosci.* **2023**, *17* (February), 1–21. <https://doi.org/10.3389/fnins.2023.1085682>.
- (216) Wang, T.; Wu, C.; Ouzounov, D. G.; Gu, W.; Xia, F.; Kim, M.; Yang, X.; Warden, M. R.; Xu, C. Quantitative Analysis of 1300-Nm Three-Photon Calcium Imaging in the Mouse Brain. *Elife* **2020**, *9*. <https://doi.org/10.7554/eLife.53205>.
- (217) Yildirim, M.; Sugihara, H.; So, P. T. C.; Sur, M. Functional Imaging of Visual Cortical Layers and Subplate in Awake Mice with Optimized Three-Photon Microscopy. *Nat. Commun.* **2019**, *10* (1). <https://doi.org/10.1038/s41467-018-08179-6>.
- (218) Xu, C.; Webb, W. W. Measurement of Two-Photon Excitation Cross Sections of Molecular Fluorophores with Data from 690 to 1050 Nm. *J. Opt. Soc. Am. B* **1996**, *13* (3), 481. <https://doi.org/10.1364/josab.13.000481>.
- (219) Ouzounov, D. G.; Wang, T.; Wang, M.; Feng, D. D.; Horton, N. G.; Cruz-Hernández, J. C.; Cheng, Y. T.; Reimer, J.; Tolia, A. S.; Nishimura, N.; Xu, C. In Vivo Three-Photon Imaging of Activity of Gcamp6-Labeled Neurons Deep in Intact Mouse Brain. *Nat. Methods* **2017**, *14* (4), 388–390. <https://doi.org/10.1038/nmeth.4183>.
- (220) Tao, X.; Lu, J.; Lam, T.; Rodriguez, R.; Zuo, Y.; Kubby, J. A Three-Photon Microscope with Adaptive Optics for Deep-Tissue in Vivo Structural and Functional Brain Imaging. *Neural Imaging Sens.* **2017**, *10051*, 100510R. <https://doi.org/10.1117/12.2253922>.
- (221) Wang, T.; Ouzounov, D. G.; Wu, C.; Horton, N. G.; Zhang, B.; Wu, C. H.; Zhang, Y.; Schnitzer, M. J.; Xu, C. Three-Photon Imaging of Mouse Brain Structure and Function through the Intact Skull. *Nat. Methods* **2018**, *15* (10), 789–792. <https://doi.org/10.1038/s41592-018-0115-y>.
- (222) Klioutchnikov, A.; Wallace, D. J.; Frosz, M. H.; Zeltner, R.; Sawinski, J.; Pawlak, V.; Voit, K. M.; Russell, P. S. J.; Kerr, J. N. D. Three-Photon Head-Mounted Microscope for Imaging Deep Cortical Layers in Freely Moving Rats. *Nat. Methods* **2020**, *17* (5), 509–513. <https://doi.org/10.1038/s41592-020-0817-9>.
- (223) Theer, P.; Denk, W. On the Fundamental Imaging-Depth Limit in Two-Photon Microscopy. *J. Opt. Soc. Am. A* **2006**, *23* (12), 3139. <https://doi.org/10.1364/JOSAA.23.003139>.
- (224) Takasaki, K.; Abbasi-Asl, R.; Waters, J. Superficial Bound of the Depth Limit of Two-Photon Imaging in Mouse Brain. *eNeuro* **2020**, *7* (1), 1–10. <https://doi.org/10.1523/ENEURO.0255-19.2019>.
- (225) Wang, K.; Horton, N. G.; Charan, K.; Xu, C. Advanced Fiber Soliton Sources for Nonlinear Deep Tissue Imaging in Biophotonics. *IEEE J. Sel. Top. Quantum Electron.* **2014**, *20* (2). <https://doi.org/10.1109/JSTQE.2013.2276860>.

- (226) Liu, H.; Deng, X.; Tong, S.; He, C.; Cheng, H.; Zhuang, Z.; Gan, M.; Li, J.; Xie, W.; Qiu, P.; Wang, K. In Vivo Deep-Brain Structural and Hemodynamic Multiphoton Microscopy Enabled by Quantum Dots. *Nano Lett.* **2019**, *19* (8), 5260–5265. <https://doi.org/10.1021/acs.nanolett.9b01708>.
- (227) Sun, B.; Wang, M.; Hoerder-Suabedissen, A.; Xu, C.; Packer, A. M.; Szele, F. G. Intravital Imaging of the Murine Subventricular Zone with Three Photon Microscopy. *Cereb. Cortex* **2022**, *32* (14), 3057–3067. <https://doi.org/10.1093/cercor/bhab400>.
- (228) Zhao, C.; Chen, S.; Zhang, L.; Zhang, D.; Wu, R.; Hu, Y.; Zeng, F.; Li, Y.; Wu, D.; Yu, F.; Zhang, Y.; Zhang, J.; Chen, L.; Wang, A.; Cheng, H. Miniature Three-Photon Microscopy Maximized for Scattered Fluorescence Collection. *Nat. Methods* **2023**. <https://doi.org/10.1038/s41592-023-01777-3>.
- (229) Wang, Y.; Wen, W.; Wang, K.; Zhai, P.; Qiu, P.; Wang, K. Measurement of Absorption Spectrum of Deuterium Oxide (D₂O) and Its Application to Signal Enhancement in Multiphoton Microscopy at the 1700-Nm Window. *Appl. Phys. Lett.* **2016**, *108* (2). <https://doi.org/10.1063/1.4939970>.
- (230) Wang, K.; Liang, R.; Qiu, P. Fluorescence Signal Generation Optimization by Optimal Filling of the High Numerical Aperture Objective Lens for High-Order Deep-Tissue Multiphoton Fluorescence Microscopy. *IEEE Photonics J.* **2015**, *7* (6), 1–8. <https://doi.org/10.1109/JPHOT.2015.2505145>.
- (231) Streich, L.; Boffi, J. C.; Wang, L.; Alhalaseh, K.; Barbieri, M.; Rehm, R.; Deivasigamani, S.; Gross, C. T.; Agarwal, A.; Prevedel, R. High-Resolution Structural and Functional Deep Brain Imaging Using Adaptive Optics Three-Photon Microscopy. *Nat. Methods* **2021**, *18* (10), 1253–1258. <https://doi.org/10.1038/s41592-021-01257-6>.
- (232) Rodríguez, C.; Chen, A.; Rivera, J. A.; Mohr, M. A.; Liang, Y.; Natan, R. G.; Sun, W.; Milkie, D. E.; Bifano, T. G.; Chen, X.; Ji, N. An Adaptive Optics Module for Deep Tissue Multiphoton Imaging in Vivo. *Nat. Methods* **2021**, *18* (10), 1259–1264. <https://doi.org/10.1038/s41592-021-01279-0>.
- (233) Sinefeld, D.; Xia, F.; Wang, M.; Wang, T.; Wu, C.; Yang, X.; Paudel, H. P.; Ouzounov, D. G.; Bifano, T. G.; Xu, C. Three-Photon Adaptive Optics for Mouse Brain Imaging. *Front. Neurosci.* **2022**, *16* (May), 1–10. <https://doi.org/10.3389/fnins.2022.880859>.
- (234) Qin, Z.; She, Z.; Chen, C.; Wu, W.; Lau, J. K. Y.; Ip, N. Y.; Qu, J. Y. Deep Tissue Multi-Photon Imaging Using Adaptive Optics with Direct Focus Sensing and Shaping. *Nat. Biotechnol.* **2022**, *40* (11), 1663–1671. <https://doi.org/10.1038/s41587-022-01343-w>.
- (235) Zinter, J. P.; Levene, M. J. Maximizing Fluorescence Collection Efficiency in Multiphoton Microscopy. *Opt. Express* **2011**, *19* (16), 15348. <https://doi.org/10.1364/oe.19.015348>.
- (236) Singh, A.; McMullen, J. D.; Doris, E. A.; Zipfel, W. R. Comparison of Objective Lenses for Multiphoton Microscopy in Turbid Samples. *Biomed. Opt. Express* **2015**, *6* (8), 3113. <https://doi.org/10.1364/boe.6.003113>.
- (237) Beaurepaire, E.; Oheim, M.; Mertz, J. Ultra-Deep Two-Photon Fluorescence Excitation in Turbid Media. *Opt. Commun.* **2001**, *188* (1–4), 25–29. [https://doi.org/10.1016/S0030-4018\(00\)01156-1](https://doi.org/10.1016/S0030-4018(00)01156-1).
- (238) Wang, K.; Wang, Y.; Wang, K.; Wen, W.; Qiu, P. Comparison of Signal Detection of GaAsP and GaAs PMTs for Multiphoton Microscopy at the 1700-Nm Window. *IEEE Photonics J.* **2016**, *8* (3), 1–6. <https://doi.org/10.1109/JPHOT.2016.2570005>.
- (239) Rowlands, C. J.; Park, D.; Bruns, O. T.; Piatkevich, K. D.; Fukumura, D.; Jain, R. K.; Bawendi, M. G.; Boyden, E. S.; So, P. T. C. Wide-Field Three-Photon Excitation in

- Biological Samples. *Light Sci. Appl.* **2016**, *6* (5), e16255–e16255.
<https://doi.org/10.1038/lisa.2016.255>.
- (240) Sinefeld, D.; Paudel, H. P.; Ouzounov, D. G.; Bifano, T. G.; Xu, C. Adaptive Optics in Multiphoton Microscopy: Comparison of Two, Three and Four Photon Fluorescence. *Opt. Express* **2015**, *23* (24), 31472. <https://doi.org/10.1364/oe.23.031472>.
- (241) Sun, W.; Tan, Z.; Mensh, B. D.; Ji, N. Thalamus Provides Layer 4 of Primary Visual Cortex with Orientation- and Direction-Tuned Inputs. *Nat. Neurosci.* **2016**, *19* (2), 308–315. <https://doi.org/10.1038/nn.4196>.
- (242) Wang, K.; Sun, W.; Richie, C. T.; Harvey, B. K.; Betzig, E.; Ji, N. Direct Wavefront Sensing for High-Resolution in Vivo Imaging in Scattering Tissue. *Nat. Commun.* **2015**, *6*, 1–6. <https://doi.org/10.1038/ncomms8276>.
- (243) Tuchin, V. V. *Tissue Optics: Light Scattering Methods and Instruments for Medical Diagnosis*; Society of Photo-Optical Instrumentation Engineers (SPIE), 2015.
<https://doi.org/10.1117/3.1003040>.
- (244) Hampson, K. M.; Turcotte, R.; Miller, D. T.; Kurokawa, K.; Males, J. R.; Ji, N.; Booth, M. J. Adaptive Optics for High-Resolution Imaging. *Nat. Rev. Methods Prim.* **2021**, *1* (1).
<https://doi.org/10.1038/s43586-021-00066-7>.
- (245) Liu, R.; Li, Z.; Marvin, J. S.; Kleinfeld, D. Direct Wavefront Sensing Enables Functional Imaging of Infragranular Axons and Spines. *Nat. Methods* **2019**, *16* (7), 615–618.
<https://doi.org/10.1038/s41592-019-0434-7>.
- (246) Ji, N.; Sato, T. R.; Betzig, E. Characterization and Adaptive Optical Correction of Aberrations during in Vivo Imaging in the Mouse Cortex. *Proc. Natl. Acad. Sci. U. S. A.* **2012**, *109* (1), 22–27. <https://doi.org/10.1073/pnas.1109202108>.
- (247) Zhang, Q.; Hu, Q.; Berlage, C.; Kner, P.; Judkewitz, B.; Booth, M.; Ji, N. Adaptive Optics for Optical Microscopy [Invited]. *Biomed. Opt. Express* **2023**, *14* (4), 1732.
<https://doi.org/10.1364/BOE.479886>.
- (248) Rodríguez, C.; Ji, N. Adaptive Optical Microscopy for Neurobiology. *Curr. Opin. Neurobiol.* **2018**, *50*, 83–91. <https://doi.org/10.1016/j.conb.2018.01.011>.
- (249) Wang, K.; Milkie, D. E.; Saxena, A.; Engerer, P.; Misgeld, T.; Bronner, M. E.; Mumm, J.; Betzig, E. Rapid Adaptive Optical Recovery of Optimal Resolution over Large Volumes. *Nat. Methods* **2014**, *11* (6), 625–628. <https://doi.org/10.1038/nmeth.2925>.
- (250) Yao, P.; Liu, R.; Broggin, T.; Thunemann, M.; Kleinfeld, D. Construction and Use of an Adaptive Optics Two-Photon Microscope with Direct Wavefront Sensing. *Nat. Protoc.* **2023**, *18* (12). <https://doi.org/10.1038/s41596-023-00893-w>.
- (251) Aviles-Espinosa, R.; Andilla, J.; Porcar-Guezenc, R.; Olarte, O. E.; Nieto, M.; Levecq, X.; Artigas, D.; Loza-Alvarez, P. Measurement and Correction of in Vivo Sample Aberrations Employing a Nonlinear Guide-Star in Two-Photon Excited Fluorescence Microscopy. *Biomed. Opt. Express* **2011**, *2* (11).
<https://doi.org/10.1364/boe.2.003135>.
- (252) Ji, N.; Milkie, D. E.; Betzig, E. Adaptive Optics via Pupil Segmentation for High-Resolution Imaging in Biological Tissues. *Nat. Methods* **2010**, *7* (2).
<https://doi.org/10.1038/nmeth.1411>.
- (253) Wang, C.; Liu, R.; Milkie, D. E.; Sun, W.; Tan, Z.; Kerlin, A.; Chen, T. W.; Kim, D. S.; Ji, N. Multiplexed Aberration Measurement for Deep Tissue Imaging in Vivo. *Nat. Methods* **2014**, *11* (10). <https://doi.org/10.1038/nmeth.3068>.
- (254) Champelovier, D.; Teixeira, J.; Conan, J. M.; Balla, N.; Mugnier, L. M.; Tressard, T.; Reichinnek, S.; Meimon, S.; Cossart, R.; Rigneault, H.; Monneret, S.; Malvache, A.

- Image-Based Adaptive Optics for in Vivo Imaging in the Hippocampus. *Sci. Rep.* **2017**, 7. <https://doi.org/10.1038/srep42924>.
- (255) Débarre, D.; Botcherby, E. J.; Watanabe, T.; Srinivas, S.; Booth, M. J.; Wilson, T. Image-Based Adaptive Optics for Two-Photon Microscopy. *Opt. Lett.* **2009**, 34 (16), 2495. <https://doi.org/10.1364/OL.34.002495>.
- (256) Li, Z.; Zhang, Q.; Chou, S. W.; Newman, Z.; Turcotte, R.; Natan, R.; Dai, Q.; Isacoff, E. Y.; Ji, N. Fast Widefield Imaging of Neuronal Structure and Function with Optical Sectioning in Vivo. *Sci. Adv.* **2020**, 6 (19). <https://doi.org/10.1126/sciadv.aaz3870>.
- (257) Sohmen, M.; Muñoz-Bolaños, J. D.; Rajaeipour, P.; Ritsch-Martens, M.; Ataman, Ç.; Jesacher, A. Optofluidic Adaptive Optics in Multi-Photon Microscopy. *Biomed. Opt. Express* **2023**, 14 (4). <https://doi.org/10.1364/boe.481453>.
- (258) Chung, C. L.; Furieri, T.; Lin, J. Y.; Chang, T. C.; Lee, J. C.; Chen, Y. F.; Pan, M. K.; Bonora, S.; Chu, S. W. Plug-And-Play Adaptive Optics for Two Photon High-Speed Volumetric Imaging. *JPhys Photonics* **2022**, 4 (2). <https://doi.org/10.1088/2515-7647/ac6120>.
- (259) Xia, F.; Rimoli, C. V.; Akemann, W.; Ventalon, C.; Bourdieu, L.; Gigan, S.; de Aguiar, H. B. Neurophotonics beyond the Surface: Unmasking the Brain's Complexity Exploiting Optical Scattering. *Neurophotonics* **2024**, 11 (S1), 1–14. <https://doi.org/10.1117/1.NPh.11.S1.S11510>.
- (260) Wu, T.; Zhang, Y.; Blochet, B.; Arjmand, P.; Berto, P.; Guillon, M. Single-Shot Digital Optical Fluorescence Phase Conjugation through Forward Multiple-Scattering Samples. *Sci. Adv.* **2024**, 10 (3), 1–10. <https://doi.org/10.1126/sciadv.adi1120>.
- (261) Vellekoop, I. M.; Mosk, A. P. Focusing Coherent Light through Opaque Strongly Scattering Media. *Opt. Lett.* **2007**, 32 (16), 2309. <https://doi.org/10.1364/OL.32.002309>.
- (262) Katz, O.; Small, E.; Guan, Y.; Silberberg, Y. Noninvasive Nonlinear Focusing and Imaging through Strongly Scattering Turbid Layers. *Optica* **2014**, 1 (3), 170. <https://doi.org/10.1364/OPTICA.1.000170>.
- (263) Qureshi, M. M.; Brake, J.; Jeon, H.-J.; Ruan, H.; Liu, Y.; Safi, A. M.; Eom, T. J.; Yang, C.; Chung, E. In Vivo Study of Optical Speckle Decorrelation Time across Depths in the Mouse Brain. *Biomed. Opt. Express* **2017**, 8 (11). <https://doi.org/10.1364/boe.8.004855>.
- (264) Blochet, B.; Joaquina, K.; Blum, L.; Bourdieu, L.; Gigan, S. Enhanced Stability of the Focus Obtained by Wavefront Optimization in Dynamical Scattering Media. *Optica* **2019**, 6 (12). <https://doi.org/10.1364/optica.6.001554>.
- (265) Boniface, A.; Dong, J.; Gigan, S. Non-Invasive Focusing and Imaging in Scattering Media with a Fluorescence-Based Transmission Matrix. *Nat. Commun.* **2020**, 11 (1), 6154. <https://doi.org/10.1038/s41467-020-19696-8>.
- (266) Popoff, S. M.; Lerosey, G.; Carminati, R.; Fink, M.; Boccara, A. C.; Gigan, S. Measuring the Transmission Matrix in Optics: An Approach to the Study and Control of Light Propagation in Disordered Media. *Phys. Rev. Lett.* **2010**, 104 (10), 100601. <https://doi.org/10.1103/PhysRevLett.104.100601>.
- (267) Zhao, S.; Rauer, B.; Valzania, L.; Dong, J.; Liu, R.; Li, F.; Gigan, S.; de Aguiar, H. B. Single-Pixel Transmission Matrix Recovery via Two-Photon Fluorescence. *Sci. Adv.* **2024**, 10 (3), 1–7. <https://doi.org/10.1126/sciadv.adi3442>.
- (268) Tang, J.; Germain, R. N.; Cui, M. Superpenetration Optical Microscopy by Iterative Multiphoton Adaptive Compensation Technique. *Proc. Natl. Acad. Sci. U. S. A.* **2012**,

- 109 (22), 8434–8439. <https://doi.org/10.1073/pnas.1119590109>.
- (269) Papadopoulos, I. N.; Jouhanneau, J. S.; Poulet, J. F. A.; Judkewitz, B. Scattering Compensation by Focus Scanning Holographic Aberration Probing (F-SHARP). *Nat. Photonics* **2017**, *11* (2), 116–123. <https://doi.org/10.1038/nphoton.2016.252>.
- (270) May, M. A.; Barré, N.; Kummer, K. K.; Kress, M.; Ritsch-Marte, M.; Jesacher, A. Fast Holographic Scattering Compensation for Deep Tissue Biological Imaging. *Nat. Commun.* **2021**, *12* (1). <https://doi.org/10.1038/s41467-021-24666-9>.
- (271) Park, J. H.; Sun, W.; Cui, M. High-Resolution in Vivo Imaging of Mouse Brain through the Intact Skull. *Proc. Natl. Acad. Sci. U. S. A.* **2015**, *112* (30). <https://doi.org/10.1073/pnas.1505939112>.
- (272) Park, J. H.; Kong, L.; Zhou, Y.; Cui, M. Large-Field-of-View Imaging by Multi-Pupil Adaptive Optics. *Nat. Methods* **2017**, *14* (6), 581–583. <https://doi.org/10.1038/nmeth.4290>.
- (273) Blochet, B.; Akemann, W.; Gigan, S.; Bourdieu, L. Fast Wavefront Shaping for Two-Photon Brain Imaging with Multipatch Correction. *Proc. Natl. Acad. Sci.* **2023**, *120* (51). <https://doi.org/10.1073/pnas.2305593120>.
- (274) Zhu, L.; Boutet de Monvel, J.; Berto, P.; Brasselet, S.; Gigan, S.; Guillon, M. Chromato-Axial Memory Effect through a Forward-Scattering Slab. *Optica* **2020**, *7* (4), 338. <https://doi.org/10.1364/OPTICA.382209>.
- (275) Wu, T.; Berto, P.; Guillon, M. Reference-Less Complex Wavefields Characterization with a High-Resolution Wavefront Sensor. *Appl. Phys. Lett.* **2021**, *118* (25). <https://doi.org/10.1063/5.0050036>.
- (276) Wu, T.; Guillon, M.; Tessier, G.; Berto, P. Multiplexed Wavefront Sensing with a Thin Diffuser. *Optica* **2024**, *11* (2), 297. <https://doi.org/10.1364/OPTICA.500780>.
- (277) Tzang, O.; Niv, E.; Singh, S.; Labouesse, S.; Myatt, G.; Piestun, R. Wavefront Shaping in Complex Media with a 350 KHz Modulator via a 1D-to-2D Transform. *Nat. Photonics* **2019**, *13* (11), 788–793. <https://doi.org/10.1038/s41566-019-0503-6>.
- (278) Zhou, Z. C.; Gordon-Fennell, A.; Piantadosi, S. C.; Ji, N.; Smith, S. L. V.; Bruchas, M. R.; Stuber, G. D. Deep-Brain Optical Recording of Neural Dynamics during Behavior. *Neuron* **2023**, *111* (23), 3716–3738. <https://doi.org/10.1016/j.neuron.2023.09.006>.
- (279) Jung, J. C.; Schnitzer, M. J. Multiphoton Endoscopy. *Opt. Lett.* **2003**, *28* (11), 902. <https://doi.org/10.1364/ol.28.000902>.
- (280) Attardo, A.; Fitzgerald, J. E.; Schnitzer, M. J. Impermanence of Dendritic Spines in Live Adult CA1 Hippocampus. *Nature* **2015**, *523* (7562), 592–596. <https://doi.org/10.1038/nature14467>.
- (281) Wang, C.; Ji, N. Characterization and Improvement of Three-Dimensional Imaging Performance of GRIN-Lens-Based Two-Photon Fluorescence Endomicroscopes with Adaptive Optics. *Opt. Express* **2013**, *21* (22), 27142. <https://doi.org/10.1364/OE.21.027142>.
- (282) Li, Y.; Cheng, Z.; Wang, C.; Lin, J.; Jiang, H.; Cui, M. Geometric Transformation Adaptive Optics (GTAO) for Volumetric Deep Brain Imaging through Gradient-Index Lenses. *Nat. Commun.* **2024**, *15* (1). <https://doi.org/10.1038/s41467-024-45434-5>.
- (283) Qin, Z.; Chen, C.; He, S.; Wang, Y.; Tam, K. F.; Ip, N. Y.; Qu, J. Y. Adaptive Optics Two-Photon Endomicroscopy Enables Deep-Brain Imaging at Synaptic Resolution over Large Volumes. *Sci. Adv.* **2020**, *6* (40), 2020.05.29.124727. <https://doi.org/10.1126/sciadv.abc6521>.
- (284) Antonini, A.; Sattin, A.; Moroni, M.; Bovetti, S.; Moretti, C.; Succol, F.; Forli, A.;

- Vecchia, D.; Rajamanickam, V. P.; Bertocini, A.; Panzeri, S.; Liberale, C.; Fellin, T. Extended Field-of-View Ultrathin Microendoscopes for High-Resolution Two-Photon Imaging with Minimal Invasiveness. *Elife* **2020**, *9*, 1–76. <https://doi.org/10.7554/eLife.58882>.
- (285) Sattin, A.; Nardin, C.; Daste, S.; Moroni, M.; Reddy, I.; Liberale, C.; Panzeri, S.; Fleischmann, A.; Fellin, T. Aberration Correction in Long GRIN Lens-Based Microendoscopes for Extended Field-of-View Two-Photon Imaging in Deep Brain Regions. *bioRxiv* **2024**, 2024.07.24.604890. <https://doi.org/10.7554/eLife.101420.1>.
- (286) Stark, S. L.; Gross, H.; Reglinski, K.; Messerschmidt, B.; Eggeling, C. Field Curvature Reduction in Miniaturized High Numerical Aperture and Large Field-of-View Objective Lenses with Sub 1 Mm Lateral Resolution. *Biomed. Opt. Express* **2023**, *14* (12), 6190. <https://doi.org/10.1364/boe.499785>.
- (287) Accanto, N.; Chen, I. W.; Ronzitti, E.; Molinier, C.; Tourain, C.; Papagiakoumou, E.; Emiliani, V. Multiplexed Temporally Focused Light Shaping through a Gradient Index Lens for Precise In-Depth Optogenetic Photostimulation. *Sci. Rep.* **2019**, *9* (1), 1–10. <https://doi.org/10.1038/s41598-019-43933-w>.
- (288) Piantadosi, S. C.; Zhou, Z. C.; Pizzano, C.; Pedersen, C. E.; Nguyen, T. K.; Thai, S.; Stuber, G. D.; Bruchas, M. R. Holographic Stimulation of Opposing Amygdala Ensembles Bidirectionally Modulates Valence-Specific Behavior via Mutual Inhibition. *Neuron* **2024**, *112* (4), 593-610.e5. <https://doi.org/10.1016/j.neuron.2023.11.007>.
- (289) Wei, B.; Wang, C.; Cheng, Z.; Lai, B.; Gan, W. B.; Cui, M. Clear Optically Matched Panoramic Access Channel Technique (COMPACT) for Large-Volume Deep Brain Imaging. *Nat. Methods* **2021**, *18* (8), 959–964. <https://doi.org/10.1038/s41592-021-01230-3>.
- (290) Redman, W. T.; Wolcott, N. S.; Montelisciani, L.; Luna, G.; Marks, T. D.; Sit, K. K.; Yu, C. H.; Smith, S.; Goard, M. J. Long-Term Transverse Imaging of the Hippocampus with Glass Microperiscopes. *Elife* **2022**, *11*, 1–28. <https://doi.org/10.7554/elife.75391>.
- (291) Hjort, M. M.; Gowrishankar, R.; Tian, L.; Gordon-Fennell, A.; Namboodiri, V. M. K.; Bruchas, M. R.; Stuber, G. D. Microprisms Enable Enhanced Throughput and Resolution for Longitudinal Tracking of Neuronal Ensembles in Deep Brain Structures. *Neurophotonics* **2024**, *11* (3), 33407. <https://doi.org/10.1117/1.NPh.11.3.033407>.
- (292) Wang, Y.; DeMarco, E. M.; Witzel, L. S.; Keighron, J. D. A Selected Review of Recent Advances in the Study of Neuronal Circuits Using Fiber Photometry. *Pharmacol. Biochem. Behav.* **2021**, *201*, 173113. <https://doi.org/10.1016/j.pbb.2021.173113>.
- (293) Sych, Y.; Chernysheva, M.; Sumanovski, L. T.; Helmchen, F. High-Density Multi-Fiber Photometry for Studying Large-Scale Brain Circuit Dynamics. *Nat. Methods* **2019**, *16* (6), 553–560. <https://doi.org/10.1038/s41592-019-0400-4>.
- (294) Pisanello, F.; Sileo, L.; Oldenburg, I. A.; Pisanello, M.; Martiradonna, L.; Assad, J. A.; Sabatini, B. L.; De Vittorio, M. Multipoint-Emitting Optical Fibers for Spatially Addressable in Vivo Optogenetics. *Neuron* **2014**, *82* (6), 1245–1254. <https://doi.org/10.1016/j.neuron.2014.04.041>.
- (295) Pisano, F.; Pisanello, M.; Lee, S. J.; Lee, J.; Maglie, E.; Balena, A.; Sileo, L.; Spagnolo, B.; Bianco, M.; Hyun, M.; De Vittorio, M.; Sabatini, B. L.; Pisanello, F. Depth-Resolved Fiber Photometry with a Single Tapered Optical Fiber Implant. *Nat. Methods* **2019**, *16* (11), 1185–1192. <https://doi.org/10.1038/s41592-019-0581-x>.
- (296) Ohayon, S.; Caravaca-Aguirre, A.; Piestun, R.; DiCarlo, J. J. Minimally Invasive Multimode Optical Fiber Microendoscope for Deep Brain Fluorescence Imaging.

- Biomed. Opt. Express* **2018**, 9 (4), 1492. <https://doi.org/10.1364/boe.9.001492>.
- (297) Uhlířová, H.; Stibůrek, M.; Pikálek, T.; Gomes, A.; Turtaev, S.; Kolbábková, P.; Čižmár, T. “There’s Plenty of Room at the Bottom”: Deep Brain Imaging with Holographic Endo-Microscopy. *Neurophotonics* **2024**, 11 (S1), 1–11. <https://doi.org/10.1117/1.nph.11.s1.s11504>.
- (298) Stibůrek, M.; Ondráčková, P.; Tučková, T.; Turtaev, S.; Šiler, M.; Pikálek, T.; Jákl, P.; Gomes, A.; Krejčí, J.; Kolbábková, P.; Uhlířová, H.; Čižmár, T. 110 Mm Thin Endo-Microscope for Deep-Brain in Vivo Observations of Neuronal Connectivity, Activity and Blood Flow Dynamics. *Nat. Commun.* **2023**, 14 (1), 1897. <https://doi.org/10.1038/s41467-023-36889-z>.
- (299) Du, Y.; Dylida, E.; Stibůrek, M.; Gomes, A. D.; Turtaev, S.; Pagan, J. M. P.; Čižmár, T. Advancing the Path to In-Vivo Imaging in Freely Moving Mice via Multimode-Multicore Fiber Based Holographic Endoscopy. *Neurophotonics* **2024**, 11 (S1), 1–11. <https://doi.org/10.1117/1.nph.11.s1.s11506>.
- (300) Badt, N.; Katz, O. Real-Time Holographic Lensless Micro-Endoscopy through Flexible Fibers via Fiber Bundle Distal Holography. *Nat. Commun.* **2022**, 13 (1), 6055. <https://doi.org/10.1038/s41467-022-33462-y>.
- (301) Kang, M.; Choi, W.; Choi, W.; Choi, Y. Fourier Holographic Endoscopy for Imaging Continuously Moving Objects. *Opt. Express* **2023**, 31 (7), 11705. <https://doi.org/10.1364/oe.482923>.
- (302) Tsvirkun, V.; Sivankutty, S.; Baudelle, K.; Habert, R.; Bouwmans, G.; Vanvincq, O.; Andresen, E. R.; Rigneault, H. Flexible Lensless Endoscope with a Conformationally Invariant Multi-Core Fiber. *Optica* **2019**, 6 (9), 1185. <https://doi.org/10.1364/optica.6.001185>.
- (303) Aharoni, D.; Khakh, B. S.; Silva, A. J.; Golshani, P. All the Light That We Can See: A New Era in Miniaturized Microscopy. *Nat. Methods* **2019**, 16 (1), 11–13. <https://doi.org/10.1038/s41592-018-0266-x>.
- (304) Klioutchnikov, A.; Kerr, J. N. D. Chasing Cortical Behavior: Designing Multiphoton Microscopes for Imaging Neuronal Populations in Freely Moving Rodents. *Neurophotonics* **2023**, 10 (04), 1–8. <https://doi.org/10.1117/1.NPh.10.4.044411>.
- (305) Lorca-Cámara, A.; Blot, F. G. C.; Accanto, N. Recent Advances in Light Patterned Optogenetic Photostimulation in Freely Moving Mice. *Neurophotonics* **2024**, 11 (S1). <https://doi.org/10.1117/1.NPh.11.S1.S11508>.
- (306) Accanto, N.; Blot, F. G. C.; Lorca-Cámara, A.; Zampini, V.; Bui, F.; Tourain, C.; Badt, N.; Katz, O.; Emiliani, V. A Flexible Two-Photon Fiberscope for Fast Activity Imaging and Precise Optogenetic Photostimulation of Neurons in Freely Moving Mice. *Neuron* **2023**, 111 (2), 176–189.e6. <https://doi.org/10.1016/j.neuron.2022.10.030>.
- (307) Guo, C.; Blair, G. J.; Sehgal, M.; Sangiuliano Jimka, F. N.; Bellafard, A.; Silva, A. J.; Golshani, P.; Basso, M. A.; Blair, H. T.; Aharoni, D. Miniscope-LFOV: A Large-Field-of-View, Single-Cell-Resolution, Miniature Microscope for Wired and Wire-Free Imaging of Neural Dynamics in Freely Behaving Animals. *Sci. Adv.* **2023**, 9 (16), 1–14. <https://doi.org/10.1126/sciadv.adg3918>.
- (308) Scherrer, J. R.; Lynch, G. F.; Zhang, J. J.; Fee, M. S. An Optical Design Enabling Lightweight and Large Field-of-View Head-Mounted Microscopes. *Nat. Methods* **2023**, 20 (4), 546–549. <https://doi.org/10.1038/s41592-023-01806-1>.
- (309) Juneau, J.; Duret, G.; Chu, J.; Rodriguez, A.; Morozov, S.; Aharoni, D.; Robinson, J.; St-Pierre, F.; Kemere, C. MiniFAST: A Sensitive and Fast Miniaturized Microscope for in

- Vivo Neural Recording. *bioRxiv* **2020**. <https://doi.org/10.1101/2020.11.03.367466>.
- (310) Tian, F.; Mattison, B.; Yang, W. DeepLeMiN: Deep-Learning-Empowered Physics-Aware Lensless Miniscope. *bioRxiv* **2024**. <https://doi.org/10.1101/2024.05.03.592471>.
- (311) Zong, W.; Obenaus, H. A.; Skytøen, E. R.; Eneqvist, H.; de Jong, N. L.; Vale, R.; Jorge, M. R.; Moser, M. B.; Moser, E. I. Large-Scale Two-Photon Calcium Imaging in Freely Moving Mice. *Cell* **2022**, *185* (7), 1240-1256.e30. <https://doi.org/10.1016/j.cell.2022.02.017>.
- (312) Li, A.; Guan, H.; Park, H.-C.; Yue, Y.; Chen, D.; Liang, W.; Li, M.-J.; Lu, H.; Li, X. Twist-Free Ultralight Two-Photon Fiberscope Enabling Neuroimaging on Freely Rotating/Walking Mice. *Optica* **2021**, *8* (6), 870. <https://doi.org/10.1364/optica.422657>.
- (313) Zhao, C.; Zhu, Y.; Zhang, D.; Fu, Q.; Pan, M.; Wu, R.; Wang, A.; Cheng, H. Millimeter Field-of-View Miniature Two-Photon Microscopy for Brain Imaging in Freely Moving Mice. *Opt. Express* **2023**, *31* (20), 32925. <https://doi.org/10.1364/oe.492674>.
- (314) Klioutchnikov, A.; Wallace, D. J.; Sawinski, J.; Voit, K.-M.; Groemping, Y.; Kerr, J. N. D. A Three-Photon Head-Mounted Microscope for Imaging All Layers of Visual Cortex in Freely Moving Mice. *Nat. Methods* **2023**, *20* (4), 610–616. <https://doi.org/10.1038/s41592-022-01688-9>.
- (315) Berto, P.; Philippet, L.; Osmond, J.; Liu, C. F.; Afridi, A.; Montagut Marques, M.; Molero Agudo, B.; Tessier, G.; Quidant, R. Tunable and Free-Form Planar Optics. *Nat. Photonics* **2019**, *13* (9), 649–656. <https://doi.org/10.1038/s41566-019-0486-3>.
- (316) Panadés, J. M.; Rutz, N.; Robert, H. M. L.; Steffen, R. T.; García-Guirado, J.; Tessier, G.; Quidant, R.; Berto, P. Reconfigurable Integrated Thermo-Optics for Aberration Correction. *ACS Photonics* **2024**, *11* (11), 4804–4811. <https://doi.org/10.1021/acsp Photonics.4c01290>.
- (317) Robert, H. L. M.; Faini, G.; Liu, C.; Rutz, N.; Aggoun, A.; Putti, E.; Garcia-Guirado, J.; Del Bene, F.; Quidant, R.; Tessier, G.; Berto, P. Thermally Adaptive Surface Microscopy for Brain Functional Imaging. *ArXiv* **2025**. <https://doi.org/10.48550/arXiv.2501.039657>.
- (318) Li, S.-Q.; Xu, X.; Maruthiyodan Veetil, R.; Valuckas, V.; Paniagua-Domínguez, R.; Kuznetsov, A. I. Phase-Only Transmissive Spatial Light Modulator Based on Tunable Dielectric Metasurface. *Science (80-.)*. **2019**, *364* (6445), 1087–1090. <https://doi.org/10.1126/science.aaw6747>.
- (319) Göbel, W.; Kerr, J. N. D.; Nimmerjahn, A.; Helmchen, F. Miniaturized Two-Photon Microscope Based on a Flexible Coherent Fiber Bundle and a Gradient-Index Lens Objective. *Opt. Lett.* **2004**, *29* (21), 2521. <https://doi.org/10.1364/OL.29.002521>.
- (320) Ozbay, B. N.; Futia, G. L.; Ma, M.; Bright, V. M.; Gopinath, J. T.; Hughes, E. G.; Restrepo, D.; Gibson, E. A. Three Dimensional Two-Photon Brain Imaging in Freely Moving Mice Using a Miniature Fiber Coupled Microscope with Active Axial-Scanning. *Sci. Rep.* **2018**, *8* (1), 8108. <https://doi.org/10.1038/s41598-018-26326-3>.
- (321) Dussaux, C.; Szabo, V.; Chastagnier, Y.; Fodor, J.; Léger, J. F.; Bourdieu, L.; Perroy, J.; Ventalon, C. Fast Confocal Fluorescence Imaging in Freely Behaving Mice. *Sci. Rep.* **2018**, *8* (1), 16262. <https://doi.org/10.1038/s41598-018-34472-x>.
- (322) Supekar, O. D.; Sias, A.; Hansen, S. R.; Martinez, G.; Peet, G. C.; Peng, X.; Bright, V. M.; Hughes, E. G.; Restrepo, D.; Shepherd, D. P.; Welle, C. G.; Gopinath, J. T.; Gibson, E. A. Miniature Structured Illumination Microscope for in Vivo 3D Imaging of Brain Structures with Optical Sectioning. *Biomed. Opt. Express* **2022**, *13* (4), 2530. <https://doi.org/10.1364/boe.449533>.

- (323) Andresen, E. R.; Bouwmans, G.; Monneret, S.; Rigneault, H. Toward Endoscopes with No Distal Optics: Video-Rate Scanning Microscopy through a Fiber Bundle. *Opt. Lett.* **2013**, *38* (5), 609. <https://doi.org/10.1364/ol.38.000609>.
- (324) Sun, J.; Kuschmierz, R.; Katz, O.; Koukourakis, N.; Czarske, J. W. Lensless Fiber Endomicroscopy in Biomedicine. *Photonix* **2024**, *5* (1). <https://doi.org/10.1186/s43074-024-00133-8>.
- (325) Choi, W.; Kang, M.; Hong, J. H.; Katz, O.; Lee, B.; Kim, G. H.; Choi, Y.; Choi, W. Flexible-Type Ultrathin Holographic Endoscope for Microscopic Imaging of Unstained Biological Tissues. *Nat. Commun.* **2022**, *13* (1), 1–10. <https://doi.org/10.1038/s41467-022-32114-5>.
- (326) Sun, J.; Wu, J.; Wu, S.; Goswami, R.; Girardo, S.; Cao, L.; Guck, J.; Koukourakis, N.; Czarske, J. W. Quantitative Phase Imaging through an Ultra-Thin Lensless Fiber Endoscope. *Light Sci. Appl.* **2022**, *11* (1). <https://doi.org/10.1038/s41377-022-00898-2>.
- (327) Ren, H.; Jang, J.; Li, C.; Aigner, A.; Plidschun, M.; Kim, J.; Rho, J.; Schmidt, M. A.; Maier, S. A. An Achromatic Metafiber for Focusing and Imaging across the Entire Telecommunication Range. *Nat. Commun.* **2022**, *13* (1). <https://doi.org/10.1038/s41467-022-31902-3>.
- (328) Sivankutty, S.; Bertocini, A.; Tsvirkun, V.; Gajendra Kumar, N.; Brévalle, G.; Bouwmans, G.; Andresen, E. R.; Liberale, C.; Rigneault, H. Miniature 120-Beam Coherent Combiner with 3D-Printed Optics for Multicore Fiber-Based Endoscopy. *Opt. Lett.* **2021**, *46* (19), 4968. <https://doi.org/10.1364/ol.435063>.
- (329) Schmidt, S.; Thiele, S.; Toulouse, A.; Bösel, C.; Tiess, T.; Herkommer, A.; Gross, H.; Giessen, H. Tailored Micro-Optical Freeform Holograms for Integrated Complex Beam Shaping. *Optica* **2020**, *7* (10), 1279. <https://doi.org/10.1364/optica.395177>.
- (330) Gissibl, T.; Thiele, S.; Herkommer, A.; Giessen, H. Two-Photon Direct Laser Writing of Ultracompact Multi-Lens Objectives. *Nat. Photonics* **2016**, *10* (8), 554–560. <https://doi.org/10.1038/nphoton.2016.121>.
- (331) Schmid, M.; Sterl, F.; Thiele, S.; Herkommer, A.; Giessen, H. 3D Printed Hybrid Refractive/Diffractive Achromat and Apochromat for the Visible Wavelength Range. *Opt. Lett.* **2021**, *46* (10), 2485. <https://doi.org/10.1364/OL.423196>.
- (332) Liberale, C.; Cojoc, G.; Candeloro, P.; Das, G.; Gentile, F.; De Angelis, F.; Di Fabrizio, E. Micro-Optics Fabrication on Top of Optical Fibers Using Two-Photon Lithography. *IEEE Photonics Technol. Lett.* **2010**, *22* (7), 474–476. <https://doi.org/10.1109/LPT.2010.2040986>.